ČESKÉ VYSOKÉ UČENÍ TECHNICKÉ V PRAZE

FAKULTA STROJNÍ

OPTIMALIZACE FOTOVOLTAICKÉHO SYSTÉMU PRO POTŘEBY DOMÁCNOSTI

MARTIN HODEK

2021

ZADÁNÍ DIPLOMOVÉ PRÁCE

I. OSOBNÍ A STUDIJNÍ ÚDAJE

Příjmení: **Hodek** Jméno: **Martin** Osobní číslo: **459873**

Fakulta/ústav: **Fakulta strojní**

Zadávající katedra/ústav: **Ústav energetiky**

Studijní program: **Strojní inženýrství**

Studijní obor: **Energetika**

II. ÚDAJE K DIPLOMOVÉ PRÁCI

Název diplomové práce:

Optimalizace fotovoltaického systému pro potřeby domácnosti

Název diplomové práce anglicky:

Optimization of a photovoltaic system for household needs

Pokyny pro vypracování:

Na základě modelování osvitu během roku sestavte a aplikujte model pro parametrickou optimalizaci fotovoltraického systému určeného pro krytí energetické spotřeby typické domácnosti
Dílčí cíle:
1) Zpracujte rešerši malých fotovoltaických systémů pro domácnosti a možností optimalizace jejich využití.
2) Proveďte rešerši metod a modelů pro bilancování solárního svitu a energetického zisku FV elektrárny.
3) Navrhněte a verifikujte model pro predikci solárního svitu a výroby FV elektrárny ve vybrané lokalitě na hodinové bázi během roku.
4) Vytvořte profil celoroční energetické potřeby typické domácnosti v hodinovém rozlišení.
5) Sestavte model pro parametrickou optimalizaci FV systému a na základě typizovaných vstupů proveďte výpočet pro více variant.
6) Proveďte techniko-ekonomické srovnání výsledků a výběr nejvýhodnějších variant realizace.

Seznam doporučené literatury:

Loutzenhiser, P. G., Manz, H., Felsmann, C., Strachan, P. A., Frank, T., Maxwell, G. M. Empirical: validation of models to compute solar irradiance on inclined surfaces for building energy simulation. Solar Energy, 2007, vol. 81
Yang, D. Solar radiation on inclined surfaces: Corrections and benchmarks. Solar Energy, 2016, vol.136, p. 288–302.

Jméno a pracoviště vedoucí(ho) diplomové práce:

doc. Ing. Tomáš Dlouhý, CSc., ústav energetiky FS

Jméno a pracoviště druhé(ho) vedoucí(ho) nebo konzultanta(ky) diplomové práce:

Datum zadání diplomové práce: **22.04.2021** Termín odevzdání diplomové práce: **04.06.2021**

Platnost zadání diplomové práce: **31.12.2022**

_____
doc. Ing. Tomáš Dlouhý, CSc.
podpis vedoucí(ho) práce

_____
podpis vedoucí(ho) ústavu/katedry

_____
prof. Ing. Michael Valášek, DrSc.
podpis děkana(ky)

III. PŘEVZETÍ ZADÁNÍ

Diplomant bere na vědomí, že je povinen vypracovat diplomovou práci samostatně, bez cizí pomoci, s výjimkou poskytnutých konzultací.
Seznam použité literatury, jiných pramenů a jmen konzultantů je třeba uvést v diplomové práci.

._____
Datum převzetí zadání

_____
Podpis studenta

Prohlášení

Prohlašuji, že jsem předloženou práci vypracoval samostatně a že jsem uvedl veškeré použité informační zdroje v souladu s Metodickým pokynem o dodržování etických principů při přípravě vysokoškolských závěrečných prací.

Martin Hodek, v. r., 1. června 2021

Kuba, J.: Metodický pokyn č. 1/2009 O dodržování etických principů při přípravě vysokoškolských závěrečných prací, ČVUT v Praze, 1. července 2009, https://www.cvut.cz/sites/default/files/content/d1dc93cd-5894-4521-b799-c7e715d3c59e/cs/20180605-metodicky-pokyn-c-12009-o-dodrzovani-etickych-principu-pri-priprave-vysokoskolskych.pdf [10. srpna 2018]

Anotační list

Anotace

Diplomová práce řeší problematiku optimalizace fotovoltaických systémů dle energetických potřeb domácností v České republikce. Aplikovaný přístup vychází z numerické simulace výkonu fotovoltaické elektrárny a energetické spotřeby domácnosti.

V úvodní části studie je stručně představena problematika fotovoltaických elektráren pro domácnosti, solárních radiačních modelů a modelování energetických potřeb domácnosti. Na základě uvedené teorie je následně implementován a verifikován radiační model, společně s parametrickým modelem energetických nároků domácnosti.

Propojením zmíněných modelů výpočetní logikou je získán nástroj pro simulaci energetických toků v domácnostech s fotovoltaickými systémy. Ten je dále použit pro vyhodnocení vlivu velikosti solární elektrárny, bateriového úložiště a energetickcých potřeb domácnosti na využití vyráběné energie společně s posouzením prosté návratnosti fotovoltaického systému.

Závěrem práce jsou diskutovány získané výsledky a zmíněna obecná doporučení pro projektování fotovoltaických systémů pro domácnosti.

Anotation

The diploma thesis addresses the issue of the optimization of photovoltaic systems in accordance with the households energy needs in the Czech Republic. The applied approach is based on a numerical simulation of the power output of a photovoltaic power plant and the energy consumption of a household.

Within the introduction, topics of photovoltaic power plants for households, solar radiation models and modeling of household energy needs are briefly presented. Based on the theory, the radiation model is implemented and verified, together with the parametric model of household energy requirements.

Connecting the mentioned models by computational logic, a tool for simulation of energy flows in households with photovoltaic systems is obtained. Further it is used to evaluate the effect of the size of solar array, battery storage and energy needs of the household, on the utilization rate of energy produced, along with an assessment of the bare return on investment of the photovoltaic system.

In the end, obtained results are discussed and general recommendations for the household photovoltaic systems design are proposed.

Poděkování

Předně bych chtěl poděkovat vedoucímu mé diplomové práce, za jeho čas, trpělivost a vloženou důvěru. Současně také děkuji rodině, která mě při psaní diplomové práce podporovala, stejně tak jako ve všem ostatním, čemu se věnuji.

Contents

Symbols and abbreviations

DHW	Domestic Hot Water
HDKR	Hay, Davies, Klutcher and Reindl
HT	High Tariff
ICT	Information and Communication Technologies
LT	Low Tariff
PV	Photovoltaic
PVGIS	Photovoltaic Geographical Information System
SH	Space Heating

A_i	Anisotropy index	$-$
a	Solid angle	deg
B	Variable	deg
b	Solid angle	deg
DNI	Direct normal irradiance	$\mathrm{W\,m^{-2}}$
E	Equation of time	hr
E_t	Electrical energy generated	kWh
F_t	Fuel expenditures	CZK
F_x	Horizon brightness coefficient	$-$
f	Modulation factor	$-$
f_{PV}	Derating factor	%
f_{xx}	Perez coefficient	$-$
G	Global horizontal irradiance	$\mathrm{W\,m^{-2}}$
G_b	Global horizontal beam irradiance	$\mathrm{W\,m^{-2}}$
G_d	Global horizontal diffuse irradiance	$\mathrm{W\,m^{-2}}$
G_{on}	Extraterrestrial normal radiation	$\mathrm{W\,m^{-2}}$
G_{sc}	Solar constant	$\mathrm{W\,m^{-2}}$
G_T	Total solar irradiance on tilted surface	$\mathrm{W\,m^{-2}}$
$G_{T,STC}$	Incident irradiance at standard conditions	$\mathrm{W\,m^{-2}}$
$G_{T_{ERR-A}}$	Absolute error of G_T prediction	kW
$G_{T_{ERR-R}}$	Relative error of G_T prediction	%
I_t	Investment expenditures	CZK
k_t	Clearness index	$-$
LCOE	Levelized cost of energy	$\mathrm{CZK\,kWh^{-1}}$
M_t	Maintenance expenditures	CZK
n	Day of year	$-$
P_{PV}	Output of PV array	kW
$P_{PV_{ERR-A}}$	Absolute error of P_{PV} prediction	kW
$P_{PV_{ERR-R}}$	Relative error of P_{PV} prediction	%
R_b	Geometric factor	$-$
r	Discount rate	%
t	Time	Years
t_c	Civil time	hr
t_s	Solar time	hr
W_b	Grid bought electricity price	CZK
W_c	Consumed electricity	kWh
W_s	Grid sold electricity price	CZK
Y_{PV}	Standard rated capacity of PV array	kW
Z_C	Time zone	hr

β	Slope of the surface	deg
γ	Azimuth	deg
ϵ	Bin of clearness	–
θ	Angle of incidence	deg
θ_z	Zenith angle	deg
λ	Longitude	deg
ρ_g	Albedo	%
ϕ	Latitude	deg
ω	Hour angle	deg

Chapter 1

Household photovoltaics

Approaching the 70th anniversary of first silicon based photovoltaic cell created in the United States, 1954, it is obvious that photovoltaic sector has undergone a great development. Within the last decade, installed capacity of photovoltaic power plants increased rapidly, whereas the growth rate keeps further accelerating, as it can be seen in Figure 1.1. The reason for such expansion lies in technological advancements, improving operating parameters of PV systems, while also decreasing the price. As a result, photovoltaic power plants become a viable option not only for the utility and commercial scale, but also in the residential sector.

If we focus more closely on residential photovoltaic systems, it is clear that they have significant specifics. The primary functioning of the PV system is here in the sense of a decentralized source, to cover owners self-consumption. In comparison with larger installations, the approach of maximizing production is therefore not applicable, yet it is necessary to optimize the output of the PV plant according to the consumption of the household.
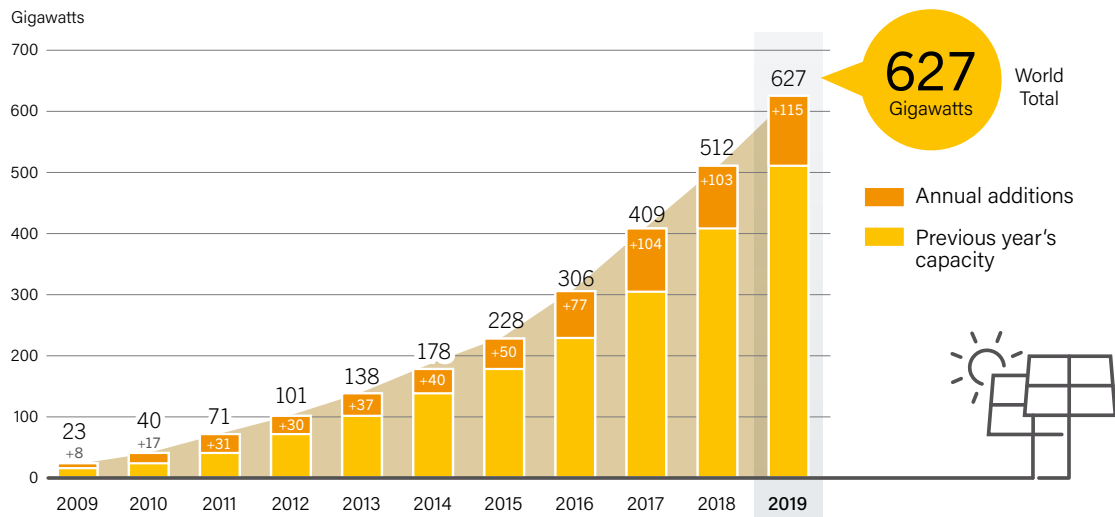

Fig. 1.1: Solar PV global capacity and annual additions
REN21 (2020)

1.1 Overview

Despite the residential photovoltaic systems accounting for less than a quarter of the total installed capacity, while this share is presumed to decrease, as stated by Olson and Baklen (2019), their importance is high, nevertheless.

The main reason for that, is their potential as a local source of electricity, reducing the load on the distribution network, if designed and operated properly. On top of that, local energy source allows for partial independence from the electrical grid, stabilizing (owners) electricity prices and serving as a back-up in the event of a blackout.

Speaking of residential solar systems, various configurations can be found. For clarification, it is necessary to distinguish between on-grid, off-grid and hybrid systems.

- On-grid systems, as the name suggests, are fully reliant on their connection to the grid. Such arrangement consists of solar panels and PV inverter only, lacking the battery storage. As a result, electricity produced can be either directly utilized, or it needs to be sold to the grid. On a plus side, on-grid systems are the cheapest available, however, falling behind due to lower produced electricity utilization rate and absence of back-up. Because of the inverter being completely dependent on grid, the system is rendered useless in case of black out.

- Off-grid systems, on the other hand, are completely independent on the grid, furthermore, they are unable to operate in the presence of the grid. This setup contains all previously mentioned parts - solar panels, inverter and battery pack, and thus can operate in detached areas. Due to the battery storage, however, the system price is noticeably higher.

- Hybrid systems lie somewhat in between, being able to operate both, connected to a grid, or off-grid. The advantage of such system is a higher PV electricity utilization, thanks to the batteries and also the option to function in different regimes. A mode using the produced energy to optimize self-consumption needs comes as a standard. However, hybrid systems even allow for charging batteries from the grid, during the off-peak electricity price and discharging to the loads during a high tariff.

Each of this systems has its upsides and downsides, mostly originating from its initial design and application purpose. The choice of a specific system therefore depends primarily on the selected boundary conditions.

In order to power a dwelling in a remote area, no other option than the off-grid system is applicable. The selection for a grid connected application is not that simple.

Unless the household is located in an area, where blackouts occur frequently, both on-grid and hybrid systems may be a viable option. The determining factor is electricity billing approach, whereas two different options exist - a net metering and a feed-in tariff.

In general, for the net metering, all surpluses send to the grid is credited at the retail electricity price. In other words, amount of electricity send to the grid is deduced from the total electrical consumption of the household. Given the same "value" of solar electricity, no matter whether it was directly consumed or send to the grid, on-grid systems are a preferable solution in such case.

Regarding the feed-in tariff, surplus energy is credited at a rate notably lower than is the electricity retail price. In such case, value of consumed PV electricity is higher, than the value of grid sold PV electricity. Therefore, storing the surplus energy in a battery occurs as a viable option. For that reason, hybrid systems are preferred in this case.

Provided the study being primarily focused on photovoltaic systems in Czech Republic, where the feed-in tariff is applicable, hybrid systems only will be considered in the whole work. Another reason for such choice is a higher potential for optimization, when it comes to hybrid systems.

Chapter 2

Goals and methodology

Targeting the hybrid PV systems with battery storage, it comes as no surprise, that the bigger the battery is, the higher the utilization rate probably will be. Photovoltaic system design is yet not that simple.

As it was mentioned previously, residential PV systems should comply to the household energy needs. Creating the system too big, results in increased costs and extended payback period, whereas too small systems may be insufficient to properly meet the needs.

In addition to that, hybrid systems can be also connected to heat storage tanks, increasing the surplus energy storage capacity.

All things considered, a techno-economic optimization is required to properly design PV system. Many articles have already provided guidelines for that purpose, e.g. Vaz (2020), USA, or Angenendt et al. (2019), Germany. Publications are, however, area specific and thus inapplicable in general means. For that reason, it was decided to examine mentioned topic under conditions of the Czech Republic in this study.

2.1   Adopted approach

In order to accurately evaluate and make full use of the potential of various hybrid photovoltaic system setups, possibly even coupled with thermal storage, it was necessary to choose a fitting approach. Simple method of comparing PV power output with household electrical demand on monthly or daily basics would fail to capture the mismatch between electricity production and consumption. Therefore, finer resolution was needed. Readily available tools, however, were unable to fulfill the study requirements and thus it was decided to implement the evaluation tool from a scratch.

Simulation model was decided to combine solar irradiation model, used to predict photovoltaic plant power output, with household consumption model, accounting for the energy needs of the dwelling. Although, not everything was possible to be simulated from the very beginning and thus the real world data measurements were also needed.

Addressing the initial difficulty, simulation step was decided to follow the best obtainable data sets resolution, that being 1 hour. Such value was also considered to provide reasonable ratio of computational time and results precision.

Once the simulation tool preliminary design was decided, computational logic was implemented, in order to utilize PV system produced electricity efficiently. As such, both solar irradiation and household energy demand models were combined into one.

Having the modeling tool established, test cases were designed next. In order to acknowledge the hybrid PV systems potential under various circumstances, diverse household types were included into the study. The differentiation was done primarily based on the ways of covering their energy demands.

Once all the simulation components were prepared and evaluation criteria set, modeling run was performed for each examined dwelling with various PV systems sizes. On top of that, optimized PV setup for shortest bare payback time and best LCOE was determined for each household type.

Chapter 3

Radiation model

In order to perform comparison of various photovoltaic systems, it was necessary to create a radiation model, so that the power output of solar array can be calculated through the day.

Given that the topic of modelling solar radiation incident to Earth's surface was already well-researched and extensively studied, in this work, only brief overview is provided, keeping in mind, that the radiation model is rather a tool for further calculations, than the primary field of study.

3.1 Introduction

In general, solar radiation incident to earth's surface is a result of complex interactions of solar rays between the atmosphere and ground, whereas the determining factors can be divided into three groups. First, Earth's geometry, revolution and rotation, next, terrain and the last, atmospheric attenuation.

Regarding the first group, it is necessary to consider declination, latitude and solar hour angle, to acknowledge the relative position of the Sun and the Earth. Next, to account for the terrain effects, elevation, surface inclination and orientation, and shadows needs to be estimated. Furthermore, elevation can also be connected to the third group, atmospheric attenuation, as the thickness of atmospheric layer above the surface affects the radiation intensity.

The main drivers of atmospheric attenuation are scattering and absorption of solar rays, caused by

- air molecules, especially ozone, carbon dioxide and oxygen,

- aerosols, thus solid and liquid particles, and

- clouds, therefore condensed water (strongest attenuation).

Based on these effects, overall global radiation reaching the given surface, can be divided into three components. Namely

- beam radiation, also called direct solar radiation, which, as the name suggests, reaches the surface directly, without being reflected or scattered,

- diffuse radiation, accounting for the scattered part of global radiation, and

- reflected radiation, striking the given surface after reflection from ground.

Provided, that meteorological stations mostly measure only global radiation, sometimes also diffuse radiation intensities on horizontal planes, the solar radiation incident on a tilted surface has to be determined mathematically (empirically) from these values.

Previously mentioned beam radiation can be calculated from geometrical relationship between horizontal and tilted surfaces, by utilizing relatively simple trigonometry. Ground reflected radiation may be obtained with reasonable accuracy under simplifying assumption of "isotropic sky", expecting the sky to be uniform over the whole sky dome. Unfortunately, the calculation of diffuse radiation is not that straight forward, whereas the approach to this problem makes one of the key differences among solar radiation models.

One of the fundamental models, on which majority of consecutive models are based, is the isotropic sky model, developed by Liu and Jordan (1962), therefore referred to as Liu-Jordan model. Total solar irradiance incident on tilted surface is in that case calculated by using the equation below, whereas diffuse radiation is determined using a single uniform formula.

$$G_T = G_b \, R_b + G_d \left(\frac{1 + \cos\beta}{2}\right) + G \, \rho_g \left(\frac{1 - \cos\beta}{2}\right)$$

Total solar irradiance on tilted surface	Global horizontal beam irradiance	Geometric factor	Global horizontal diffuse irradiance	Tilted surface view factor	Global horizontal irradiance	Albedo	Tilted surface view factor
	Beam component		**Diffuse component**		**Ground reflected component**		
			Sky diffuse				

Fig. 3.1: Liu and Jordan

This approach was later largely replaced by more complex ones, as Klucher (1979) concluded that Liu-Jordan model compares well to empirical data at low intensity conditions, found during overcast skies, however underestimates the amount of solar irradiance under clear skies. Such observations were confirmed many times since, recently by Li et al. (2017), whereas Muneer (1990), even recommended to discontinue its use, due to poor performance.

In general, as mentioned by Jakhrani et al. (2012), utilization of Liu-Jordan model is only suggested for prediction of solar irradiation in cloudy weather conditions, thus estimating available solar radiation incident on the tilted surfaces in overcast skies.

Overall, isotropic sky models remain in use, mainly for its simplicity and low computational complexity, while for some geographical locations and weather conditions, it still provides reasonable results.

As the research in the field of modeling solar radiation progressed, isotropic approach, often considered oversimplifying, was replaced with more advanced approach, accounting for anisotropy of the sky. Reasoning behind this progression can be derived from the idea, that in reality, tilted surface facing the sun receive more diffuse radiation than the surface of the same tilt in the opposite direction.

Anisotropic sky models differ from isotropic ones in the manner of computing diffuse radiation inclined on tilted plane, whereas based on number of "components" used to calculate diffuse radiation, anisotropic models can be divided into various sub-categories. For simplicity, only "three components" models will be discussed further, with a single exception, Hay and Davies (1980) model, being "two components" one.

In case of "three components" anisotropic models, diffuse radiation is, as the name suggests, divided into three components. In particular, sky diffuse radiation (also called isotropic diffuse radiation), circumsolar diffuse radiation and horizon diffuse radiation. Visual representation of these constituents of diffuse radiation can be seen in Figure 3.2.
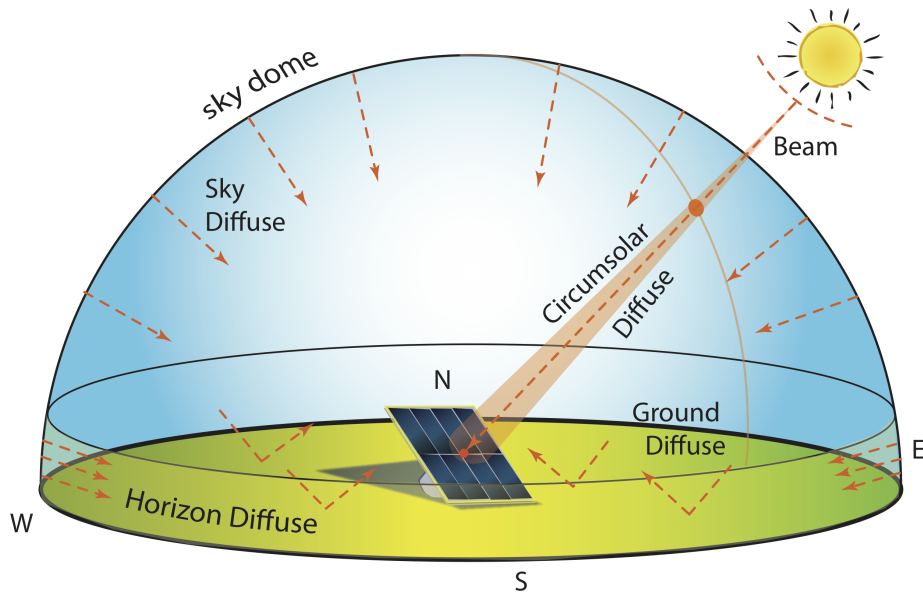
Fig. 3.2: Diagram of the multiple components of the clear sky
Brownson (2020b)

Regarding the "three components" anisotropic models, the two quite often used, are HDKR and Perez model. Speaking of HDKR model, it originates from another "three components" model, developed by Temps and Coulson (1977). This model was further improved by Klucher (1979), who significantly increased its accuracy by introducing a function to account for the degree of a cloud cover. Subsequently, Reindl et al. (1990) utilized the term referring to horizon diffuse radiation from Klutcher's model, adding it to "two components" model by Hay and Davies (1980), which already contained terms for circumsolar diffuse radiation and isotropic diffuse radiation.

This newly established model was then often referred as HDKR anisotropic sky model, where the acronym HDKR stands for names Hay, Davies, Klucher and Reindl. The final equation to calculate global solar irradiance on tilted surface is provided below.

$$G_T = G_b \quad R_b \quad + \quad G \quad \rho_g \quad (\frac{1 - \cos\beta}{2})$$

	Total solar irradiance on tilted surface	Global horizontal beam irradiance	Geometric factor		Global horizontal irradiance	Albedo	Tilted surface view factor

<div style="text-align:center">Beam component   Ground reflected component</div>

$$+ \quad G_d \quad [(1 - A_i) \quad (\frac{1 + \cos\beta}{2}) \quad (1 + f \quad \sin^3(\frac{\beta}{2})) + (A_i \quad R_b)]$$

	Global horizontal diffuse irradiance		Anisotropy index	Tilted surface view factor		Modulation factor	Horizon brightening factor		Anisotropy index	Geometric factor

<div style="text-align:center">Diffuse component</div>

<div style="text-align:center">Sky diffuse   Horizon diffuse component   Circumsolar component</div>

Fig. 3.3: HDKR

Another option for modeling solar radiation incident on tilted surface provides already mentioned Perez model, similarly to HDKR, being also "three components" anisotropic model. The main difference between these two (and in general among Perez and all other models, on that matter) is, that previously presented models separated isotropic, circumsolar and horizon components explicitly, whereas Perez introduced a more complex model, utilizing empirical coefficients for each of these terms.

These coefficients were derived from experimental data sets, obtained from measurements performed in various cities, mainly in the USA, however, including also Geneva in Switzerland and Trappes and Carpentras in France. As the experimental data sets varied, distinct variants of Perez model emerged in years, namely Perez I, II, and III, published by Perez et al. (1987), Perez et al. (1988) and Perez et al. (1990) respectively. The last quoted is the most widely accepted one.

The final equation for Perez model is to be seen in Figure 3.4, which, in its general form, is the same for all three Perez models, while the diversity can be found in a way of calculating empirical coefficients $F1$ and $F2$.

$$G_T \quad = \quad \underbrace{G_b \qquad R_b}_{\text{Beam component}} \quad + \quad \underbrace{G \qquad \rho_g \qquad (\frac{1 - \cos\beta}{2})}_{\text{Ground reflected component}}$$

G_T		G_b	R_b		G	ρ_g	$(\frac{1-\cos\beta}{2})$
Total solar irradiance on tilted surface		Global horizontal beam irradiance	Geometric factor		Global horizontal irradiance	Albedo	Tilted surface view factor

$$+ \quad \underbrace{\underbrace{G_d \quad [(1 - F_1) \quad (\frac{1 + \cos\beta}{2})}_{\text{Sky diffuse component}} + \underbrace{F_1 \quad \frac{a}{b}}_{\text{Circumsolar component}} + \underbrace{F_2 \quad \sin\beta]}_{\text{Horizon diffuse}}}_{\text{Diffuse component}}$$

	G_d	$[(1 -$	$F_1)$	$(\frac{1+\cos\beta}{2}) +$	F_1	$\frac{a}{b}$	$+$	F_2	$\sin\beta]$
	Global horizontal diffuse irradiance		Circumsolar brightness coefficient	Tilted surface view factor	Circumsolar brightness coefficient	Solid angles ratio		Horizon brightness coefficient	Tilted surface view factor

Fig. 3.4: Perez

It is not easy to straight-forwardly decide, which model to choose, as the performance of different models vary under diverse conditions. Prior to such decision, a comparative study of numerous models is often performed, to find the one providing the best match to given location, therefore, local weather conditions. Such approach, although rigorous, is out of the scope of this work, while given the modeled data usage for relative comparison, rather than absolute conclusions, is not considered necessary.

For those reasons, an approach utilizing prevailing suggestions from literature is adopted. As a common rule, it shall be mentioned, that anisotropic models should be preferred to isotropic ones, since the isotropic sky models tend to under-predict total solar radiation inclined on tilted surface. Tian et al. (2018). At the same time, generally recommended anisotropic model appears to be Perez III, by Perez et al. (1990), indicated by TRNSYS (2014) and Yang (2016).

Regarding these implications, for further irradiance modeling, Perez III model was chosen, whereas to be able to cross check its results, HDKR model was recruited.

For further references and in-depth explanation on the topic of the development and comparison of various isotropic and anisotropic models, used to estimate global solar radiation on inclined surfaces, please see the work of Loutzenhiser et al. (2007), Demain et al. (2013), Garcia and Huld (2013) and Yang (2016).

3.2 Model set-up

Despite the complexity and diversity of ways to model various components of global solar radiation, each numerical model starts the initial calculation with the same approach to determine extra-terrestrial solar radiation on horizontal surface.

To account for geographical location and orientation of given surface, necessary initial parameters are latitude ϕ and longitude λ, slope (tilt) β and azimuth of the panel γ respectively. Using standard notation, the slope is the angle formed between the panel plane and horizon plane, so that $0°$ indicates horizontal orientation, whereas tilt of $90°$, vertical. Next, azimuth regards the orientation in which the panel faces, while azimuth of $0°$ corresponds to due south and $90°$ to due west. Finally, latitude and longitude are resembling the geographical location of the panel.

In addition to these parameters, time of the year and time of the day are required, to compute the position of sun with regard to chosen location. Based on these values, available extra-terrestrial solar radiation for given location and time, can be then calculated.

First, solar declination δ, being the latitude at which the solar rays are perpendicular to the earth's surface at solar noon, needs to be determined using the formula by Cooper (1969),

$$\delta = 23.45 \sin\left(360\,\frac{284 + n}{365}\right) \tag{3.1}$$

where n stands for the day of year, while $n = 1$ indicates 1st of January.

Next, location of the sun in the sky, given by solar hour angle ω has to be calculated, in a way suggested by Antonio and Hegedus (2010),

$$\omega = 15\,(t_s - 12) \tag{3.2}$$

where "15" stands for the sun movement through the sky, being $15°$ per hour, and t_s represents the solar time in hours, while at solar noon, $t_s = 12$ and thus $\omega = 0°$.
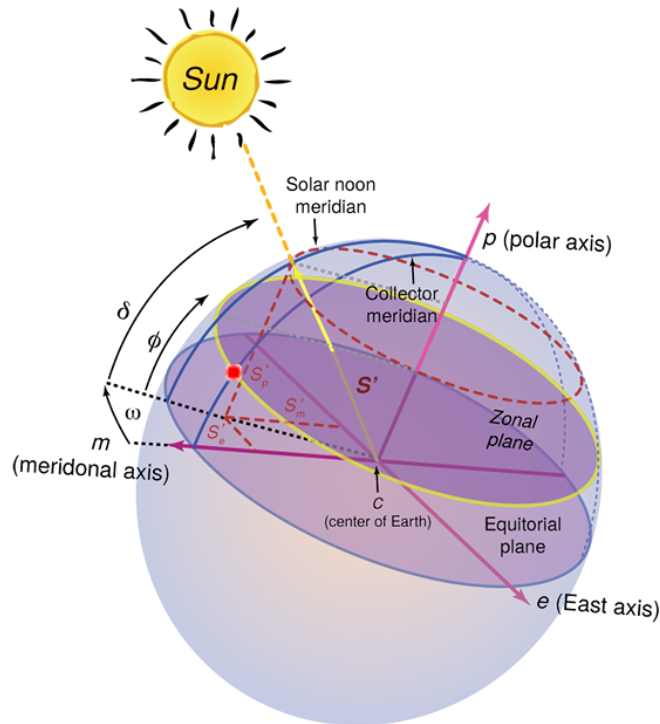
Fig. 3.5: Declination δ, latitude ϕ and solar hour ω angle
Brownson (2020a)

In the Figure 3.5, all three previously mentioned angles are depicted.

- Declination angle δ, reaching from the equator to the imagined connection between Sun and Earth centres. Its value seasonally vary from -23.45° to 23.45°, due to the tilt of Earth axis, Earth's rotation alone and also its revolution around the Sun. Limit values are achieved during winter and summer solstice respectively, whereas zero values during equinoxes.

- Latitude angle ϕ, ranging from -90° (North Pole) to 90° (South Pole), zero at equator, referring to "observer position" highlighted with red dot. That is in contrast to the declination angle, which is independent of the location on the planet.

- Solar hour angle ω, varying in range $\langle 0°, 360° \rangle$ through the day, while the zero value is reached once the sun is in its highest position in the sky that day, from the observer point of view.

Given that the solar time differ from the civil time, its value needs to be determined, as a function of civil time t_c, longitude of desired location ϕ, time zone in hours to the GMT Z_e and "equation of time", accounting for Earth's orbit and axial tilt, E.

Reasoning behind this step is, that majority of time dependent data, such as solar radiation and electric load are provided in the local or universal time.

$$t_s = t_c + \frac{\lambda}{15} - Z_c + E \tag{3.3}$$

Value of E can be further calculated using empirical equation, Antonio and Hegedus (2010), as follows,

$$
\begin{aligned}
E = 3.82 \, (0.000075 &+ 0.001868 \cos B - 0.032077 \sin B \\
&- 0.014615 \cos 2B - 0.04089 \sin 2B)
\end{aligned} \tag{3.4}
$$

where B is calculated using the day of the year, n.

$$B = 360 \, \frac{n-1}{365} \tag{3.5}$$

Now, that the collector surface position and orientation is known, angle of incidence θ, characterizing the angle between Sun's beam (direct) radiation and the normal to the panel plane, can be obtained using the equation below,

$$
\begin{aligned}
\cos \theta = \sin \delta \sin \phi \cos \beta &- \sin \delta \, \cos \phi \, \sin \beta \cos \gamma \\
&+ \cos \delta \cos \phi \cos \beta \cos \omega + \cos \delta \sin \phi \sin \beta \cos \gamma \cos \omega \\
&+ \cos \delta \sin \beta \sin \gamma \sin \omega
\end{aligned} \tag{3.6}
$$

where δ stands for declination angle, ϕ for latitude, β for tilt, γ for azimuth and ω for hour angle.

If we consider the slope of the panel to be zero, Equation 3.6 simplifies to a form provided beneath, where the particular angle of incidence for such case is called the zenith angle θ_z. Physical representation of this angle is the value between vertical line and line to the Sun. That being 0° once the Sun is directly overhead and 90° when it is at the horizon.

$$\cos \theta_z = \cos \phi \cos \delta \cos \omega + \sin \phi \sin \delta \tag{3.7}$$

Depiction of zenith angle and previously mentioned declination and latitude angles can be seen in Figure 3.20.
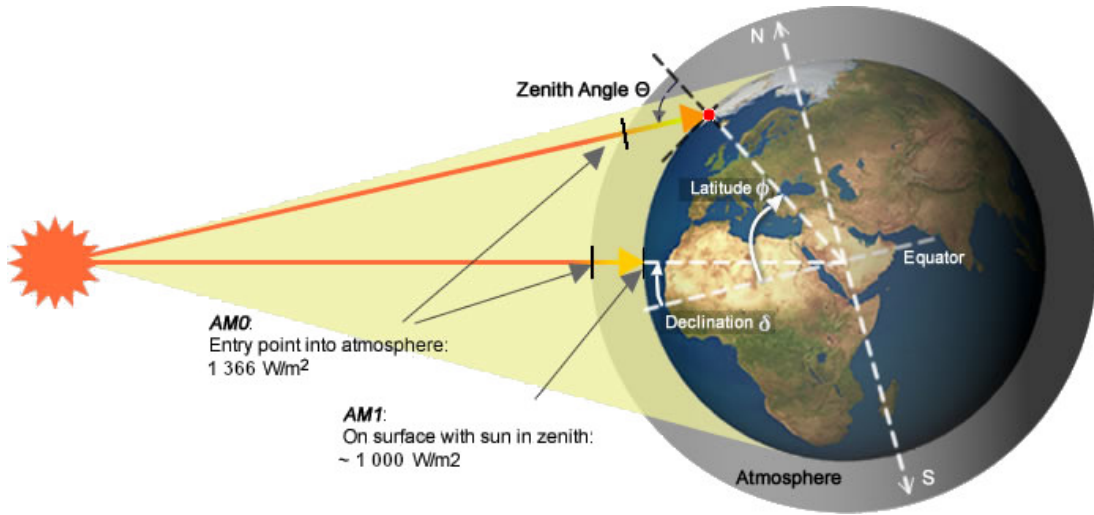
Fig. 3.6: Declination δ latitude ϕ and zenith θ_z angle
Green Rhino Energy (2016)

Given that all necessary geometrical relations are known by now, the extra-terrestrial normal radiation, is to be computed next. It can be assumed, that the Sun output is constant over time, however, due to the eccentricity of Earth's orbit, amount of solar irradiance striking the top of atmosphere varies through the year. To account for this effect, extra-terrestrial normal radiation needs to be described as a function of a day of the year, as proposed by Whiteman and Allwine (1986),

$$G_{on} = G_{sc}\left(1 + 0.033\cos\frac{360\,n}{365}\right) \tag{3.8}$$

where G_{sc} refers to solar constant, being $1.366\ \mathrm{kW/m^2}$.

Next, extra-terrestrial horizontal radiation, incident on the horizontal surface at the top of the atmosphere can be calculated as follows.

$$G_o = G_{on}\cos\theta_z \tag{3.9}$$

Once the extra-terrestrial radiation is determined, using the clearness index k_T, global horizontal radiation on Earth's surface can be obtained as provided below.

$$k_T = \frac{G}{G_o} \tag{3.10}$$

Clearness index refers to radiation attenuation by the atmosphere and clouds, before the solar rays reach the surface of the Earth. Its value ranges from 0 to 1, whereas the typical values lie between 0.25 for a very cloudy day and 0.75 during a very sunny day.

Contrary, as it was mentioned previously, the most commonly measured value is the global horizontal radiation on the Earth's surface, whereas, clearness index is generally unknown. Therefore, an opposite approach is used, calculating clearness index by using known values of G and G_o.

To further divide global horizontal radiation G into its main components, the correlation of Erbs et al. (1982) is used,

$$\frac{G_d}{G} = 1 - 0.09\,k_T \qquad\qquad\qquad \text{for } k_T \leq 0.22 \qquad (3.11)$$

$$= 0.9511 - 0.1604\,k_T + 4.388\,k_T^2 - 16.638\,k_T^3 + 12.336\,k_T^4 \quad \text{for } 0.22 < k_T \leq 0.8 \quad (3.12)$$

$$= 0.165 \qquad\qquad\qquad \text{for } k_T > 0.8 \qquad (3.13)$$

where based on the value of k_T, specific equation is chosen to calculate the diffuse radiation G_d.

Lastly, prior to different models set up itself, as we still calculate in terms of irradiance on horizontal surface, meaning that the ground reflected radiation equals zero, the beam radiation can be calculated as follows:

$$G_b = G - G_d \qquad (3.14)$$

3.2.1 Perez model

As it was mentioned previously, from the broad scale of Perez models, Perez III, by Perez et al. (1990) was chosen, calculating the global solar radiation striking the tilted surface as follows,

$$G_T = G_b\,R_b + G_d\left[(1 - F_1)\left(\frac{1 + \cos\beta}{2}\right) + F_1\,\frac{a}{b} + F_2\sin\beta\right] + G\,\rho_g\left(\frac{1 - \cos\beta}{2}\right) \qquad (3.15)$$

where β stands for the slope of PV module, R_b, (Eq. 3.18), for the ratio of beam radiation on the tilted surface to beam radiation on horizontal surface, and ρ_g for ground reflectance, also called albedo. Furthermore, F_1 and F_2 are circumsolar and horizon brightness coefficients respectively, while terms a, (Eq. 3.16), and b, (Eq. 3.17), are solid angles corresponding to the circumsolar part, as seen from the inclined plane.

$$a = \max\left(0, \cos\theta\right) \qquad (3.16)$$

$$b = \max\left(\cos 85, \cos\theta_z\right) \qquad (3.17)$$

$$R_b = \frac{\cos\theta}{\cos\theta_z} \qquad (3.18)$$

Values of F_1 and F_2 may be obtained as provided below,

$$F_1 = \max\left(0, f_{11} + f_{12}\,\Delta + \frac{\pi\,\theta_z}{180}\,f_{13}\right) \qquad (3.19)$$

$$F_2 = f_{21} + f_{22}\,\Delta + \frac{\pi\,\theta_z}{180}\,f_{23} \qquad (3.20)$$

based on empirical coefficients displayed in Table 3.1, whereas Δ being calculated as follows.

$$\Delta = \frac{G_d}{G_o} \qquad (3.21)$$

Using the Table 3.1, appropriate coefficients are chosen based on so called bins of clearness ϵ. Its value is obtained using the equation below,

$$\epsilon = \frac{(G_d + DNI)/G_d + 1.041\,\theta_z^3}{1 + 1.041\,\theta_z^3} \qquad (3.22)$$

where DNI stands for Direct Normal Irradiance, being calculated as follows.

$$DNI = \frac{G_b}{\cos\theta_z} \qquad (3.23)$$

Table 3.1 Perez III, empirical coefficients

ϵ	f_{11}	f_{12}	f_{13}	f_{21}	f_{22}	f_{23}
$\langle 1, 1.065)$	-0.008	0.588	-0.062	-0.060	0.072	-0.022
$\langle 1.065, 1.23)$	0.130	0.683	-0.151	-0.019	0.066	-0.029
$\langle 1.23, 1.50)$	0.330	0.487	-0.221	0.055	-0.064	-0.029
$\langle 1.5, 1.95)$	0.568	0.187	-0.295	0.109	-0.152	-0.014
$\langle 1.95, 2.8)$	0.873	-0.392	-0.362	0.226	-0.462	0.001
$\langle 2.8, 4.5)$	1.113	-1.237	-0.412	0.288	-0.823	0.056
$\langle 4.5, 6.2)$	1.060	-1.600	-0.359	0.264	-1.127	0.131
$\langle 6.2, \infty)$	0.678	-0.327	-0.250	0.156	-1.377	0.251

3.2.2 HDKR model

To cross validate the results provided by Perez III model, Hay-Davies-Klutcher-Reindl model was employed. In order to calculate the global radiation on the tilted surface, two more factors have to be determined for HDKR model.

First, anisotropy index, A_i, being the measure of atmospheric transmittance of beam radiation, used to estimate the amount of circumsolar diffuse radiation.

$$A_i = \frac{G_b}{G_o} \tag{3.24}$$

And next, the horizon brightening coefficient, f, related to the cloudiness. Its value acknowledge the fact, that more of diffuse radiation comes from the horizon than from the rest of the sky.

$$f = \sqrt{\frac{G_b}{G}} \tag{3.25}$$

Finally, the global solar radiation incident on the tilted plane can be computed according to the equation below.

$$G_T = (G_b + G_d A_i) R_b + G_d (1 - A_i) \left(\frac{1 + \cos\beta}{2}\right) [1 + f \sin^3 \left(\frac{\beta}{2}\right)] + G \rho_g \left(\frac{1 - \cos\beta}{2}\right) \tag{3.26}$$

3.2.3 PV array power

Once the global solar radiation incident on PV surface is obtained, the power output of the photovoltaic array can be calculated. However, to account for the real-world performance of PV module instead of the performance under standard test conditions, a derating factor f_{PV} needs to be introduced. Its value regards effects of the soiling of the panels, wiring losses, partial shading, aging and so on, typically reaching values around 0.8. Utilizing this fact, a true photovoltaic array power output can be calculated as follows,

$$P_{PV} = Y_{PV} f_{PV} \left(\frac{G_T}{G_{T,STC}}\right) \tag{3.27}$$

where, Y_{PV} stands for the rated capacity of the PV module and $G_{T,STC}$ represents the incident radiation under standard test conditions, that being 1 kW/m^2.

Furthermore, the module temperature, if known, may be addressed separately, yet for the sake of simplicity, its influence will be included within the derating factor only.

3.3   Model verification

Based on the theory presented in the previous sub-chapter, Perez III and HDKR solar radiation models were build. To test the models performance and verify the results, it was necessary to provide the only input variable, global irradiance on the horizontal plane, sampled through the year. For that purpose, PVGIS-SARAH database was used.

PVGIS, Photovoltaic Geographical Information System is the part of EU Science Hub, under European Commission, which provides information about solar radiation and photovoltaic system performance. It contains various online tools and databases, while being publicly accessible. Previously mentioned PVGIS-SARAH database, being located there, accommodates, among others, also required measurements of global irradiance on the horizontal plane at a single hour time step. The only downside is, that the entire database stores only values through the years 2005 to 2016.

However, considering the size of PVGIS-SARAH data set compared to its "obsolescence", while also keeping in mind that the yearly variation of incident solar radiation is only within units of percent, available data were assumed satisfactory for the given purpose.

3.3.1   Input values

As the database covers Europe, Africa, most of Asia, and parts of South America, having a spatial resolution of 0.05° x 0.05° ($\sim$ 5 km), test location needed to be specified. For that, the position of latitude 50.094°, longitude 14.334°, and elevation 315 meters was chosen, representing site in the Czech Republic, Prague, district n.6.

Furthermore, the photovoltaic array was stated as fixed mounted, with rated capacity of 1 kWp, tilt of 38° and azimuth 0°. Additionally, regarding the mathematical model, the derating factor was set to 0.8 and ground reflectance to 20 %. Lastly, for the sake of PVGIS online tool, PV module technology was specified as crystalline silicon, system losses kept at a default value, 14 %, and mounting position defined "free standing", allowing air circulation around the panels, thus providing natural cooling.

To verify the models performance, data of all 12 years were utilized within the calculation, which not only provided a great sample for comparison of Perez III and HDKR results, however also allowed for a cross validation with PVGIS online tool, which calculates an average monthly and yearly PV power output based on whole PVGIS-SARAH data set.

3.3.2   Results comparison

The data predicted for given inputs were of two kinds, first, the total solar irradiance on a tilted surface, and second, the power output of the photovoltaic array. For the sake of initial representation of models performance, all predicted values through the years were compared to PVGIS online tool reports, those assumed to be "correct". (In further text referred as WEB data). As a result, a total irradiance absolute/relative error and a photovoltaics power output absolute/relative error were obtained.

Additionally, it is important to note, that the results are provided in Coordinated Universal Time, same as the data from PVGIS are sampled.

$$GT_{ERR-A} = GT_{PREDICTED} - GT_{WEB} \tag{3.28}$$

$$GT_{ERR-R} = \frac{GT_{PREDICTED} - GT_{WEB}}{GT_{WEB}} \tag{3.29}$$

$$PV_{P_{ERR-A}} = PV_{P_{PREDICTED}} - PV_{P_{WEB}} \tag{3.30}$$

$$PV_{P_{ERR-R}} = \frac{PV_{P_{PREDICTED}} - PV_{P_{WEB}}}{PV_{P_{WEB}}} \tag{3.31}$$

Since the entire data set contained 105 120 samples, out of which 50 205 were non-zero values, box plot was chosen for the evaluation purpose. In order not to compromise the plot significance, zero values were excluded.
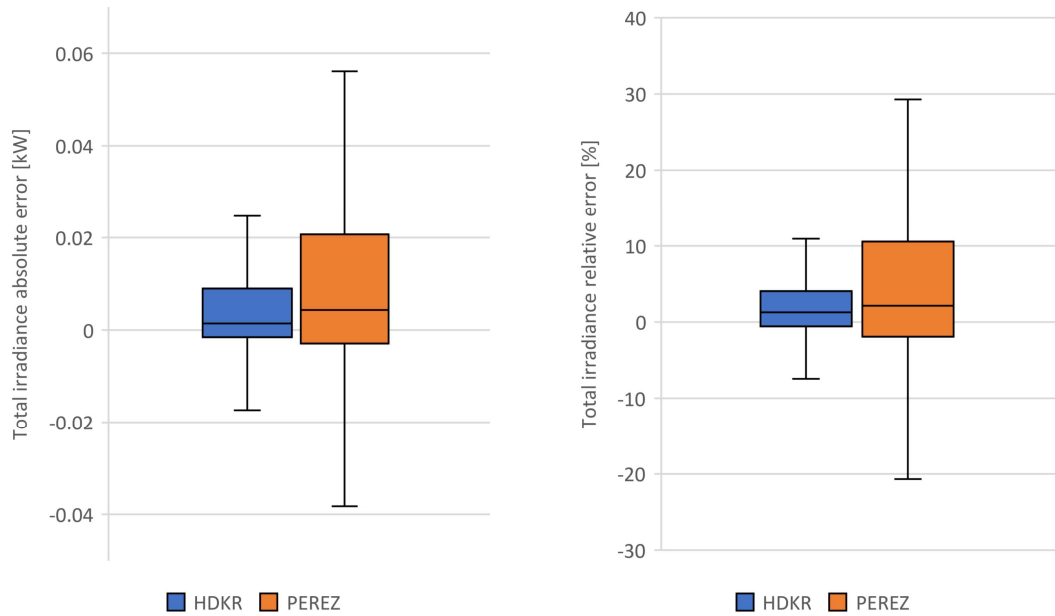

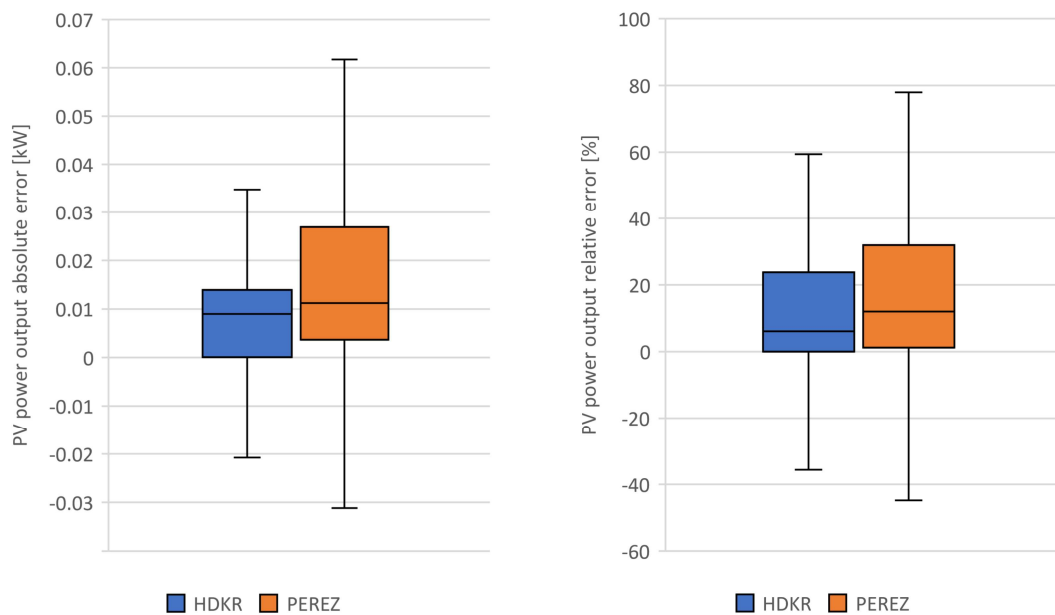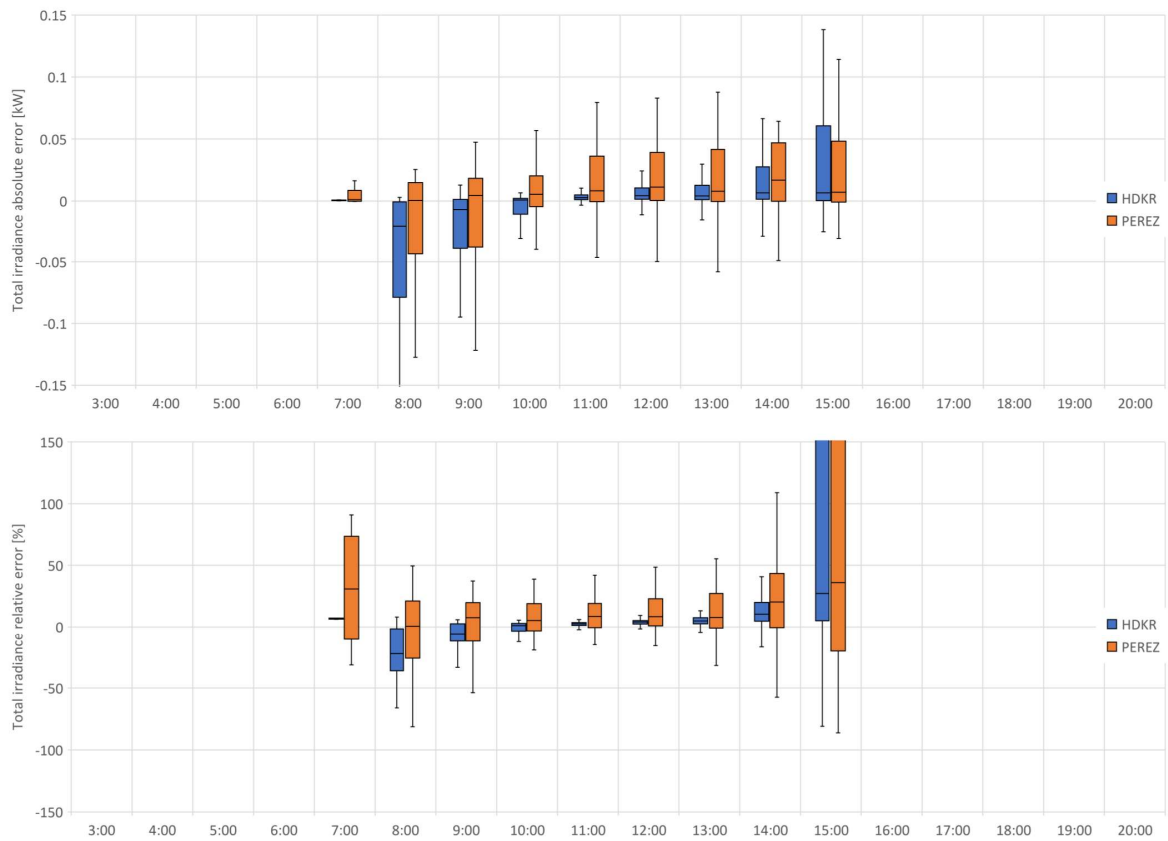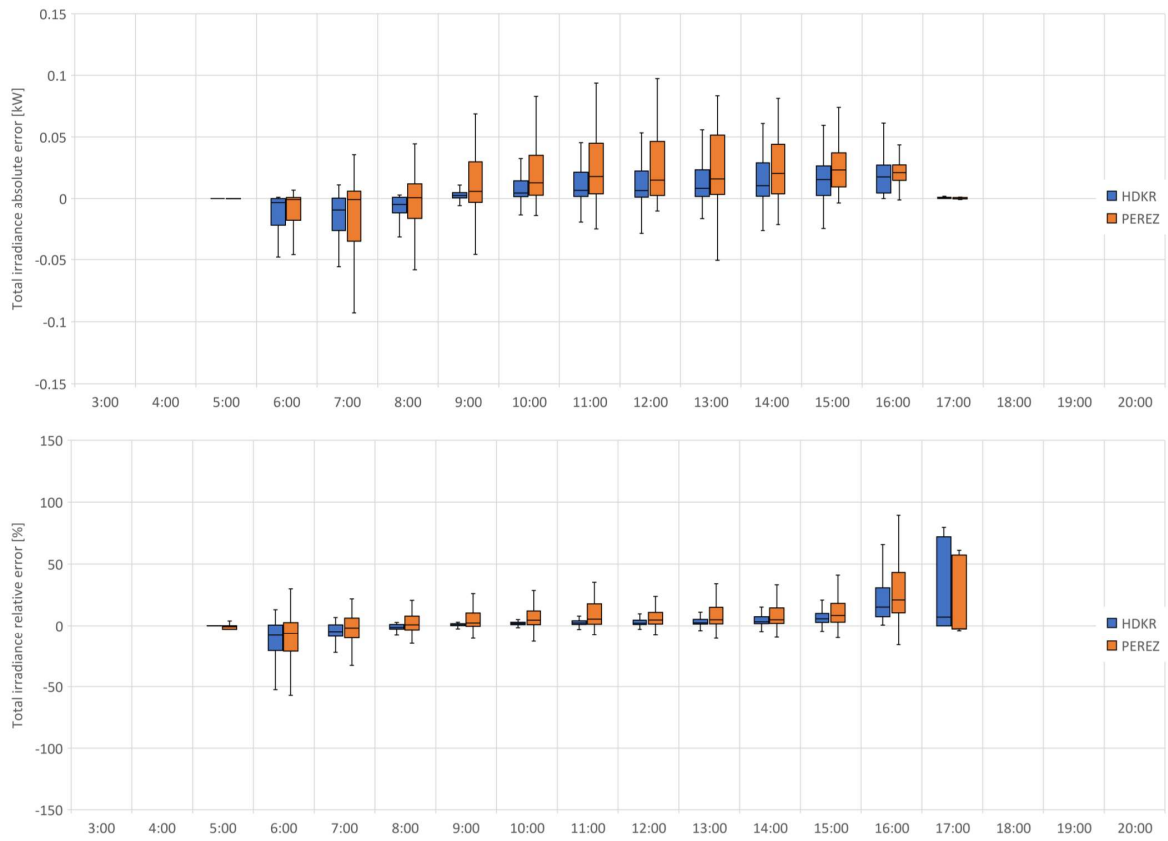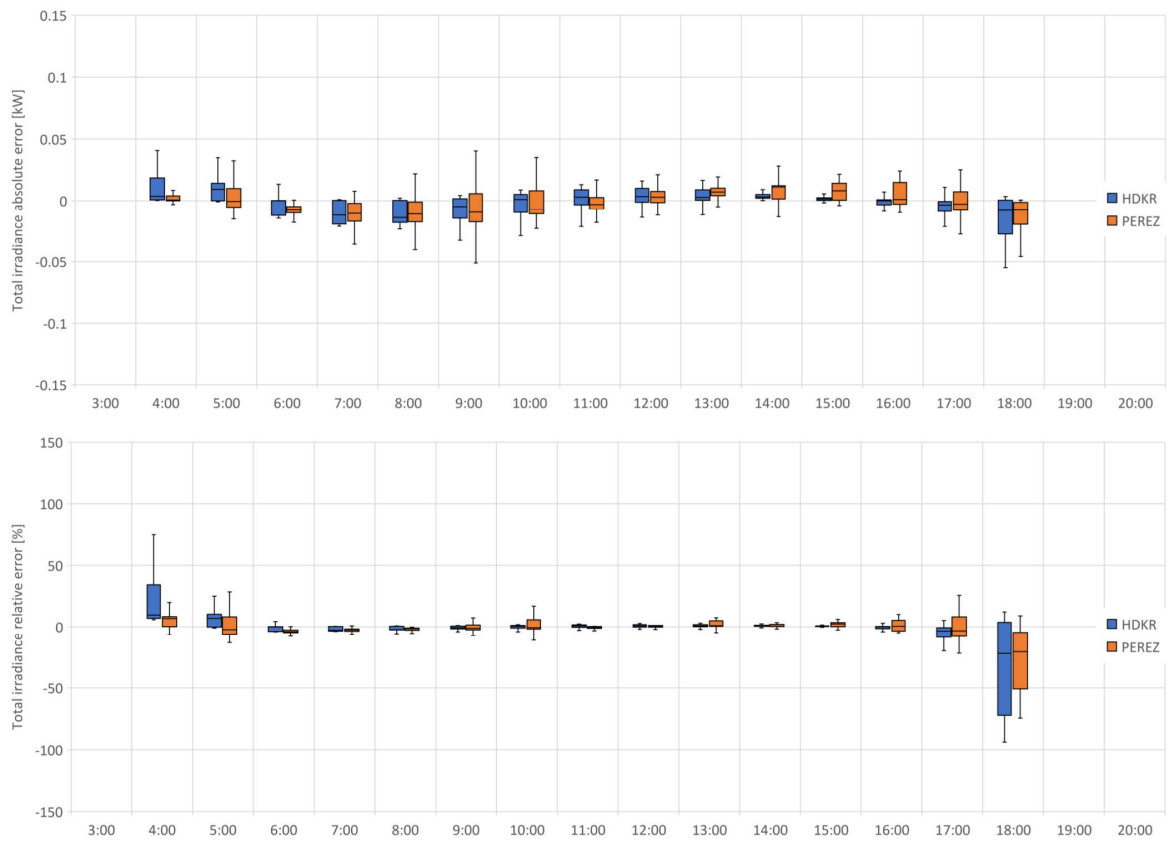Fig. 3.7: Total irradiance absolute (left) and relative (right) error

Fig. 3.8: Photovoltaics power output absolute (left) and relative (right) error

As it can be seen from both figures, (Fig: 3.7, 3.8), HDKR model provides generally closer fit to the WEB data, then PEREZ model. For both it can be also assumed, that the error from total irradiance prediction gets further expanded in PV power output prediction.

To better understand the error origins and effects on prediction precision, the complete data set was divided into months, while the box plot was compiled with regard to an hourly predictions error.

Fig. 3.9: Total irradiance absolute (top) and relative (bottom) error - January
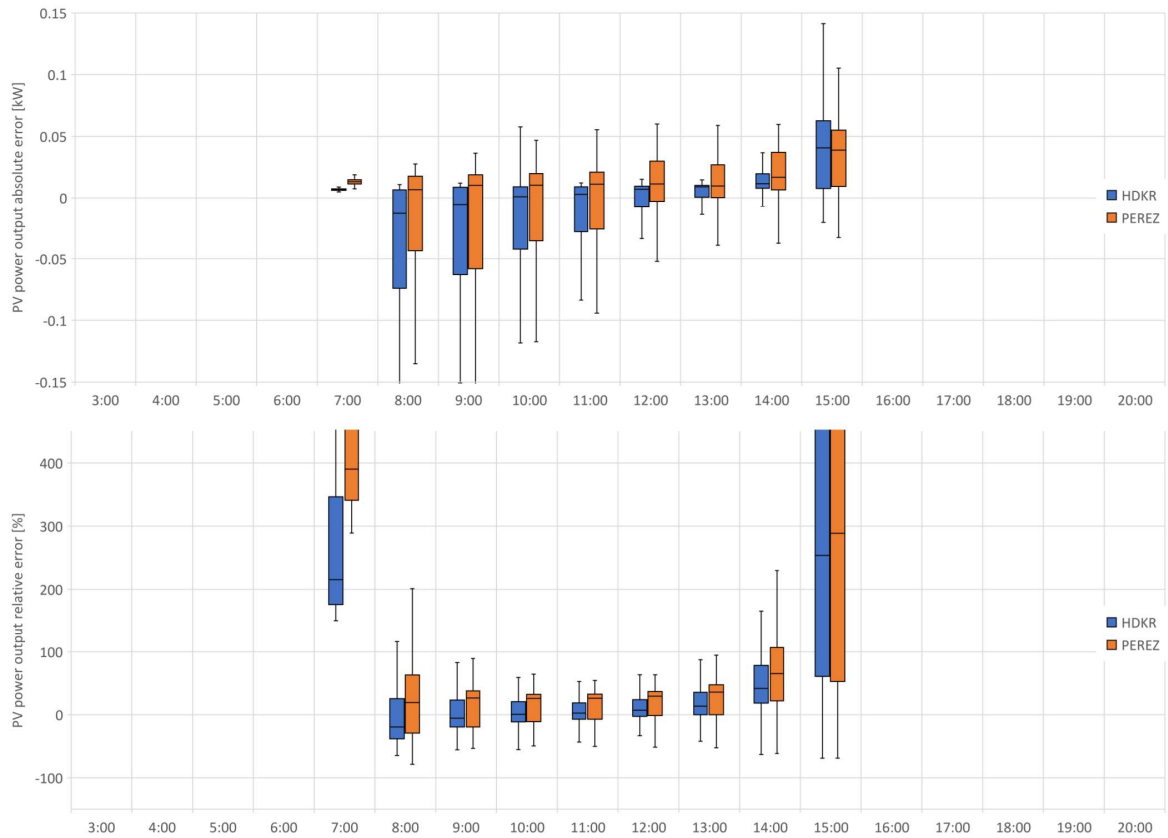
Fig. 3.10: Photovoltaics power output absolute (top) and relative (bottom) error - January

Fig. 3.11: Total irradiance absolute (top) and relative (bottom) error - March
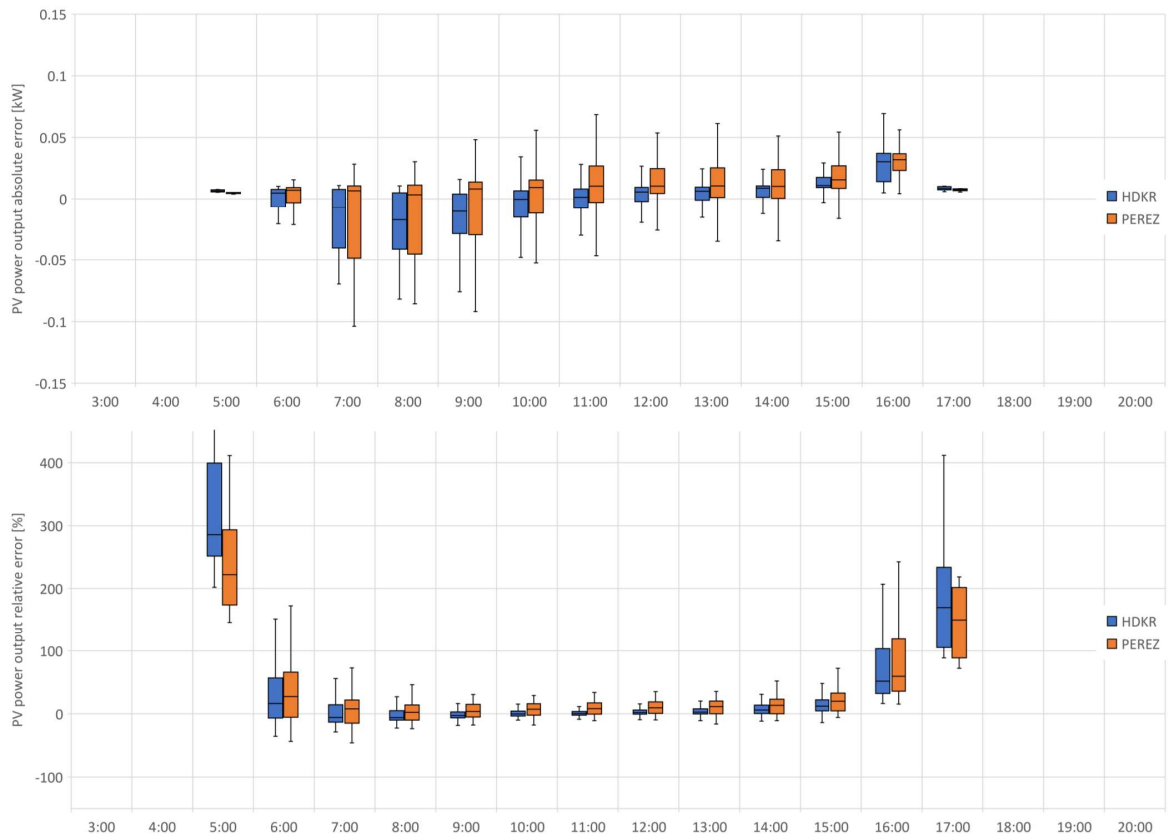
Fig. 3.12: Photovoltaics power output absolute (top) and relative (bottom) error - March

Fig. 3.13: Total irradiance absolute (top) and relative (bottom) error - June
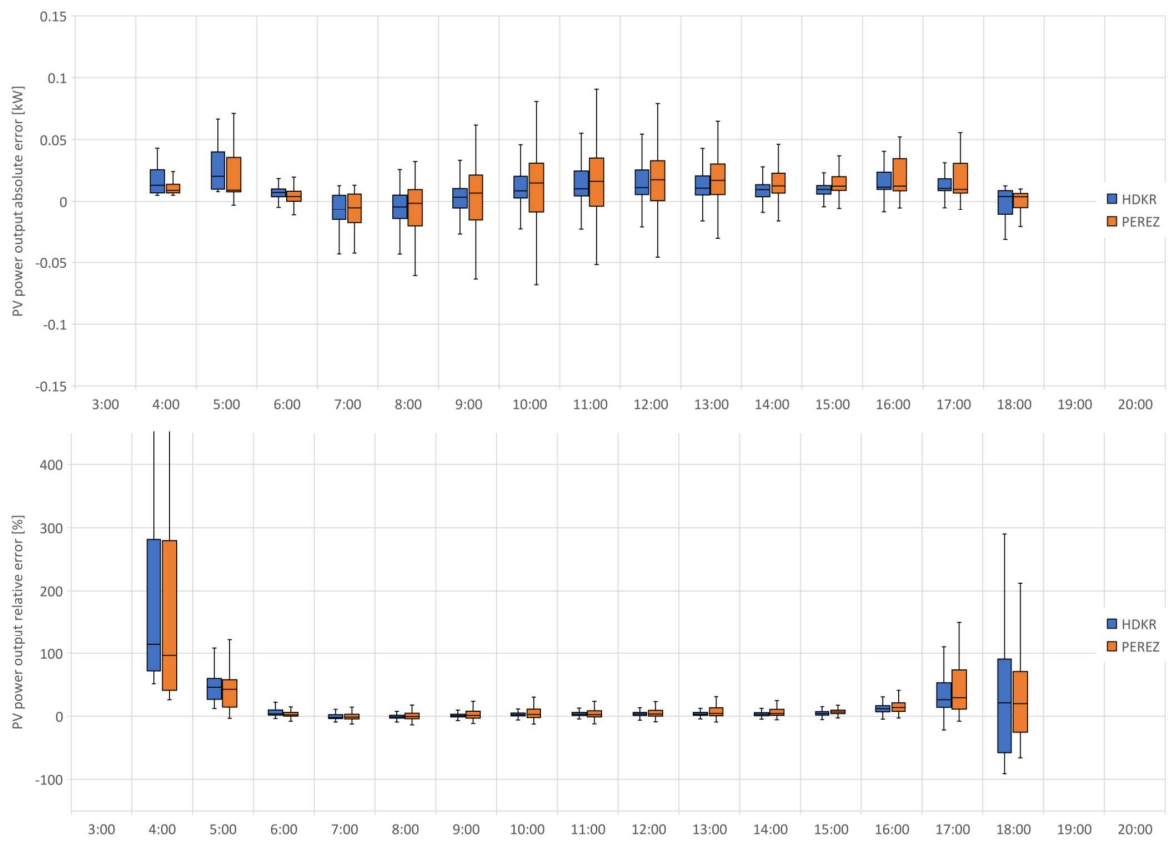
Fig. 3.14: Photovoltaics power output absolute (top) and relative (bottom) error - June

For the sake of clarity, only plots for January, March and June are presented in the chapter, whereas the whole set can be seen in the Appendix A. These three months, however, provide a great representation of models performance, during all three "periods". winter, transition and summer.

As it can be observed, given the axis scales are kept identical for all the months, during winter, the absolute prediction error is comparatively the greatest for both, the total irradiance and the photovoltaics array power output. Due to the low amount of solar radiation, also the relative error skyrockets of the range. Through the transition period and furthermore in summer, the error rate drops down, both in absolute and relative numbers.

What is common for all three data sets, is that the most recognizable relative errors occur during the sunrise and sunset, while during the forenoon, both models tend to under predict and during the afternoon, over predict. Overall, as previously implied from Figures 3.7 and 3.8, it can be noted, that HDKR model produces better estimates than PEREZ model, with regard to PVGIS online tool.

Despite the info-graphic value of the presented figures, it remains unclear, what are the actual cumulative errors and thus, whether the prediction provides reasonable data for further utilization. For that reason, aggregated plots for monthly and yearly offsets are presented next.
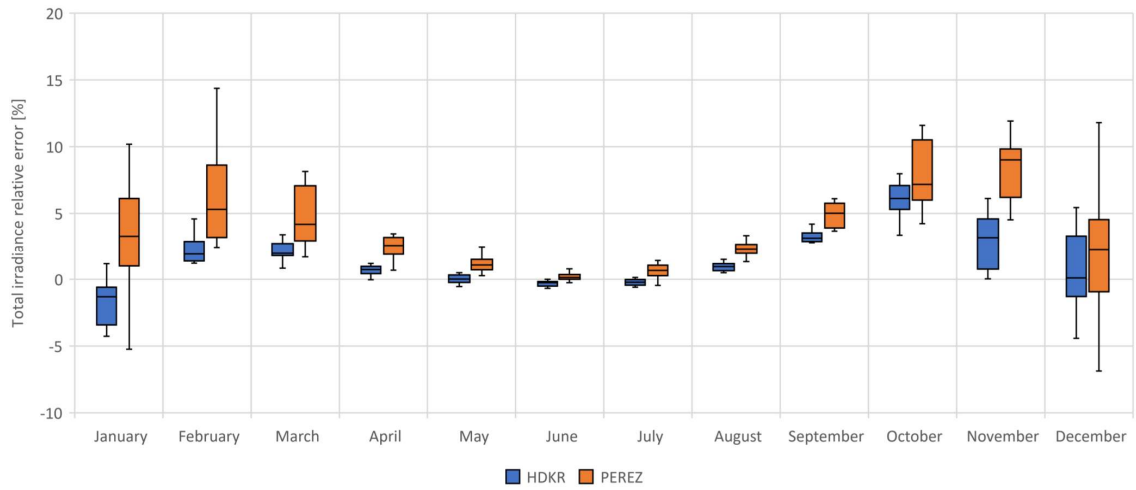
Fig. 3.15: Monthly total irradiance relative error
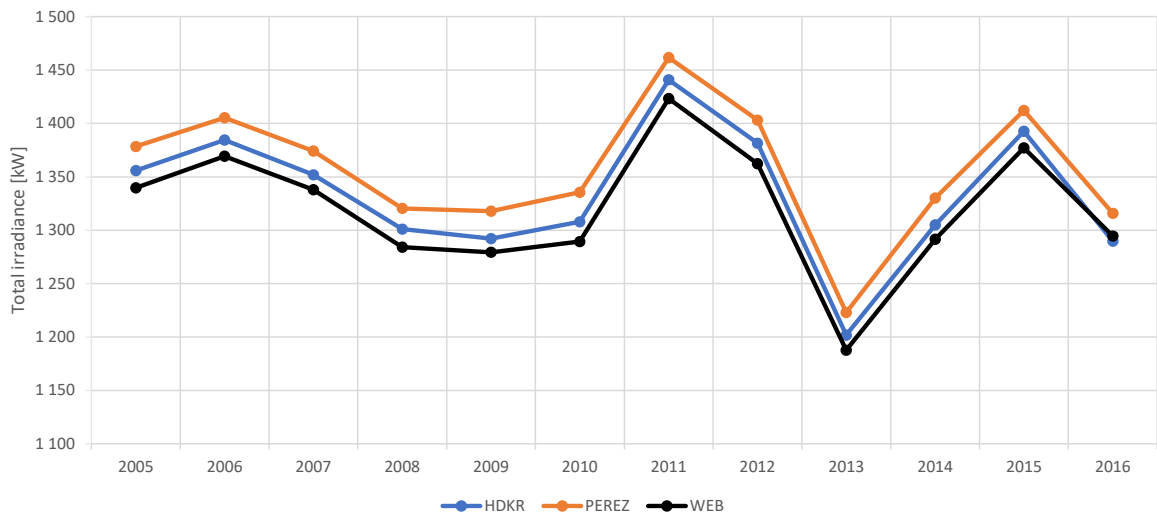
Fig. 3.16: Yearly total irradiance cross comparison
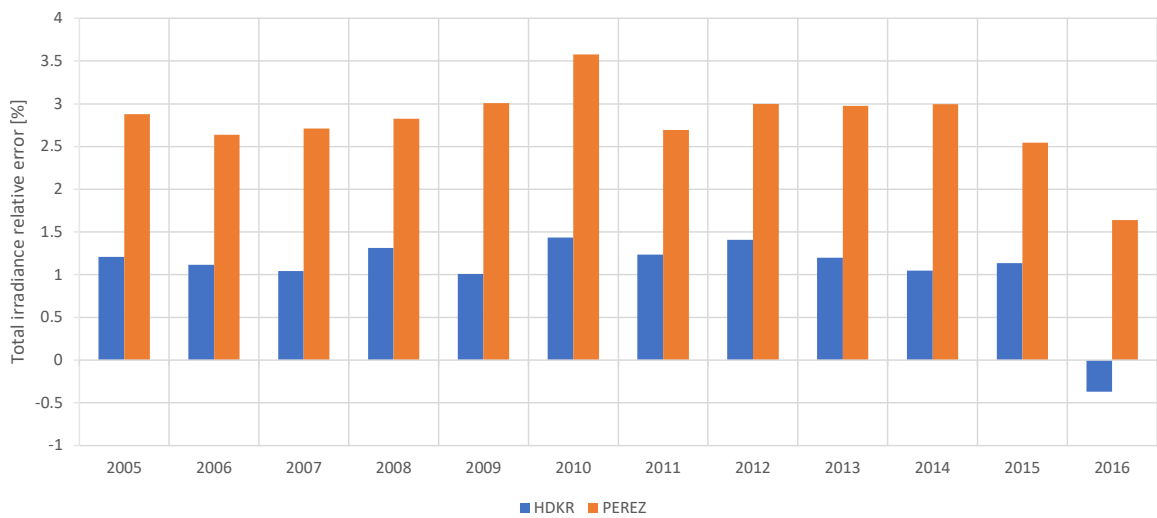
Fig. 3.17: Yearly total irradiance relative error
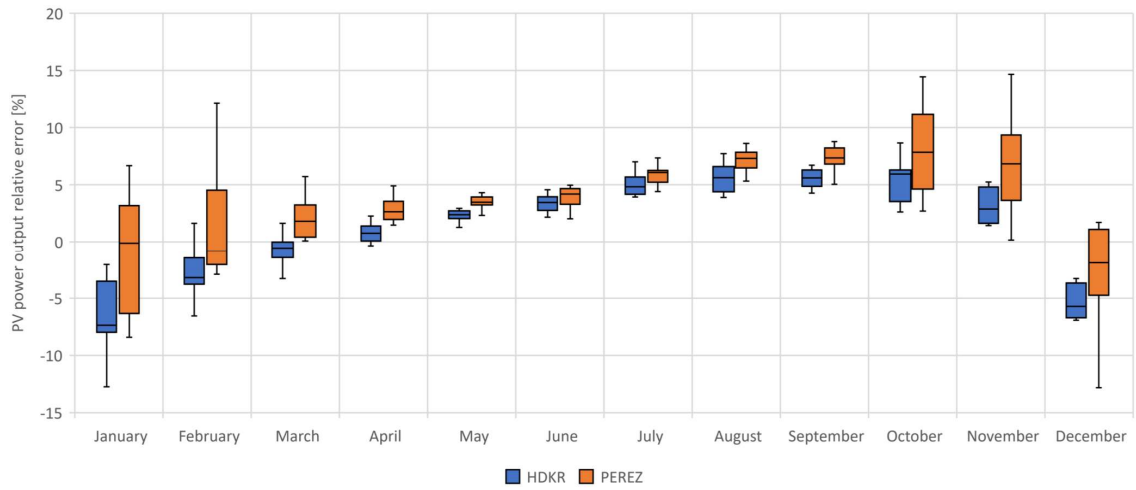
Fig. 3.18: Monthly photovoltaics power output relative error
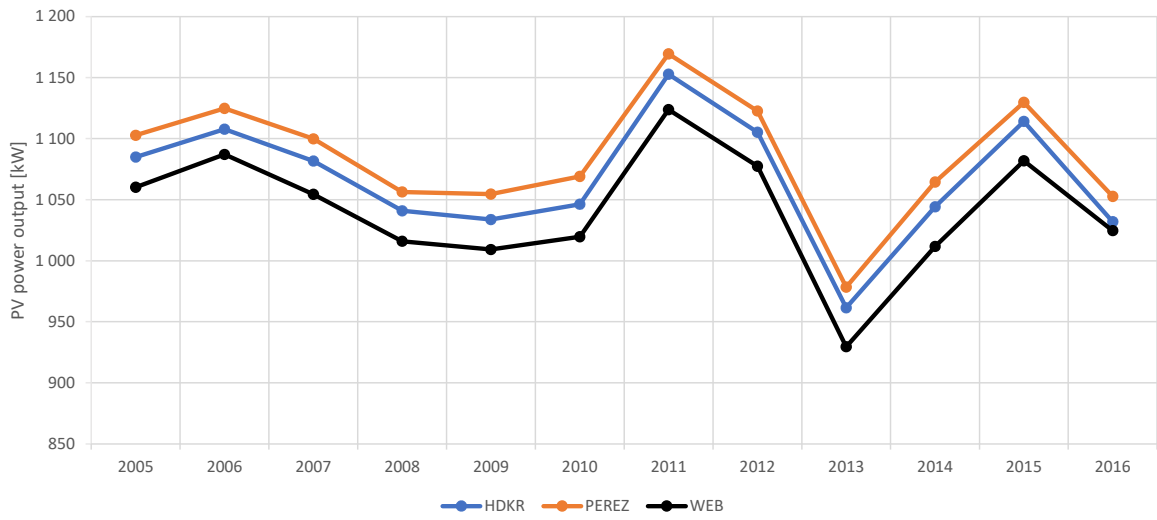

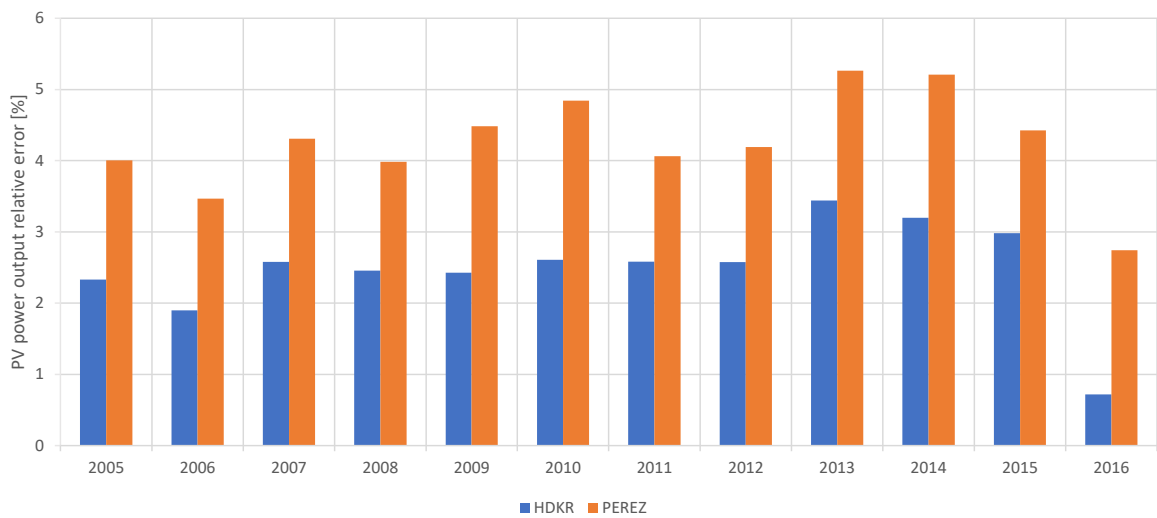Fig. 3.19: Yearly photovoltaics power output cross comparison

Fig. 3.20: Yearly photovoltaics power output relative error

As it can be deduced from the cumulative figures, despite of a slight error rate on the daily scale, both relative and absolute errors tend to be reasonably small in an bigger scope. Both models tend to over predict, with regard to WEB data, however in case of PEREZ model, that being around 2.8 % for total irradiance prediction and 4.3 % for photovoltaics power output, whereas in case of HDKR model, only 1.1 % relative error on a yearly basis for total irradiance prediction and 2.5 % error for PV power output prognosis.

Based on these results, both models are considered to perform fairly well and with acceptable prediction accuracy. Regarding the performance of both models, although HDKR initially being considered only as a cross validation platform, it turned out to produce better fitting data. For such reason, it was decided to utilize HDKR model instead of Perez III, for the following photovoltaics calculations.

3.3.3 HDKR modeling examples

Provided that bare solar irradaition and PV production curves account for only half of desired modeling outcome, missing the demand side load curves, achieved results of HDKR model are just briefly showcased.

Presented figures illustrate PV system of 1 kWp installed solar array, with tilt of $38°$ and azimuth $0°$, as specified in the Subsection 3.3.1.
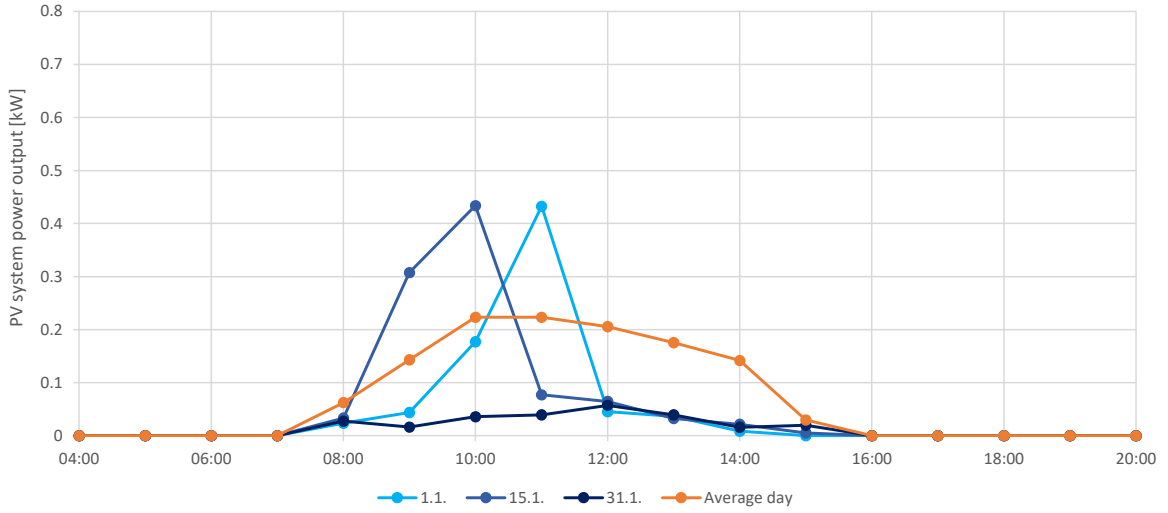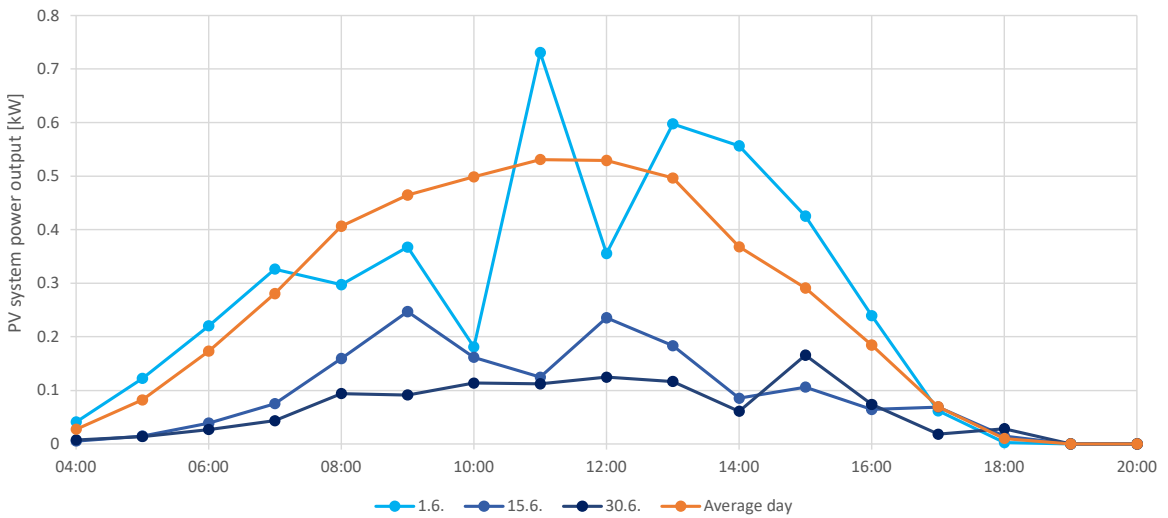

Fig. 3.21: PV system production curve - January

Fig. 3.22: PV system production curve - June

Chapter 4

Household consumption profile

Having the radiation model selected and its implementation and performance verified, energy "production side" of the photovoltaics system optimization model was established. Consequently, it was necessary to compile the energy "consumption side", thus the energy need profile of the average household through the year.

4.1 Daily load profile

Through the years, numbers of household energy consumption studies were performed for various reasons, all showing great similarity, once it came to household daily load profile. Generalized profile regarding the EU average household by Almeida et al. (2011) is provided below, yet comparable results were published by Andersen et al. (2017), Lee et al. (2014), Palmer et al. (2013) and many others.
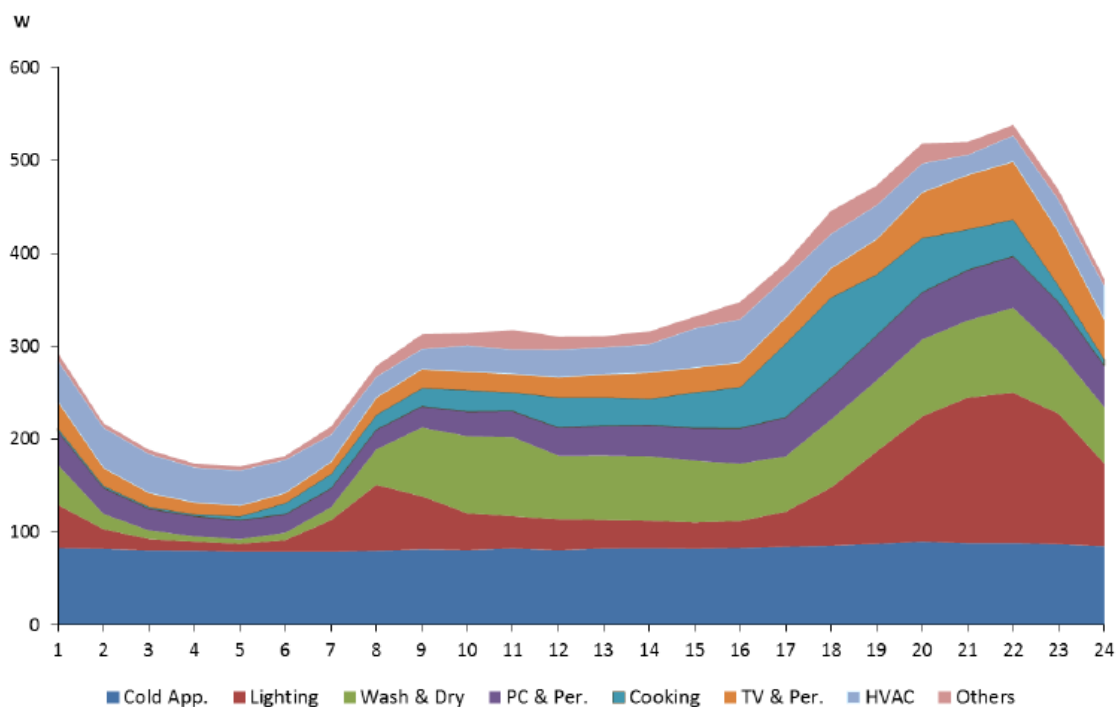
Fig. 4.1: Load profile of an average EU household
Almeida et al. (2011)

Figure 4.1 however represents only electricity related load profile, lacking a greater detail of hot water heating and space heating data. Such energy needs have to be also addressed, in order to obtain a complete household energy consumption profile.

Regarding a daily hot water heating, or rather domestic hot water (DHW) need, common patterns can be also found in various studies, Medved et al. (2019), Lutz (2017), Knight et al. (2007), showing a typical morning peak and later a smaller evening peak, as in Figure 4.2.
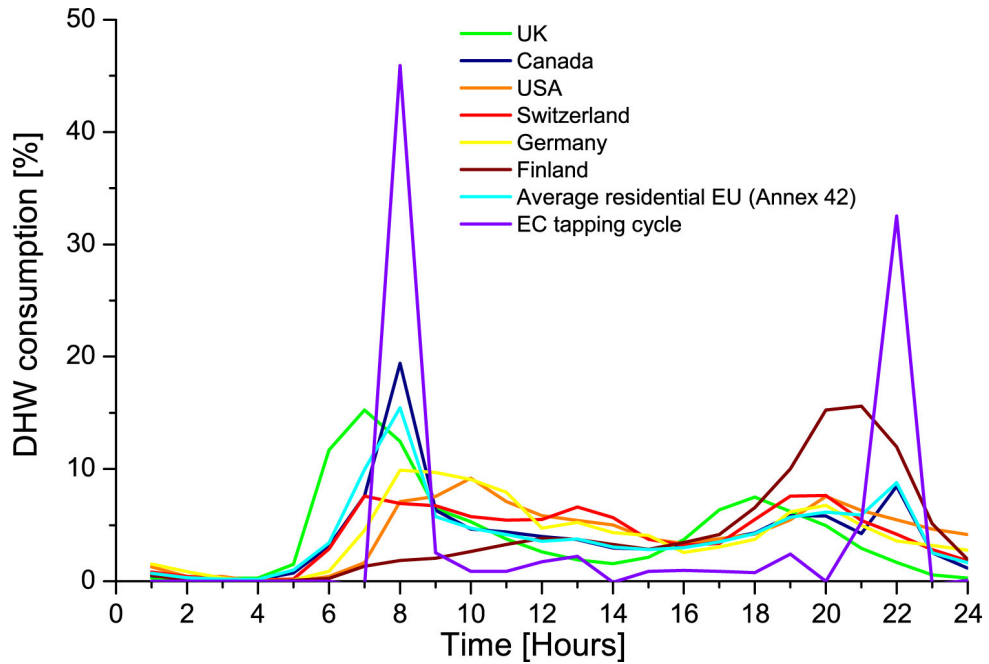

Fig. 4.2: Comparison of residential average daily DHW consumption profiles
Knight et al. (2007)

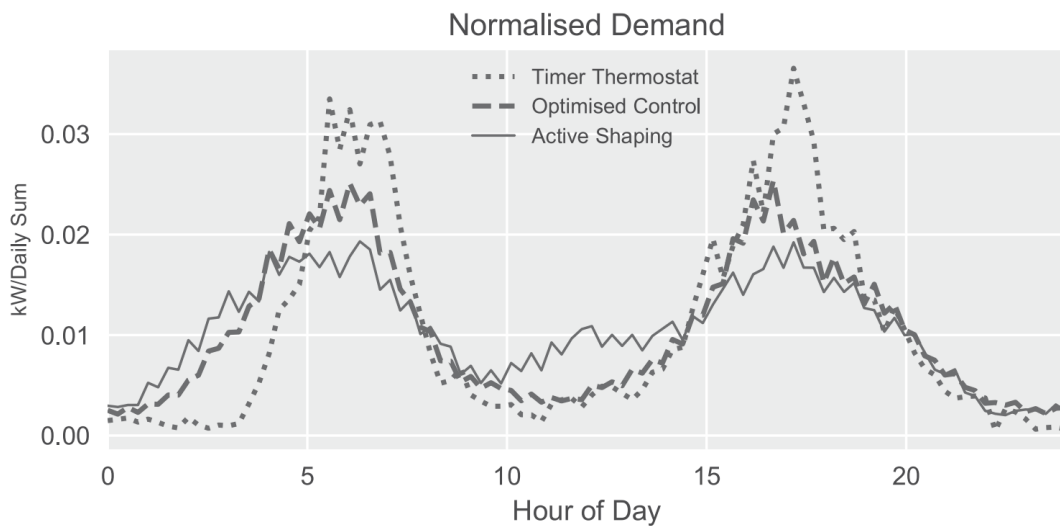The same can be applied to generic demand profile of residential space heating, presented e.g. by Sweetnam et al. (2018) or Palmer et al. (2013).

Fig. 4.3: Space heating demand profile
Sweetnam et al. (2018)

Based on an in-depth analysis of daily load profiles, an average household consumption profile was formed. In the model, energy needs of space heating, water heating, lighting, cooking, air conditioning, electric appliances and "other" are addressed separately, while "electric appliances" were subdivided into cold appliances, audiovisual, ICT and washing and drying. Such approach provides greater precision and especially an option for additional introduction of demand seasonality and other modifications.

For the sake of clarity, space heating and water heating will be further referred as to thermal loads, regardless of whether the actual heaters are powered by electricity or any other form of energy, e.g. by gas or solid fuels. Likewise, lighting, cooking, air conditioning, electric appliances and "other" purely electrical appliances, will be referred to as electrical loads.

Load curves were however made, by using relative values and thus it was necessary to get the absolute data of daily consumption. Provided that the case study location is specified in Prague, the Czech Republic, appropriate inputs were obtained from Eurostat - database of European statistics, ODYSSEE-MURE - database project containing detailed energy efficiency and CO_2-indicators with data on energy consumption, and the Czech Statistical Office.

Table 4.1 Average household yearly consumption in the Czech Republic, 2018

	kWh/dwelling	%
Space heating	14 070	69.57
Water heating	3 163	15.64
Cooking	1 291	6.38
El. appliances	1 198	5.92
Lighting	179	0.89
Air conditioning	~ 0	~ 0
Other	324	1.60
Thermal loads	17 233	85.21
Electrical loads	2 992	14.79

Given the presented values, a load profile on average day at Czech Republic household was made, while for the sake of simplification, the difference between the workdays and weekends was neglected.

4.2 Demand seasonality

Considering that every day of the year is an average day, no matter, whether it is a workday, weekend or a holiday, inevitably affects the precision of modeling, yet the effect is not marginal. On the other side, seasonality effects on the residential sector energy demand are of a great importance and thus have to be included.

In order to account for the demand variability during a year, data from an extensive survey by Zimmermann et al. (2012) on the topic of the domestic electrical product usage were utilized, seconded by works of Atanasoae (2020), Watson et al. (2019), Rehman et al. (2016) and Leeuwen et al. (2015).

Cold appliances
Seasonality effect on the consumption

Lighting
Seasonality effect on the consumption
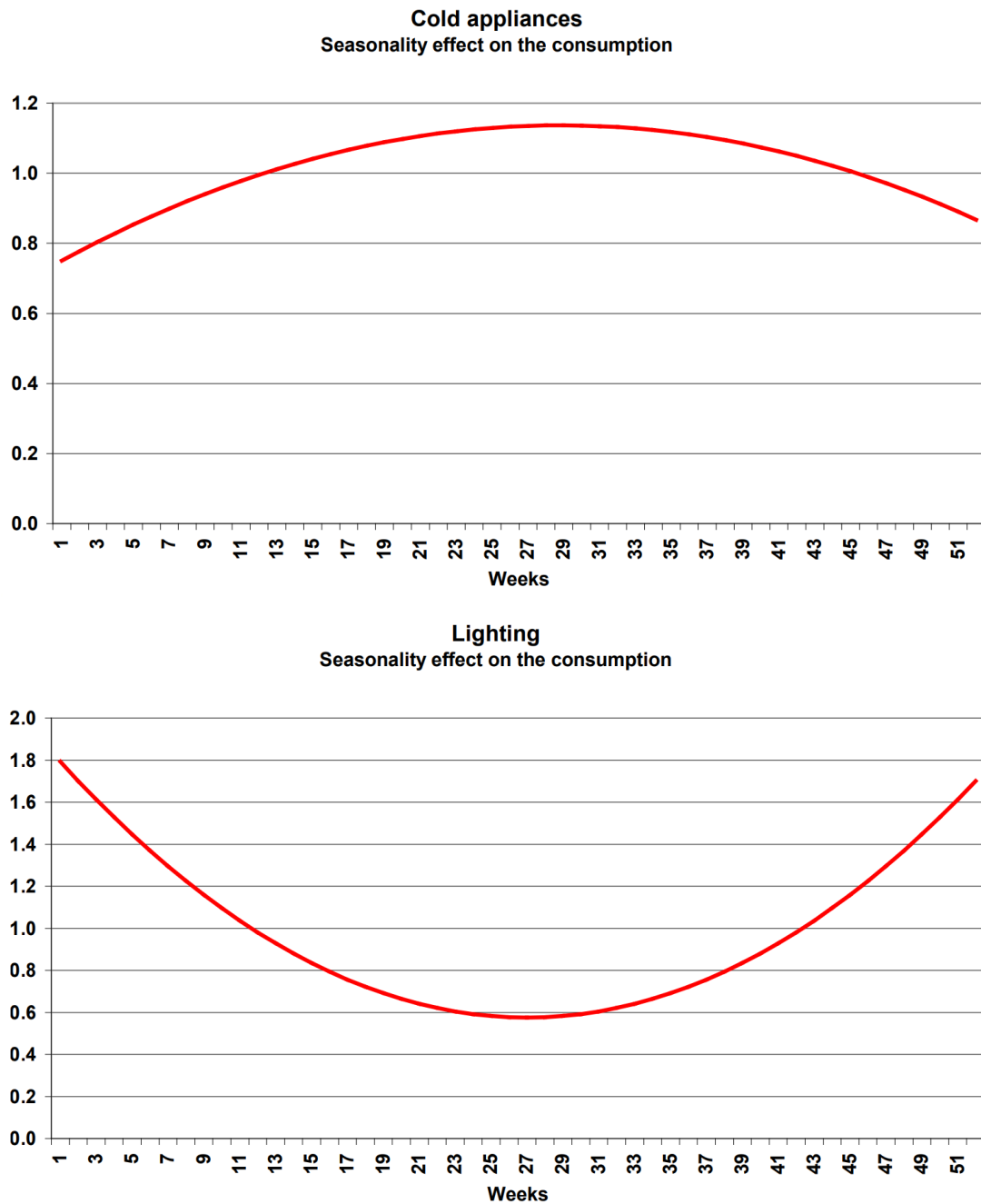
Fig. 4.4: Examples of relative seasonality effects; Zimmermann et al. (2012)
(No seasonality would result in straight line at vertical axis value = 1)

4.3 Energy needs modeling

Having both, a daily load profile and seasonality researched, a household energy demand model was built. As a combination of household energy needs through the whole day and seasonality effects, yearly load profile of an average dwelling on hourly basis was obtained.

Resulting plots for winter, transition, and summer period can be seen in the next pages, represented by months - January, April, and July.

In the Figure 4.5, the total demand for energy may be examined, where for winter and a transition period, the space heating needs are dominating. That is not the case of the last plot, illustrating the summer period.

Not to completely overlook the smaller additions to the load profile, in the Figure 4.6, the influence of space heating is ignored, while in Figure 4.7, both, space and water heating imprint is avoided.
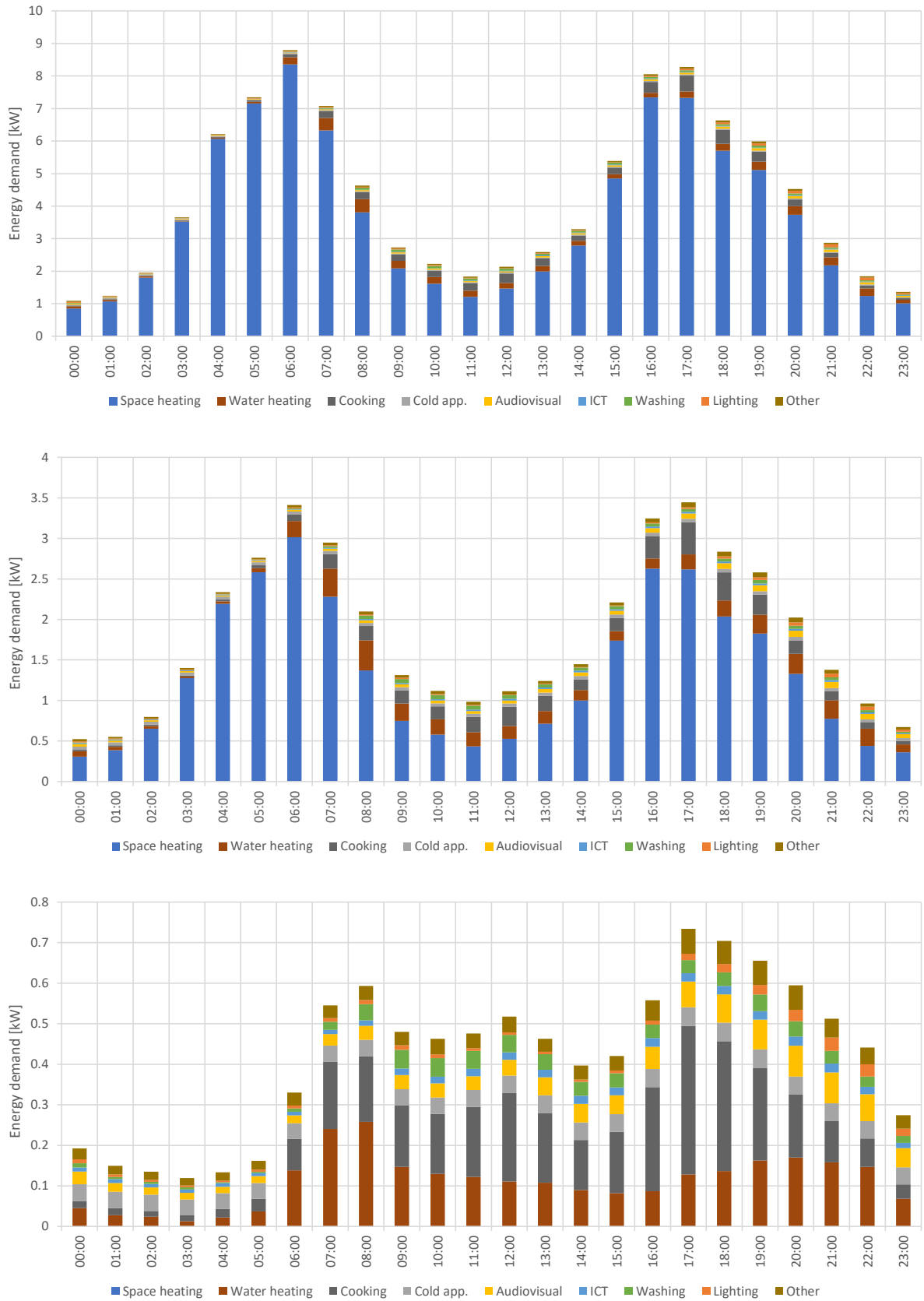
Fig. 4.5: Household energy demand - January (top), April (middle), July (bottom)
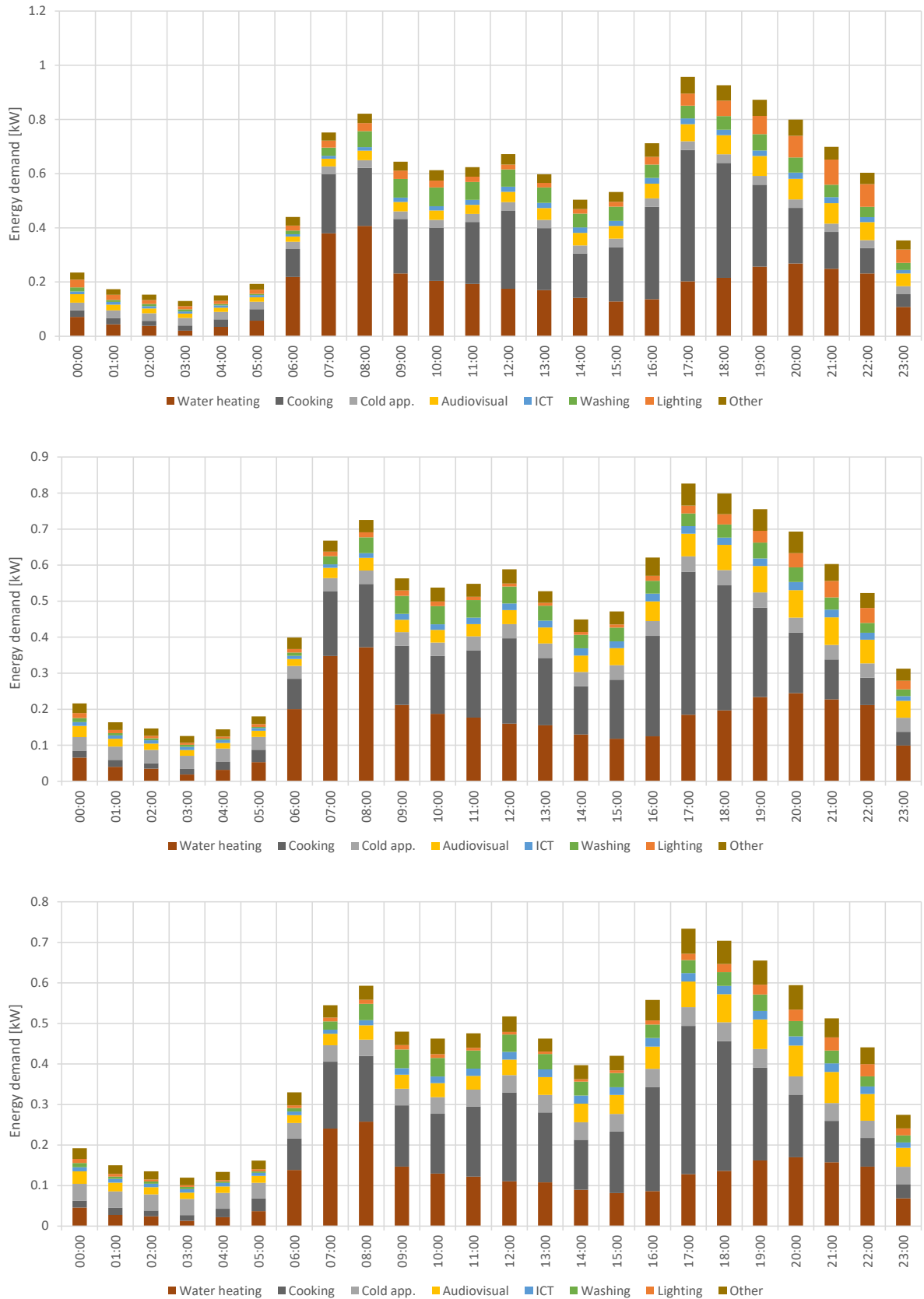
Fig. 4.6: Household energy demand, neglecting space heating
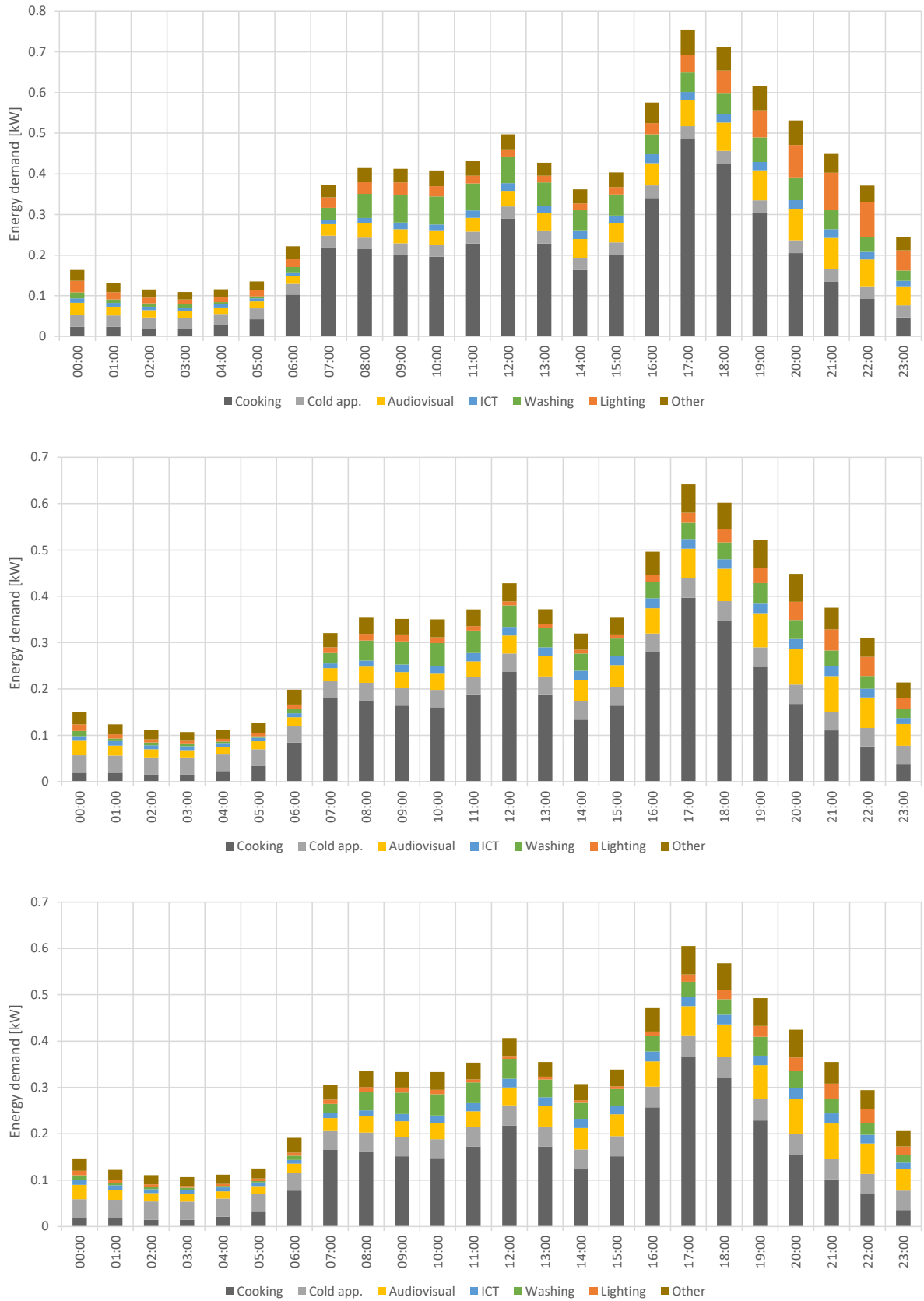- January (top), April (middle), July (bottom)

Fig. 4.7: Household energy demand, neglecting space and water heating
- January (top), April (middle), July (bottom)

Chapter 5

Optimization modeling

Having both radiation model and household consumption model implemented, therefore knowing, PV systems yields and household energy needs in a year, a desired model for photovoltaics system optimization could be made.

5.1 Calculation approach

The general idea behind a model setup is fairly simple. As input data, average household is introduced, requiring energy to cover its electrical and thermal needs. No matter what is the origin of such energy, the demand has to be met. Considering various options used in a residential sector to fulfill energy requirements, three different alternatives were taken into account.

- Household utilizing electricity only for cooking, cold appliances, audiovisual, information and communication technologies, washing and lighting, whereas both water and space heating are covered by either gas, a solid or liquid fuel burner. In such case, electricity consumption is quite low and thus it comes at a single tariff, having the same price in the whole day. Further on, this variant will be referred to as **V1_El.App**

- Household utilizing electricity for common electrical loads (same as above), plus also using an electric accumulation water heater - electric boiler. Electricity is billed at a two-tariff rate, while boiler operates only during a low tariff (LT), active 8 hours a day. Space heating is still covered by either gas, a solid or liquid fuel burner. **V2_DHW**

- Household utilizing electricity for common electrical loads, water heating and space heating. For the sake of simplicity, water heating and space heating is assumed to be a single system, sharing both, a heating element and an accumulation tank. This variant is further subdivided based on electricity tariff type.

  - Accumulation heater, preparing heat prior to its consumption. Electricity billed at two-tariff rate, heater operates only during the a low tariff, active 8 hours a day. **V3.1_DHW+SH**

  - Accumulation heater, same as in previous option, yet the low tariff is active 20 hours a day. **V3.2_DHW+SH**

In the calculation, no flow-through heaters are included. The reason for that is the operational nature of the mentioned heaters, preparing hot water directly in time of demand. Such regime is incompatible with the modeling resolution, as the time scope of matching photovoltaic surplus power against energy needs of flow through boilers would allow for even surpluses, that would in reality occur at dissimilar times to boilers energy demands, to be matched together within a single 1-hour modeling step.

The choice of the various alternatives and complementary electricity tariffs was made according to current situation in the Czech Republic, representing:

- Tariff D02d, without LT, for common electrical appliances.

- Tariff D25d, 8 hour LT, for district hot water boilers with accumulation.

- Tariff D26d, 8 hour LT, for space (and water) heating with accumulation.

- Tariff D57d, 20 hour LT, for space and water heating using hybrid heaters or heat pumps.

Through the countries, both the systems and billing tariffs may differ. In such case, the model input values would need to be modified.

Also, the distribution of low tariff periods in the day might vary, often switching between a low tariff (LT) and a high tariff (HT) on 30-minute basis. Provided that both radiation and household consumption models work with 1-hour time step, LT distribution was adjusted.

Table 5.1 Tariffs used within the model, low tariff distribution

	00:00	01:00	02:00	03:00	04:00	05:00	06:00	07:00	08:00	09:00	10:00	11:00
8-hour	LT	LT	HT	LT	LT	LT	HT	HT	HT	HT	HT	HT
20-hour	LT	LT	LT	LT	HT	LT	LT	LT	HT	LT	LT	LT

	12:00	13:00	14:00	15:00	16:00	17:00	18:00	19:00	20:00	21:00	22:00	23:00
8-hour	HT	HT	HT	HT	LT	LT	LT	HT	HT	HT	HT	HT
20-hour	LT	HT	LT	LT	LT	LT	LT	HT	LT	LT	LT	LT

Now that the alternatives of household energy systems are set, it is important to focus on how they are powered. Initially the dwelling is expected to be built without photovoltaics power station in mind, thus designed to satisfy its energy needs in another way. From that point of view, any electricity later supplied by photovoltaic system is considered an extra.

Speaking of PV system, in the whole study, always a set of solar panels, battery storage and PV inverter is considered.

5.1.1 Energy flow

If we now presume a photovoltaic power plant to be additionally installed to the household infrastructure, it is important to set the rules, so that the solar electric power is utilized efficiently. For that reason, it is important to prioritize its use, and thus the model logic goes in the following fashion.

At the beginning, the electrical demand and PV power output is estimated.

1. If PV power output is greater than the demand, the electric loads demand (no heaters) is covered and surplus energy is

   (a) used to charge the battery storage, unless it is full or the charging power would be above the maximum allowed charging rate. In such case, the surplus energy is

   (b) used to charge the heat storage, if present, unless it is fully charged (heated to the maximum temperature). In case that none of the foregoing is applicable, the surplus energy is

   (c) send to the grid.

2. If PV power output is lower than demand, all PV electricity is directly utilized, while electricity still needed is

   (a) covered from the battery, unless it is empty or the discharge current would be above the maximum allowed discharge rate. In such case, demand is

   (b) covered from the grid, no matter the electricity tariff.

In parallel, thermal demand is examined.

3. If an accumulation heater is present, the heat demand is covered from a storage tank, while afterwards, if it was not fully charged by PV surplus power,

   (a) if a low tariff is active, the heater is turned on, to recharge the accumulation capacity, using electricity from the grid. In another case,

   (b) if a high tariff is active, the heater remains off.

Side notes:
System is considered to be single phase, neglecting the possibility of asymmetric load of individual phases of a three-phase system.
System model is designed in a way, that accumulation heater has suitable power output, so that during the year, there is always minimal 10 % of accumulation capacity reserve. That apply for the settings prior to photovoltaics power station installation.
Heat storage capacity is denoted purely in kilowatt hours, thus being independent of space and water heating systems temperatures.
All energy demands are covered at 100% efficiency, ignoring conversion and dissipation loses of electrical and thermal systems. The only exception is battery storage charging and discharging, of which the efficiency is set as an input parameter.
Regarding the aforementioned, even thermal systems for **V3.2_DHW+SH** are assumed to work at 100 % efficiency, despite the fact that in case of using heat pumps, the coefficient of the performance is always higher than 1, often in the range of 3 to 4.
No battery stored energy is used for heating purposes.
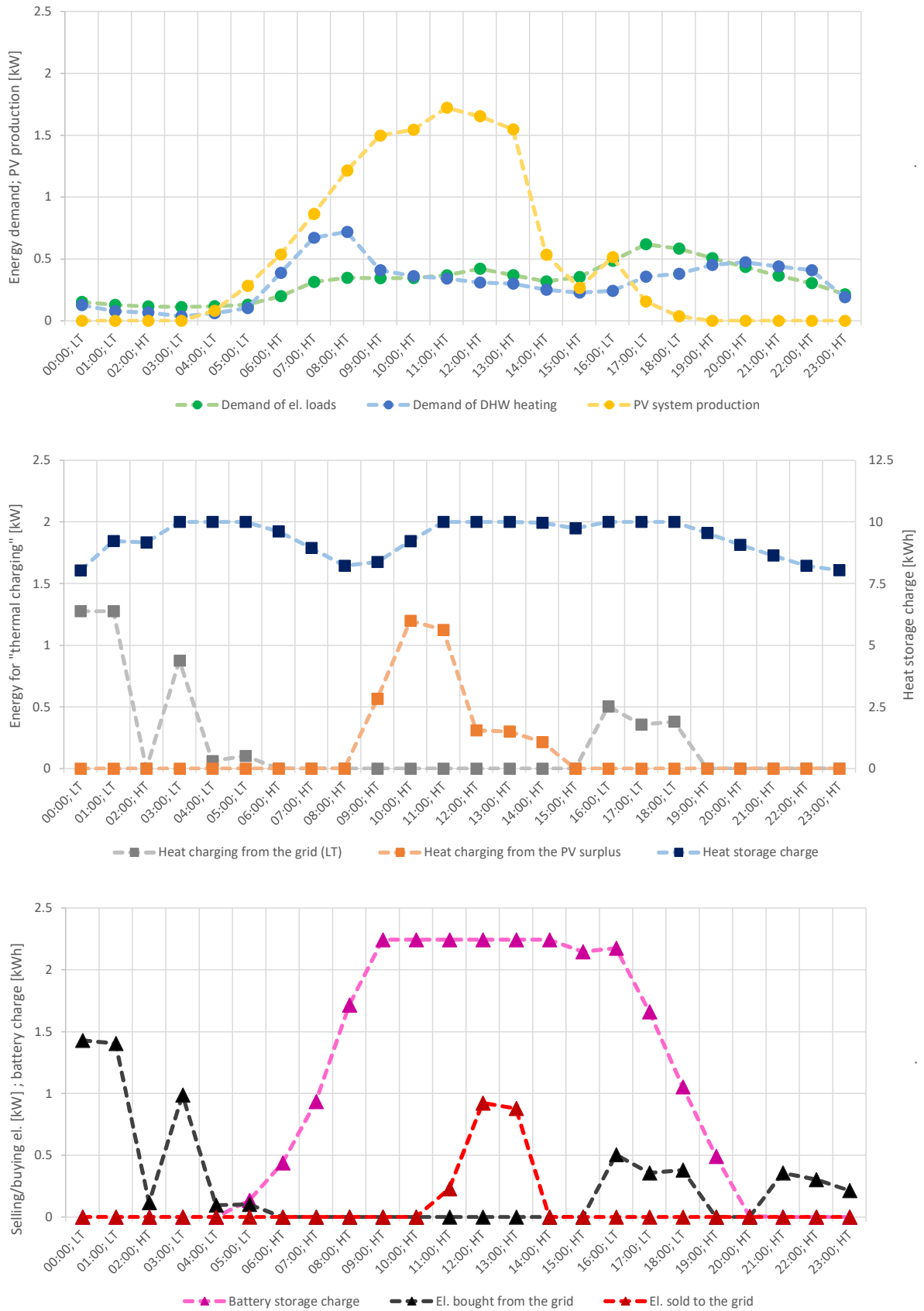Discharging battery is independent of the electric tariff.

Fig. 5.1: Model load curves and energy flows visualization

In order to better illustrate energy flows logic, graphs showing the real operation of the model are presented in Figure 5.1. Provided charts refer to photvoltaic system for household type **V2_DHW**, having the specifications of 2.24 kWp solar array, 2.80 kWh battery storage, 10 kWh heat accumulation tank and 1.28 kW heater. The data originate from the day in mid June.

Note: Both the state of the battery storage and the state of heat storage are plotted for the end of computational step. Equal discharging and recharging the battery or the heat storage may happen within single step, resulting in no visual change in plotted value. E.g. data points 11:00 to 13:00 for the accumulation tank charge.

Flowing the aforementioned logic, the case of 1.(a) can be seen from the time points 04:00 to 08:00. The PV production outweighs the demand of electrical loads and thus the surplus energy is used to charge the battery storage.

Coming to the case 1.(b), once the battery storage is full, PV surplus electricity is used to run the heater despite the active HT. Data points 09:00 and 10:00.

Furthermore, if the PV surplus energy can not be used either for heat storage or the battery storage charging, excess energy is send to the grid. The case 1.(c), data points 11:00 to 13:00.

Regarding the case 2.(a), data points 15:00 and 17:00 to 20:00 can serve as an example. For all, PV production is insufficient to cover the demands of electrical loads and thus the battery is discharged to supply the electrical loads.

Speaking of the case 2.(b), the best example can be noticed at data points 21:00 to 23:00. No PV energy is produced and the battery storage is drained. Under such conditions, electricity to cover the demand of electrical loads is obtained from the grid.

Lastly the thermal demand case 3.(a) can be recognized from the data points 00:00, 01:00, 03:00 to 05:00 and even 16:00 to 18:00. Complementary to that, the case 3.(b) can be seen at data points 03:00, 06:00 to 08:00, 15:00 and 19:00 to 23:00.

From the visualization, it is also clear, that different cases may occur together during single step. For example 1.(b) and 1.(c) at data points 11:00 to 13:00.

5.1.2   Design boundary conditions

Having the study area in the Czech Republic, especially, regulations to be eligible for a governmental subsidy need to be followed. Even though the gain of a government support is not a necessary condition for photovoltaic power plant operating permit, it is advantageous to focus in such direction. The logic behind is that the subsidy covers up to 50 % of the expenditure, which significantly affects the financial return of the system. For this reason, it is irrelevant to pay attention to systems ineligible for subsidies, given that compared to the subsidized systems they have no chance to succeed.

Speaking of the governmental directives, aside from obligations of the applicant and requirements on PV system efficiency, the most notable ones are

- to utilize at least 70 % of the theoretical PV system production for self-consumption, while

- the battery capacity needs to be at least 1.25 kWh per each kWp installed, in case of lithium based batteries, SFŽP (2020).

5.1.3   Photovoltaic system optimization

Based on the calculation logic, an entire model was compiled, providing an option for an analysis of various photovoltaic and household systems settings. For the purpose of a legitimate cross comparison, PV power utilization efficiency was chosen, referring to how much of "solar electricity" is utilized for household needs, out of all electricity produced.

The computation itself commence with an iterative sequence, (**Calc.1**), figuring the optimum battery storage capacity, for given solar array size and utilization efficiency. Within this initial step, only electrical loads demand of common appliances is taken into account. Thermal needs are not included. Such PV sizing approach corresponds to setup **V1_El.App**.

As a result of the simulation, best numerical estimate of a battery pack capacity, ideal for given conditions is obtained, which however, does not necessarily corresponds to the obtainable battery sizes on the market. Similarly, a solar array nominal power output may not match the realistically assemblable power output of the solar array. In such case, in reality, a next higher variant should be chosen.

Example: Given the annual consumption of electrical loads, 2 992 kWh, as presented in Table 4.1, and input solar array size, e.g. 2.992 kWp, PV power output and household electrical loads demand is determined, based on which the battery storage size is calculated, so that the utilization efficiency of the entire PV system match desired value, e.g. 70 %. Surplus energy is either stored in the battery or sold to the grid.

Next, utilizing the previously obtained battery pack size and the same solar array size, another calculation loop is executed, (**Calc.2**). The logic stays the same, with the exception, that the photovoltaic surplus energy can be used for charging the heat accumulation tank, while also two-tariff billing is practiced. Such approach corresponds to variants **V2_DHW**, **V3.1_DHW+SH** and **V3.2_DHW+SH**.

Provided that distinct dwellings, may operate diverse heating systems, having various sizes of heat storage tanks and included heaters, five different variants were used for every simulation example. Initial condition for any heater-accumulation set was to ensure minimal 10 % of heat storage reserve through the year, based on which, the individual cases were put together.

Once again, as a result of simulation, best numerical estimate of a heater and accumulation tank combination is obtained, ideal for input conditions. That, however, does not necessarily corresponds to the realistically obtainable products on the market.

Entire **Calc.2** is yet a bit more complex, than the initial one and therefore it is further subdivided into **Calc.2.1** and **Calc.2.2**.

First, the heater system to cover the household thermal loads is optimized as an stand-alone device, disregarding PV power station, (**Calc.2.1**). Such method corresponds to the preceding statement, that the dwelling is expected to be built without photovoltaics power plant in mind.

Example: Given the annual consumption of thermal loads, 17 233 kWh, as presented in Table 4.1, and the demand profile, accumulation storage capacity is chosen, e.g. 15 kWh and accordingly, heater power output calculated, so that the combination of both match the condition of minimal 10 % of heat storage capacity reserve through the whole year. In case this condition can not be fulfilled, bigger accumulation storage is chosen and the computational loop repeats.

Next, utilizing the accumulation heater setup from previous calculation, **Calc.2.2** modeling run is executed, allowing for PV surplus energy to be stored in a heat storage tank.

Additionally to aforementioned, another computational sequence is launched, with different setup. To acknowledge both of the governmental subsidy conditions, as presented in the Section 5.1.2, required ratio 1:1.25 of solar array size to battery storage size is set as boundary condition this time. Calculation is performed for the same solar array sizes as previously, yet the criteria of desired 70 % utilization rate is loosened.

Example: As for the original computational sequence, based on the input solar array size, e.g. 2.992 kWp, the battery storage size was calculated, so that the utilization efficiency of entire PV system match desired value, e.g. 70 %. Same solar array size, 2.992 kWp, in now used for another computational sequence, where the battery size is set in accordance with the 1:1.25 ratio, thus 3.74 kWh. As a result, value of utilization rate is obtained.

Aside from mentioned change, no other adjustments were made to the simulation loop.

5.2 Model parameters

Having the photovlotaics optimization model complied, utilizing procedures earlier declared, it is important to distinguish universally applicable "core parts" of the model, from individually adjustable inputs.

Key components of the simulation algorithm being the radiation model and household yearly load profile model, both designed with study site located in the Czech Republic in mind. As such, the operational framework was assembled to correspond the local conditions. It is assumed, that for similar geopolitical regions, their functioning should not be compromised and thus the optimization algorithm could be applicable without configuration changes.

If we now focus on actual input parameters, they can be divided into two categories. First, based on study site location, radiation model a load profile model inputs, and second, physical photovoltaic system inputs.

As previously covered in Chapter 3, Section 3.3, measurements of global irradiance on the horizontal plane are needed for studied location, as well as its latitude and longitude. In order to run the radiation model, also the de-rating factor, the slope and azimuth of referred solar array are necessary, with the addition of ground reflectance value.

Table 5.2 Radiation model input parameters

Latitude	50.094°
Longitude	14.334°
De-rating factor	0.8
Slope	38°
Azimuth	0°
Ground reflectance	20 %
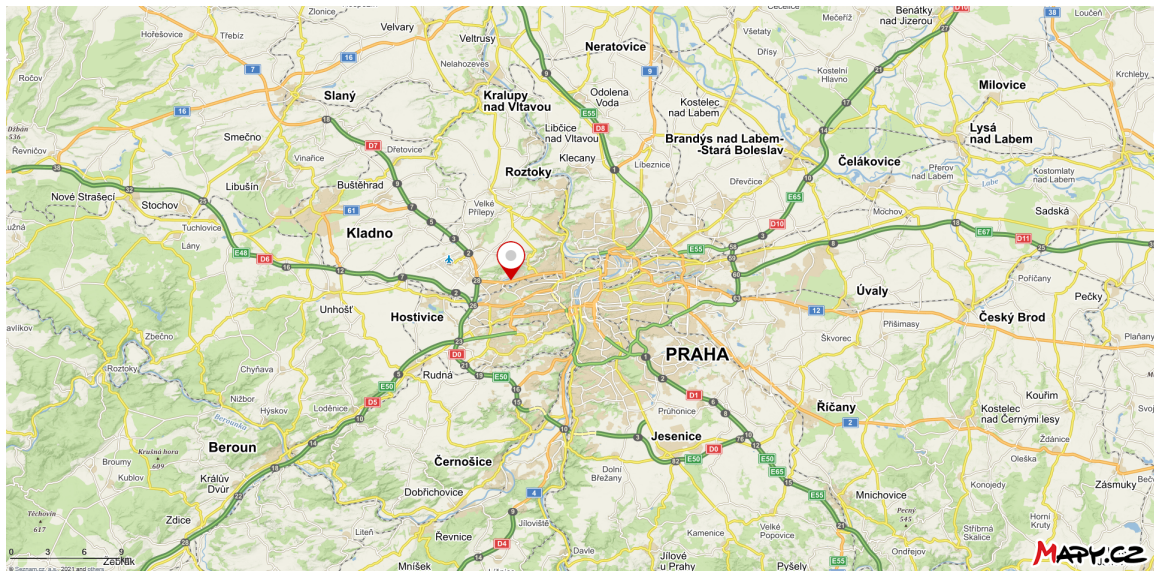
Fig. 5.2: Study site location

Focusing the household load profile model, values of yearly consumption are the required input, and thus the average values for the Czech Republic household are utilized.

Table 5.3 Load profile model input parameters

Space heating	14 070 kWh
Water heating	3 163 kWh
Cooking	1 291 kWh
El. appliances	1 198 kWh
Lighting	179 kWh
Air conditioning	~ 0 kWh
Other	324 kWh

Lastly, regarding the optimization model as a whole, household and heater type need to be specified, together with the electricity tariff, (Chapter 5, Section 5.1). Additionally, the depth of discharge, charging and discharging efficiency and maximal charging and discharging rate of battery storage is required.

Table 5.4 Battery storage input parameters

Depth of discharge	80 %
Charging efficiency	90 %
Discharging efficiency	90 %
Maximal charging rate	0.5 C
Maximal discharging rate	0.5 C

Values specified for battery storage pack generally represent prevalent guidelines for lithium iron phosphate cells, most commonly used in residential photovoltaic systems. The particular numbers however, should be specified based on actual battery manufacturer and his recommendations.

5.2.1 Economical parameters

In order to carry out a technical-economic comparison, electricity pricing and investment cost of photovoltaic power station need to be addressed. Speaking of expenses on PV system, it is important to bear in mind, that the real price is highly dependent on the solar system type, its manufacturer, supplier, and also household infrastructure readiness. For this reason, the pricing needs to be considered as indicative only.

A further presented appraisal is based on the product range and pricing of a well established photovoltaic components suppliers in the Czech Republic - Krannich Solar and GBC Solino.

Table 5.5 PV systems components pricing, taxes included

Solar panels	7 CZK/Wp
Mounting construction	2.6 CZK/Wp
Hybrid asymmetric inverter	8 CZK/Wp
LiFePO4 battery	9 400 CZK/kWh
Battery management system	18 000 CZK/piece

Additionally, project management, transportation, and assembly costs derived from a market research suggest, that the realization (and margins) account for approximately 50 % of the total price.

Together with the state subsidy, covering up to 50 % of total expenditure, it is to be assumed that PV system price consists only of the prices of individual components summed up.

Regarding electricity prices, the standard values corresponding to a two-year contract for households are presented. Precisely, the values given in the price list of ČEZ, electricity supplier, applicable in the distribution area of ČEZ Distribution.

On top of that, feed in tariff price is employed, presuming the surplus electricity to be sold to the grid. For that case, the price list of electricity supplier, Nano Energies, is used.

Table 5.6 Total unit price for electricity, including tax on electricity and system services

	HT	LT
D02d	4.476 CZK/kWh	- CZK/kWh
D25d	4.549 CZK/kWh	2.500 CZK/kWh
D26d	3.232 CZK/kWh	2.500 CZK/kWh
D57d	2.567 CZK/kWh	2.468 CZK/kWh
Feed-in	0.800 CZK/kWh	0.800 CZK/kWh

5.2.2   Examined variants

To encompass the broader perspective and obtain a wide range of results for the evaluation, each household setup was tested for various sizes of solar array, scaling its nominal power output accordingly to electrical loads demand. Namely, the values of 0.5, 0.75, 1, 1.25 and 1.5 times the electrical loads requirements divided by thousand were used.

   Example: Given the electrical loads of 2 992 kWh annually and solar array coefficient, e.g. 0.75, photovoltaic array size is estimated at 2 992 · 0.75 / 1000 = 2.244 kWp.

Additionally, PV systems were optimized in two different ways, to comply with government directives as presented in Chapter 1, Section 5.1.2.

First, to match the 70 % utilization rate for given solar array size, scaling the battery storage capacity, and second, to keep the battery capacity to solar array nominal power output ratio at 1.25:1.

Coming back to first mentioned, it is important to note, that for the sake of clearer comparison, 70 % utilization rate has to be achieved as a combination of PV electricity directly used for electrical loads and PV electricity stored in batteries. Therefore, no surplus energy used for heating was accounted. Such approach does not entirely follow the conditions of the subsidy, yet provides more valuable outcomes.

Lastly, an optimized PV system setups were examined for each of the household variant. First, searching for the best yearly benefit in comparison to system price and second, aiming for the best LCOE. Both while following the conditions of subsidy.

5.2.3 Evaluation criteria

For the purpose of PV systems evaluation, among others, three leading parameters were inspected. Photovoltaic system price, its yearly benefit and overall levelized costs of electricity.

Generally is the LCOE criteria given by equation as follows,

$$LCOE = \frac{\sum_{i=1}^{n} \frac{I_t + M_t + F_t}{(1+r)^t}}{\sum_{i=1}^{n} \frac{E_t}{(1+r)^t}} \tag{5.1}$$

where I_t stands for investment expenditures in a year t, M_t for operational and maintenance expenditures in the year t, F_t for fuel expenditures in the year t, E_t for electrical energy generated in the year t, r for discount rate and n for expected service life. As a result of Equation 5.1, price of produced energy is obtained.

In order to properly apply the criteria for residential photovoltaics, slight adjustments had to be done. Given the free solar radiation, fuel costs were removed from the equation. Similarly under assumption of negligible costs of maintenance and operation, neither M_t parameter was needed.

for the sake of simplicity, discount rate was set to zero, provided that in the case of a photovoltaic systems, it is a risk-free investment, where even the alternative risk-free investments show close to insignificant rates. As such, effect of time was eliminated from the equation, which should be remembered for future interpretation.

Based on these changes, the LCOE equation was modified to the form provided.

$$LCOE = \frac{\sum_{i=1}^{n} I_t}{\sum_{i=1}^{n} E_t} \tag{5.2}$$

Due to the varying value of PV produced electricity in households however, further alterations were necessary. To acknowledge mentioned issue, Equation 5.2 was remade as shown below,

$$LCOE = \frac{\sum_{i=1}^{n} I_t + W_b - W_s}{\sum_{i=1}^{n} W_c} \tag{5.3}$$

where W_b regards the price of electricity bought from grid in the year t, W_s the earnings form PV electricity sold to the grid in the year t and W_c the total amount of electricity consumed in the year t. As a result, unit price of household consumed electricity is achieved.

Established criteria illustrates the decrease in the household electricity price thanks to the photovoltaic system self-supply and also the sales of surplus electricity. Consequently, the lower the LCOE in comparison to the original el. price is, the greater revenue does the examined PV plant generate over its service life.

Speaking of photovoltaic system lifespan, assessment period was determined 15 years, as given interval corresponds to general PV system service life. Such choice may not be entirely rigorous, as the solar panels often come with the 25-year performance warranty. On the other hand, life span of system battery storage and inverter corresponds to a maximum of 15 years. Beltran et al. (2020); Narayan et al. (2018)

Given these components comes as the most expensive part of the system, the service life is therefore linked to them. Once their lifespan is over, it is surely an option to replace them with new ones, in order to extend PV system operational life. Nonetheless, it is highly debatable what will be the state of PV market in 15 years and thus the components replacement was not included in the simulation.

Regarding the "benefit" criteria, it was designed as an alternative to well established LCOE, offering a different point of view. Its value combines the savings thanks to the self-produced electricity covering the energy demands, with earnings due to selling the surplus energy to the grid. Electricity utilized for self-consumption is then credited in accordance with immediate electricity tariff, whereas surplus sold to the grid is credited in conformity to the feed-in tariff.

Linking the values of system price and its benefit inevitably leads to the price performance ratio, which in other words determines system bare payback time. Such benchmark can be easily used to cross compare completely dissimilar systems setups, yet it is important to keep in mind, that it favors investments with fast rate of return.

Overall, neither of the proposed criteria accounts for effects of time, regarding the discount rate, the inflation and especially the development fluctuations of electricity prices. Such influences would be hart to predict for the entire service life of the photovoltaic system, while in-depth assessment would be necessary. For that reason simplifications were adopted, not to exceed the scope of the study.

Chapter 6

Results and discussion

Having the simulation performed, obtained results follow, subdivided into sections based on household variants. For each, charts illustrating different PV systems performance is provided. In the left column, results corresponding to setup for 70 % utilization rate are presented, whereas in the right column, results corresponding to solar array size to battery capacity at 1:1.25 are showcased. Further in the text, these cases will be referred to as **70%_UT** and **1:1.25_RT**

Regarding the statement from Chapter 5, Subsection 5.1.3, that for each household type and photo-voltaics system combination, five different heater & accumulation tank combinations will be tested, it was found out, that the different variants of the assemblies do not show significant differences. For that reason, no related results are presented. (For heater & storage combinations studied, see Appendix B.)

The explanation for such a finding lies in the way of designing these systems. Due to the search for the smallest storage tank with the smallest heater, which would meet the criteria of 10 % of thermal storage capacity reserve through the year, assemblies were created with similar operational means. No matter the fact, that based on the first eligible heater & storage combination, four more variants with a bigger accumulation capacity yet a weaker heater were created and tested, all modeling results ended alike.

This outcome, however, has an overlap into the real-world, where the choice of household heating systems follows similar rules as in the mathematical model. Speaking of which, real systems are also designed having a reserve while the emphasis on price leads to purchase of smallest acceptable one.

Based on the aforementioned, it is possible to say that as long as the heating system is somewhat optimized to cover the household thermal demand, its exact scale does not play a crucial role if combined with the PV system.

On the other hand, that is only applicable in the case of "uncontrolled" thermal systems, where the accumulation tank serve as PV surplus storage, yet is not communicating with photovoltaic power station. Provided, that both systems would be connected through a control unit, it would be possible to increase potential for PV surplus energy utilization, by adjusting the heater functioning, whereas bigger storage tanks would presumably offer better options for optimization.

Considering the charts provided below, in contrast to an initial claim from Chapter 5, Subsection 5.2.2, only PV sizes of 0.5/1000, 0.75/1000 and 1/1000 of household electrical loads demand were included in the comparison of final results.

The reason behind was the impossibility to achieve 70 % utilization rate in **V1_El.App**, with solar array size at 1.25/1000 or 1.5/1000 of electrical loads demand, regardless of the battery size. Concerning the variants **V2_DHW**, **V3.1_DHW+SH** and **V3.2_DHW+SH**, desired utilization can be achieved, however due to the inadequacy of the system price in such case, mentioned solar array setups were cut out of final comparison anyway.

6.1 V1_El.App

Household utilizing electricity only for cooking, cold appliances, audiovisual, information and communication technologies, washing and lighting, whereas both water and space heating are covered by gas, solid or liquid fuel burner. Electricity billed at single tariff, D02d , having the same price through the whole day.
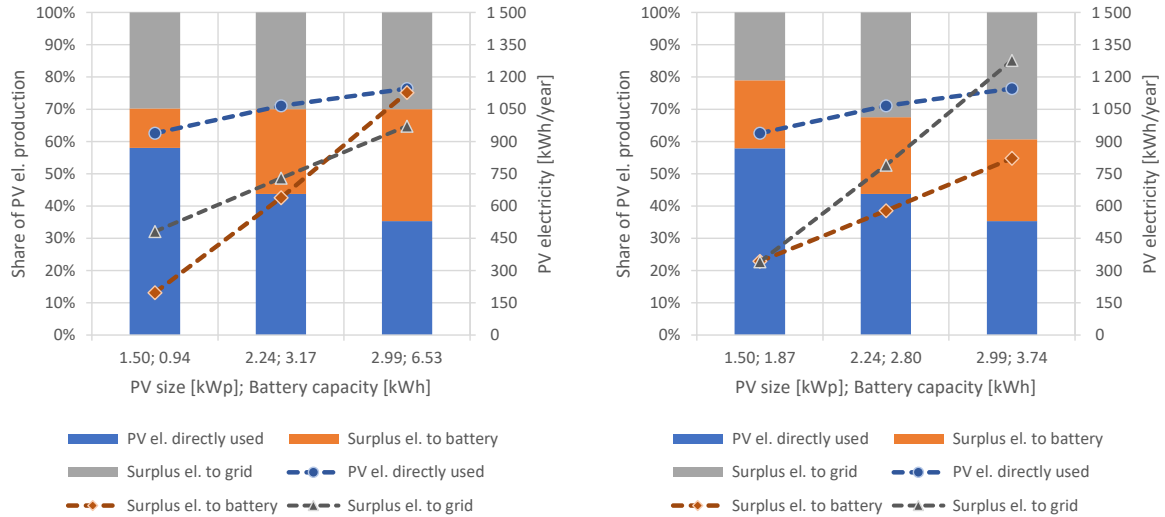
Fig. 6.1: Means of utilizing PV plant electricity, having PV system set up for
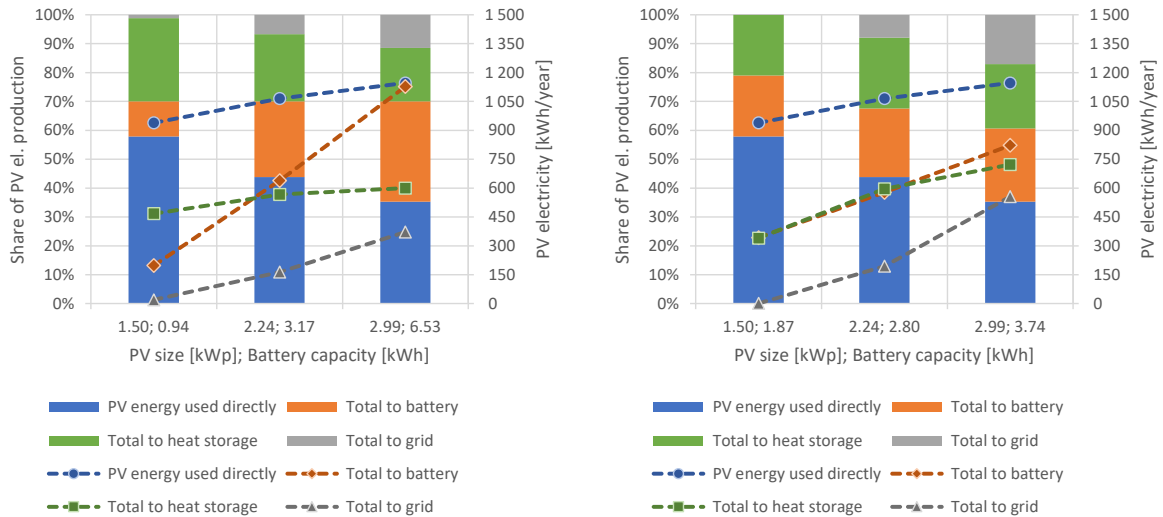a 70 % utilization (left) or with solar array size to battery capacity at 1:1.25 (right)

Comparing both **70%_UT** and **1:1.25_RT** variants, it can be clearly seen in Figure 6.1, that the formerly mentioned perfectly match desired utilization rate, however in case of PV size 1.50 kWp and battery capacity 0.94 kWh, condition of 1 kWp : 1.25 kWh is not met. Similarly, in **1:1.25_RT** chart, case of PV size 2.24 kWp, battery capacity 2.80 kWh and PV size 2.99 kWp, battery capacity 3.74 kWh, condition of minimal 70 % utilization rate is not satisfied.

Due to an identical electrical demand and solar array size, directly utilized PV electricity stays the same in corresponding setups, no matter the variant. The only difference here is hence caused by the battery storage size. That is the one compensating for the increase in PV energy output, keeping the utilization rate on required value in case of **70%_UT**.
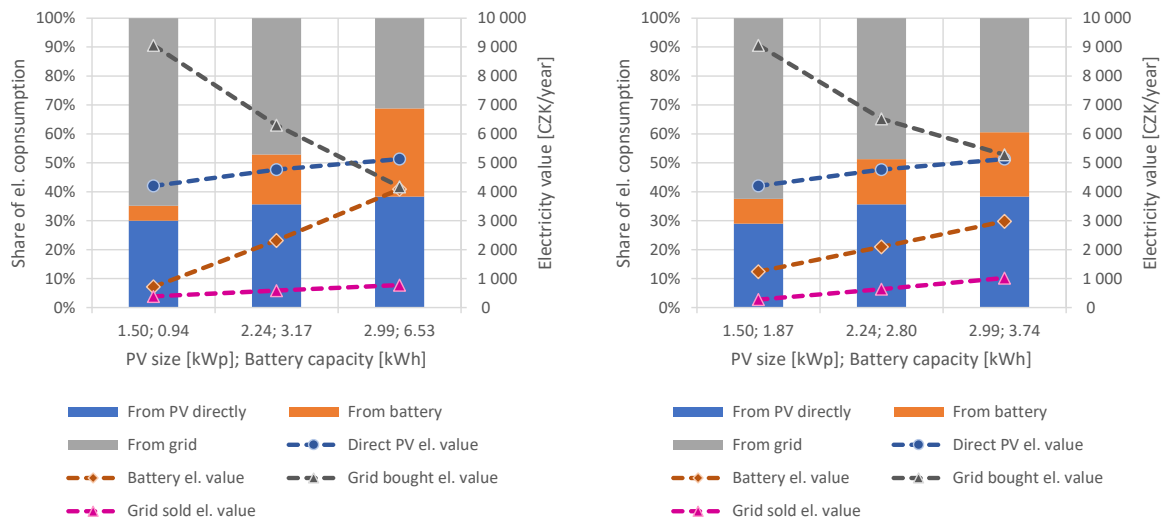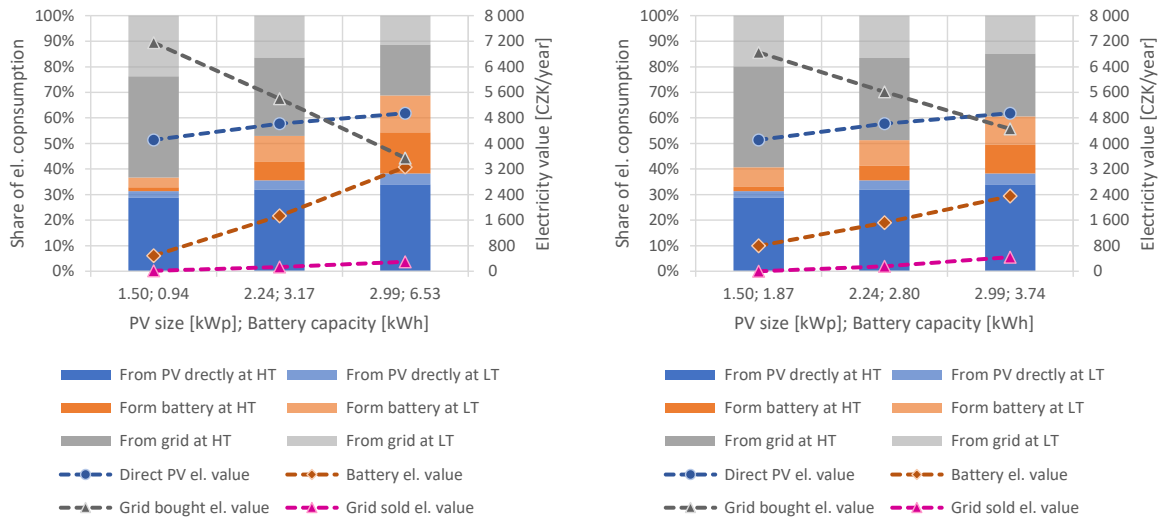

Fig. 6.2: Means of covering el. loads demand, having PV system set up for
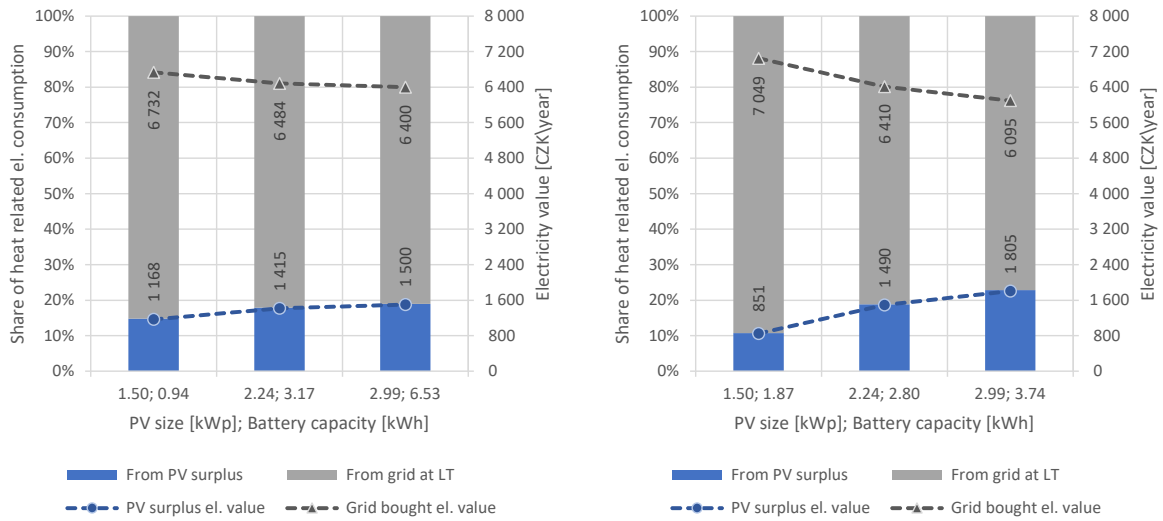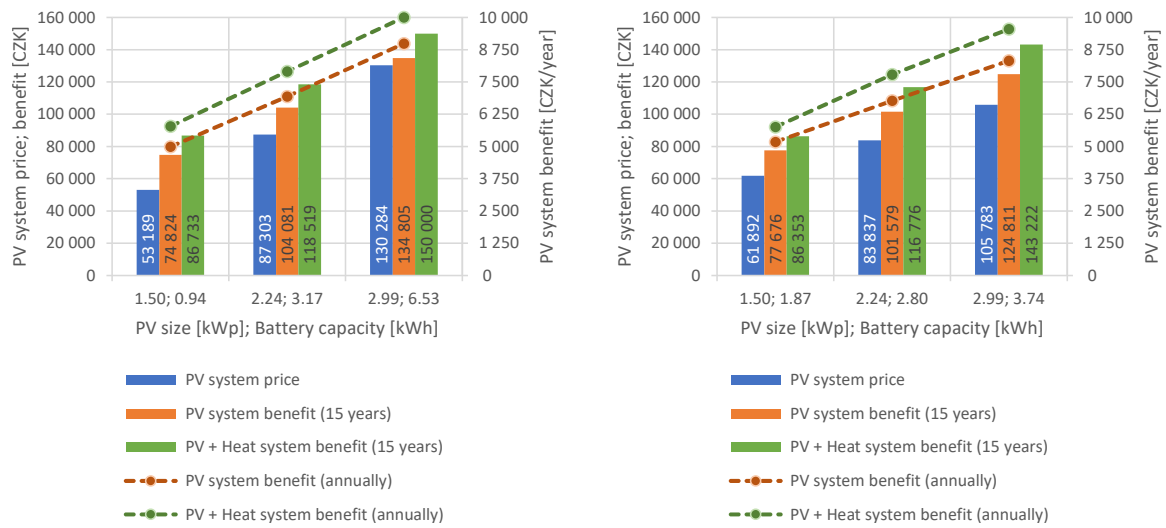a 70 % utilization (left) or with solar array size to battery capacity at 1:1.25 (right)
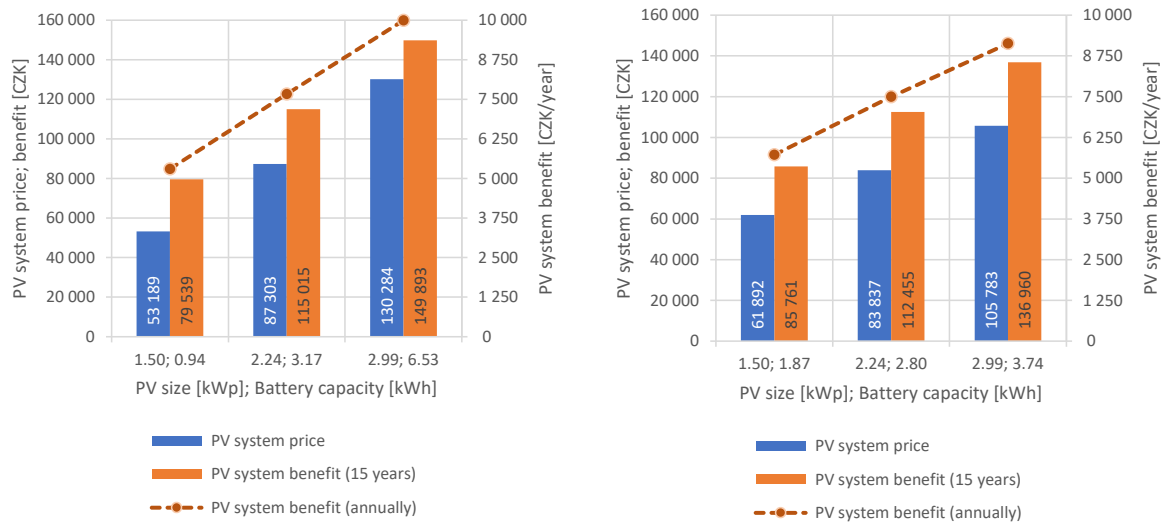
Fig. 6.3: PV system price and profit, having the system set up for
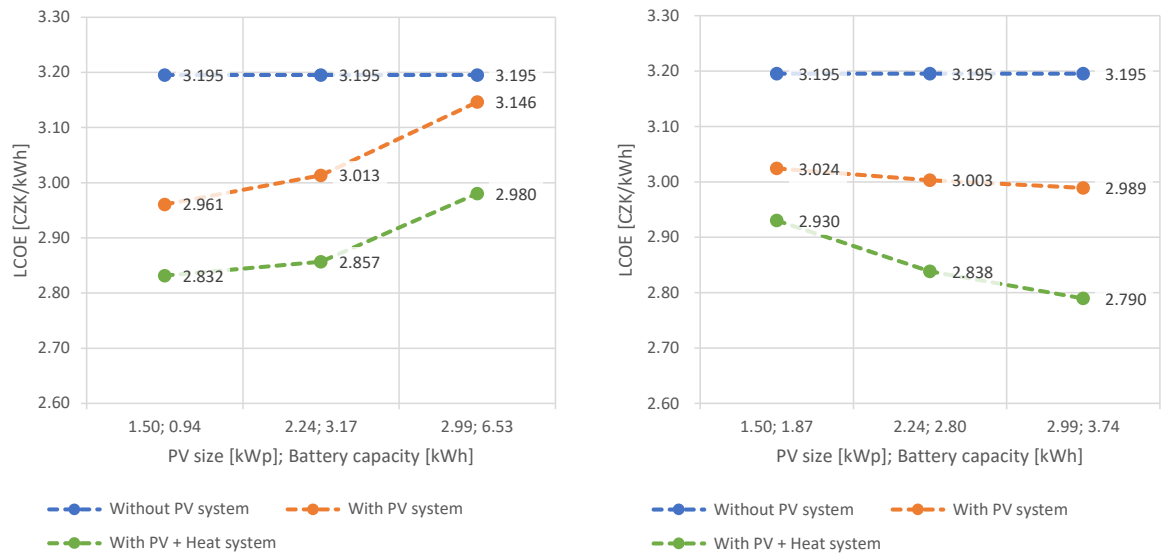a 70 % utilization (left) or with solar array size to battery capacity at 1:1.25 (right)
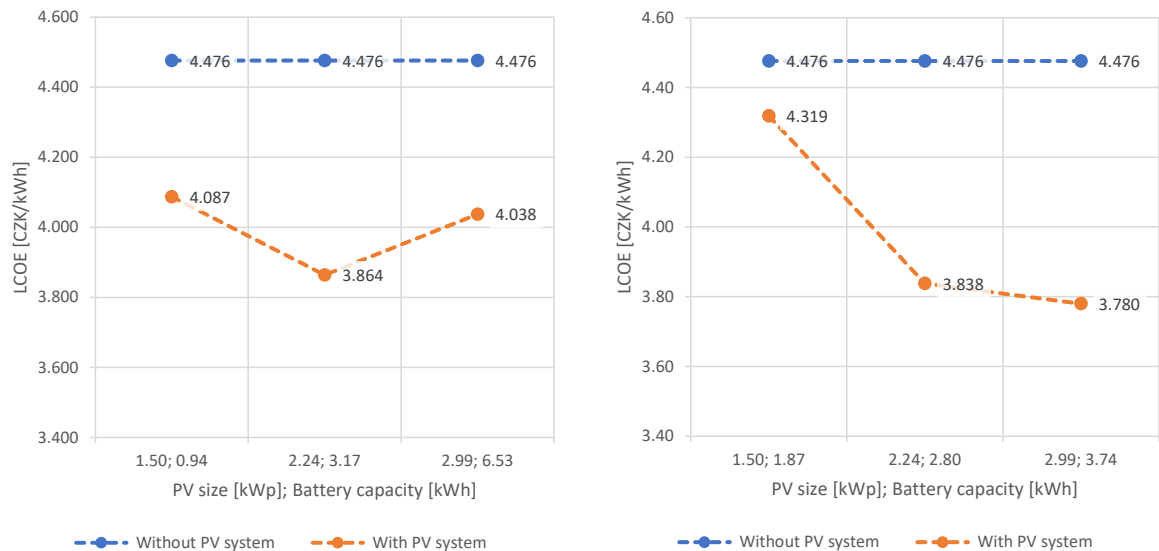
Fig. 6.4: Household LCOE, having the system set up for
a 70 % utilization (left) or with solar array size to battery capacity at 1:1.25 (right)

Speaking of the Figure 6.2, the effect of increasing the overall PV system size can be related to decreasing dependency on the grid. Accordingly, in Figure 6.3, system price rises while also the annual system benefit grows. (The value of the system benefit accounts for financial savings thanks to the reduced grid electricity need and the income from electricity sold to the grid.)

Within the Figure 6.3, a comparison of the system price and benefit over 15-year period is demonstrated. Neither inflation, nor an electricity price increase over the years are taken into consideration. Similar can be said also of Figure 6.6, showing levelized cost of electricity of various setups.

Given the evaluation parameters results, it can not be unequivocally said, whether it is better to design bigger system, showing lower LCOE, or smaller system with shorter bare payback time, under conditions of **V1_El.App**.

6.1.1 Optimized variant

In order to determine the optimal PV system setup for **V1_El.App**, calculation was performed two more times, optimizing for the best ratio of a photovoltaic plant price and an annual system benefit first, and next for the smallest household levelized cost of electricity.

Table 6.1 Optimization results

Optimization criteria	System setup kWp; kWh	Utilization efficiency	Yearly benefit	Payback period
System payback p.	1.27; 1.59	83.95 %	5 132 CZK	10.78 years
Household LCOE	2.04; 2.55	70.00 %	7 039 CZK	11.08 years
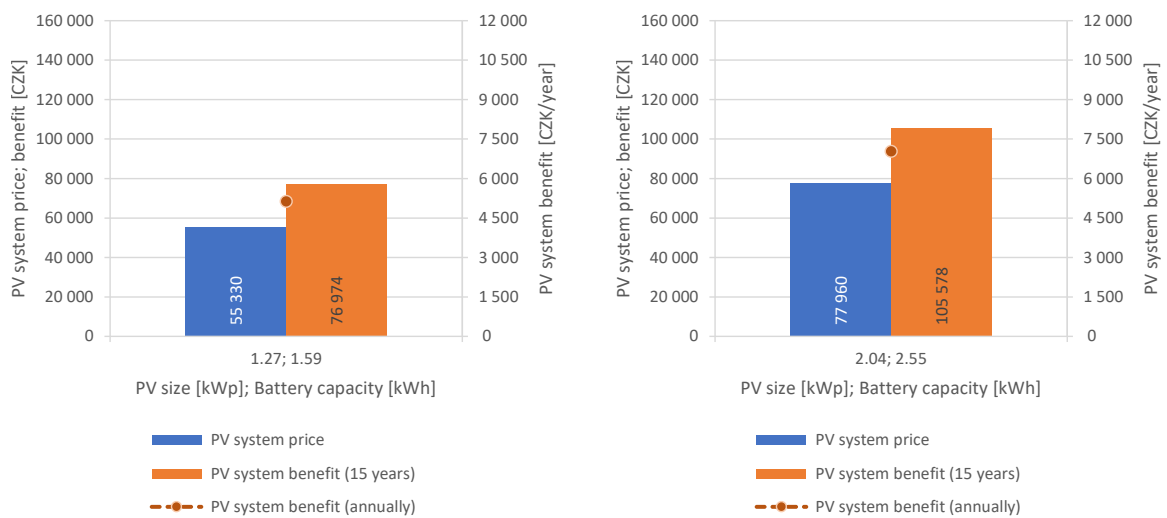
Fig. 6.5: PV system price and profit, having the system optimized for shortest bare payback period (left) or smallest LCOE (right)
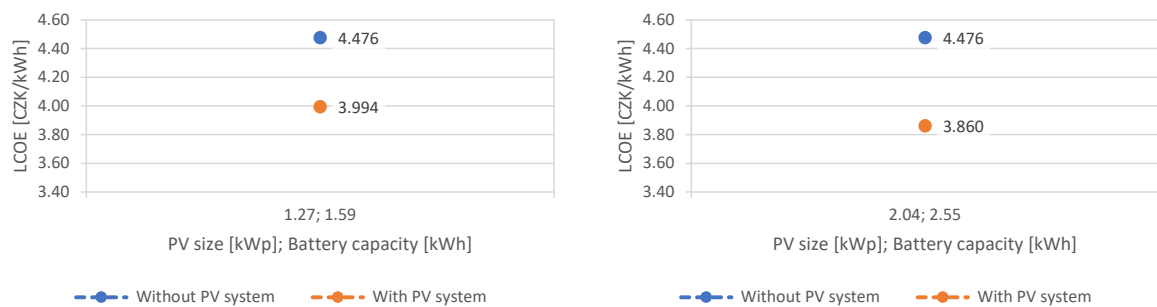
Fig. 6.6: Household LCOE, having the system optimized for shortest bare payback period (left) or smallest LCOE (right)

6.2 V2_DHW

Household utilizing electricity for common electrical loads (same as previously), plus also using an electric accumulation water heater - electric boiler. Electricity is billed at two-tariff rate, D25d, while boiler operates only during the low tariff, active 8 hours a day. Space heating is still covered by either gas, solid or liquid fuel burner.

Fig. 6.7: Means of utilizing PV plant electricity, having PV system set up for
a 70 % utilization (left) or with solar array size to battery capacity at 1:1.25 (right)

Analyzing Figures 6.1 and 6.7, studied PV systems stay the same in both occurrences. In the latter, however, surplus electricity is also used for district water heating, consequently increasing the utilization rate. The inclusion of an electric boiler in a photovoltaic system thus significantly improves the balance of electricity self-consumption, while it entitles formerly excluded systems **1:1.25_RT**, 2.24 kWp; 2.80 kWh and **1:1.25_RT**, 2.99 kWp; 3.74 kWh to a subsidy application.

Fig. 6.8: Means of covering el. loads demand, having PV system set up for
a 70 % utilization (left) or with solar array size to battery capacity at 1:1.25 (right)

Fig. 6.9: Means of covering thermal demand, having PV system set up for
a 70 % utilization (left) or with solar array size to battery capacity at 1:1.25 (right)

Examining Figures 6.2 and 6.8, proportions of the bars show no change in general means. Still, in Figure 6.8, differentiating in accordance with a high and low electricity tariff can be seen. Due to the overall lower prices in two tariff billing, household relative energy costs are reduced. On the other hand, from the point of PV system profit, this influence is negative. In comparison to single tariff billing, "PV direct" or "Battery stored" energy covering the demands during a low tariff rate is now valued at a reduced price, ultimately decreasing the photovoltaic system benefit.

Additionally, charts regarding the sources of household heat demand covering are provided in Figure 6.9. Given the boiler operating exclusively at low tariff, no HT/LT distinction is applied, whereas the "PV surplus" energy is credited at low tariff price.

Fig. 6.10: PV system price and profit, having the system set up for
a 70 % utilization (left) or with solar array size to battery capacity at 1:1.25 (right)

Fig. 6.11: Household LCOE, having the system set up for
a 70 % utilization (left) or with solar array size to battery capacity at 1:1.25 (right)

By combining the positive and negative effects of the DHW inclusion to the system of a photovoltaic power plant, a yearly profit is obtained. Unfavorable effects of reduced electricity value can be seen by comparison of Figures 6.3 and 6.10. For both, the "PV system price" stays the same while cumulated "PV system benefit after 15 years" it is clearly decreased in the latter one. Contrarily, setting the "PV system benefit after 15 years" of Figure 6.3 side by side with "PV + Heat system benefit after 15 years" of Figure 6.10, a slight beneficial effect of combining PV system with DHW system is noticeable.

The same conclusion can be reached by comparing the annual profitability of the system, also shown in the mentioned figures. for the sake of clearer comparison, numerical values regarding the aforementioned are provided within Table 6.2.

Examining Figure 6.11, interesting contrast may be seen for setups **70%_UT** and **1:1.25_RT**. In case of the former, household LCOE rises with PV system size increase, whereas in case of the latter, the opposite is true. Such effect can be linked to the battery storage capacity and its influence on the system price.

Table 6.2 Comparison of **V1 El.App** and **V2 DHW** PV systems price, profit and payback period

System setup **70% UT**	1.50; 0.94 kWp; kWh	2.24; 3.17 kWp; kWh	2.99; 6.53 kWp; kWh
PV system price	53 189 CZK	87 303 CZK	130 284 CZK
V1; PV annuall benefit	*5 303* CZK	7 668 CZK	9 993 CZK
V2; PV annuall benefit	*4 988* CZK	6 939 CZK	8 987 CZK
V2; PV+DHW annuall benefit	*5 782* CZK	7 901 CZK	10 007 CZK
V1; PV payback period	*10.03* years	11.39 years	13.04 years
V2; PV payback period	*10.66* years	12.58 years	14.50 years
V2; PV+DHW payback period	*9.20* years	11.05 years	13.02 CZK

System setup **1:1.25 RT**	1.50; 1.87 kWp; kWh	2.24; 2.80 kWp; kWh	2.99; 3.74 kWp; kWh
PV system price	61 892 CZK	83 837 CZK	105 783 CZK
V1; PV annuall benefit	5 717 CZK	*7 497* CZK	*9 131* CZK
V2; PV annuall benefit	5 178 CZK	6 772 CZK	8 321 CZK
V2; PV+DHW annuall benefit	5 757 CZK	7 785 CZK	9 548 CZK
V1; PV payback period	10.83 years	*11.18* years	*11.59* years
V2; PV payback period	11.95 years	12.38 years	12.71 years
V2; PV+DHW payback period	10.75 years	10.77 years	11.08 years

* Values in *italic* originate from systems unqualified for subsidy, thus should serve as indicative only.

6.2.1 Optimized variant

In order to determine the optimal PV system setup for **V2_DHW**, calculation was performed two more times, optimizing for the best ratio of a photovoltaic plant price and an annual system benefit first, and next for the smallest household levelized cost of electricity.

Table 6.3 Optimization results

| Optimization criteria	System setup kWp; kWh	Utilization efficiency	Yearly benefit	Payback period
System payback p.	1.81; 2.56	97.64 %	6 647 CZK	10.68 years
Household LCOE	3.54; 4.42	77.58 %	10 695 CZK	11.39 years
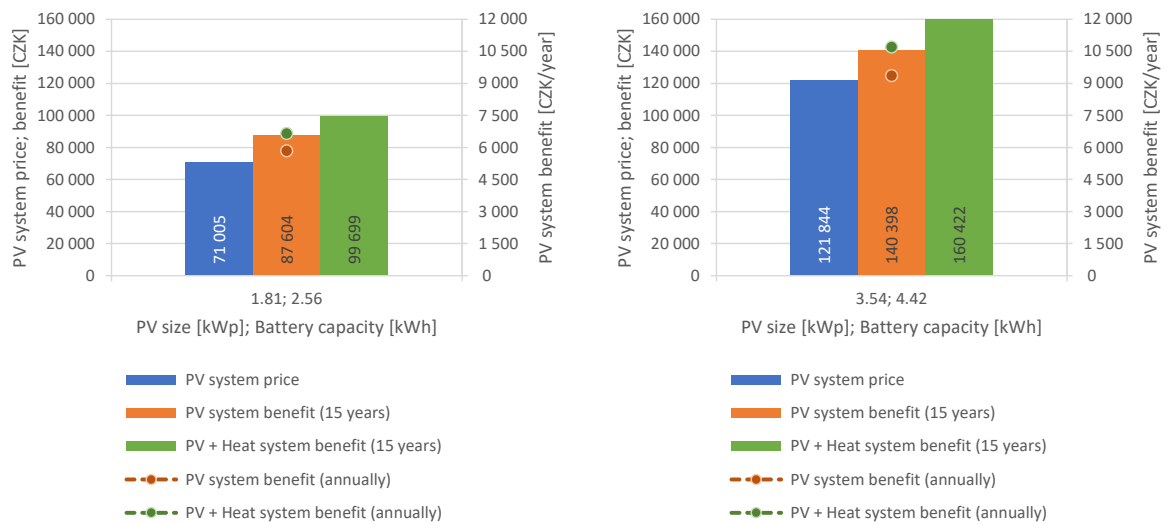
Fig. 6.12: PV system price and profit, having the system optimized for shortest bare payback period (left) or smallest LCOE (right)
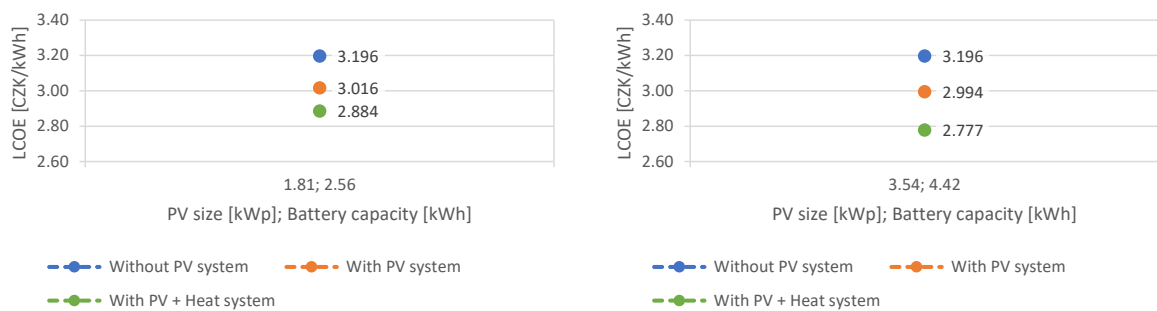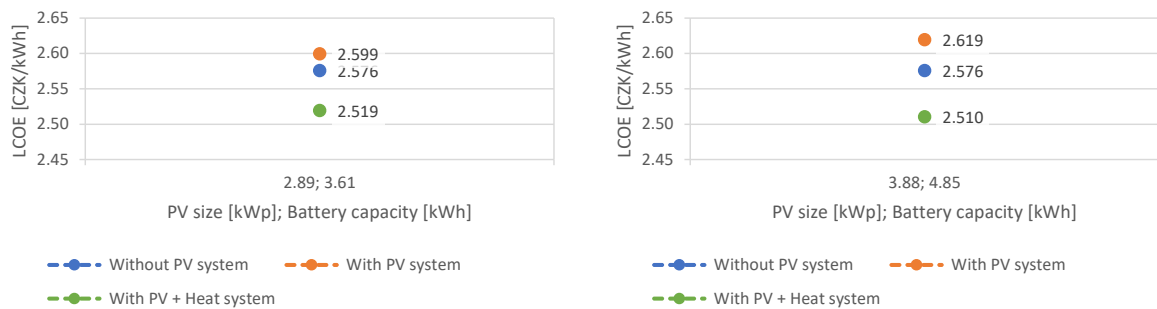

Fig. 6.13: Household LCOE, having the system optimized for shortest bare payback period (left) or smallest LCOE (right)

6.3   V3.1_DHW+SH

Household utilizing electricity for common electrical loads, water heating and space heating. Both water heating and space heating is assumed to be a single system, sharing a heating element and an accumulation tank. The electricity is billed at a two-tariff rate, D26d, while heater operates during the low tariff only, being active 8 hours a day.
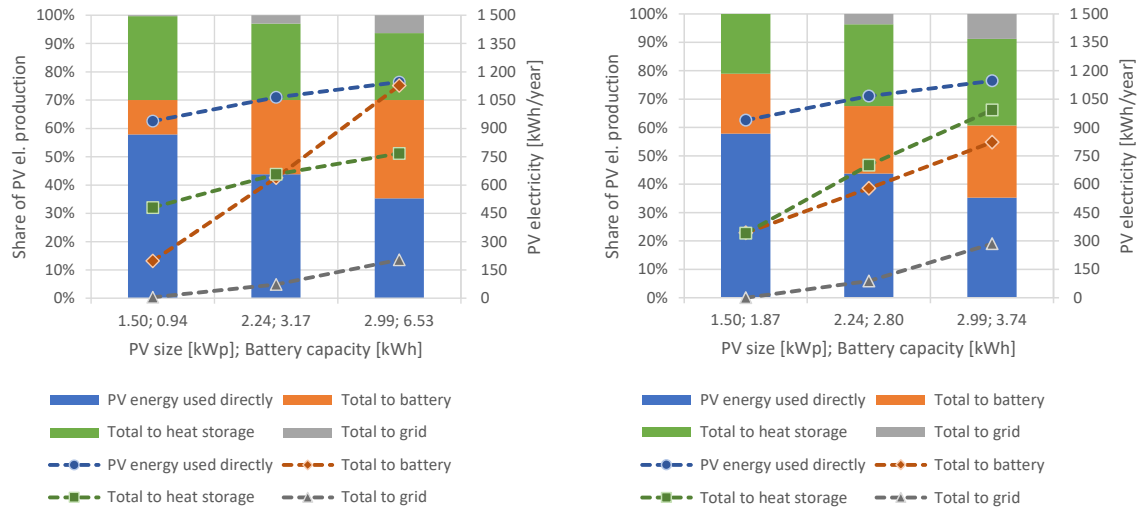
Fig. 6.14: Means of utilizing PV plant electricity, having PV system set up for
a 70 % utilization (left) or with solar array size to battery capacity at 1:1.25 (right)

Introducing the space heating on top of water heating and electrical loads, the utilization potential is further increased. The outcome of such setup can be observed examining Figures 6.7 and 6.14, yet the effect is not that significant. The reason behind is the space heating demand seasonality and relatively small PV systems studied.

Due to the discrepancy in the main heating demand period (winter) and PV system peak production period (summer), interconnection of these two systems does not show a major benefit. It is up to question, what result would be achieved in combination of a space heating and electrical loads solely, however, given this composition being used very rarely, if at all, such case was not examined.

Table 6.4 Comparison of **V2_DHW** and **V3.1_DHW+SH** PV energy utilization rate

System setup **70%_UT**	1.50; 0.94 kWp; kWh	2.24; 3.17 kWp; kWh	2.99; 6.53 kWp; kWh
V2; Total utilization rate	98.81 %	93.28 %	88.54 %
V3.1; Total utilization rate	99.68 %	97.02 %	93.71 %
System setup **1:1.25_RT**	1.50; 1.87 kWp; kWh	2.24; 2.80 kWp; kWh	2.99; 3.74 kWp; kWh
V2; Total utilization rate	99.97 %	92.02 %	82.89 %
V3.1; Total utilization rate	100.00 %	96.35 %	91.21 %
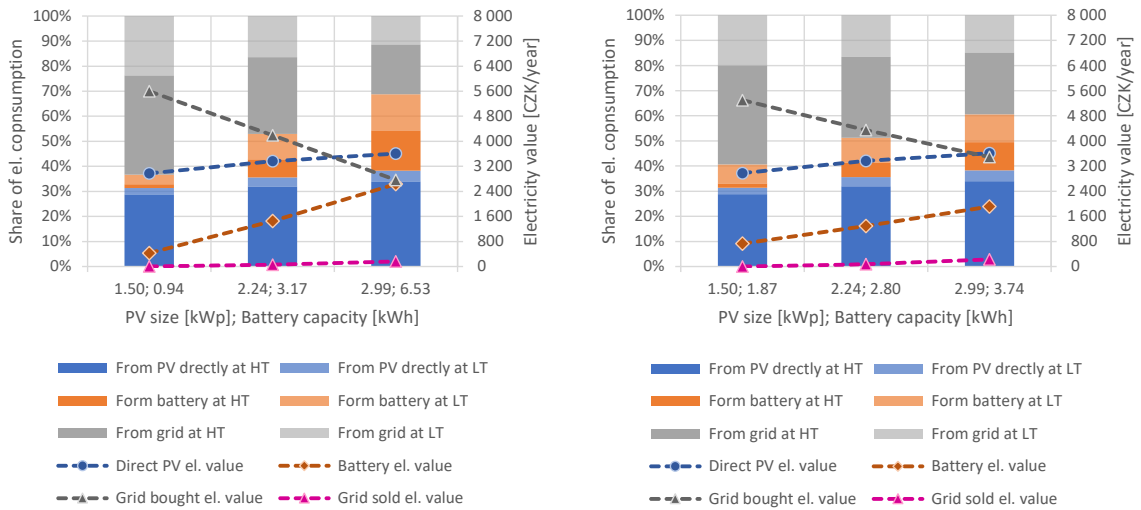
Fig. 6.15: Means of covering el. loads demand, having PV system set up for
a 70 % utilization (left) or with solar array size to battery capacity at 1:1.25 (right)
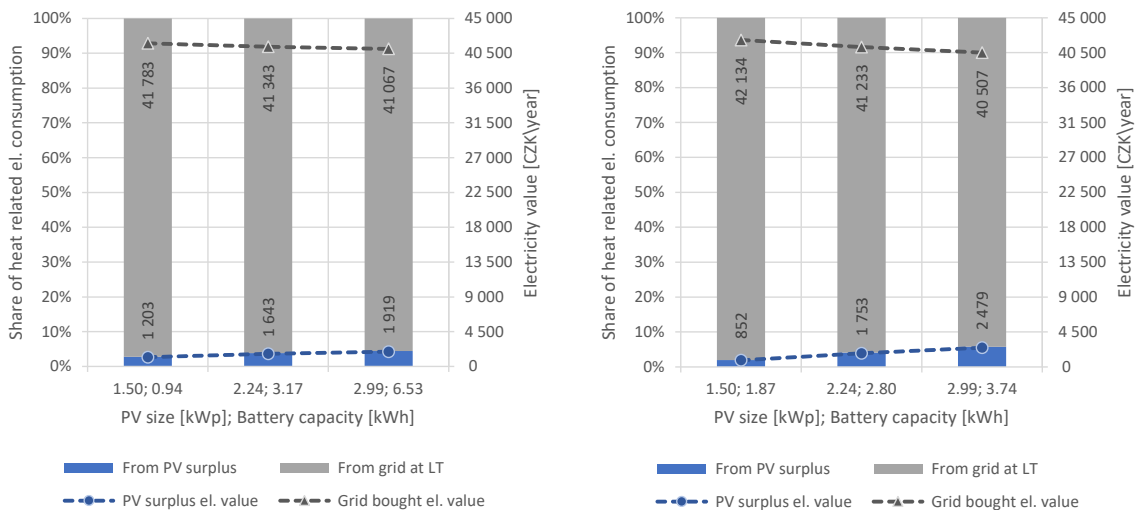
Fig. 6.16: Means of covering thermal demand, having PV system set up for
a 70 % utilization (left) or with solar array size to battery capacity at 1:1.25 (right)
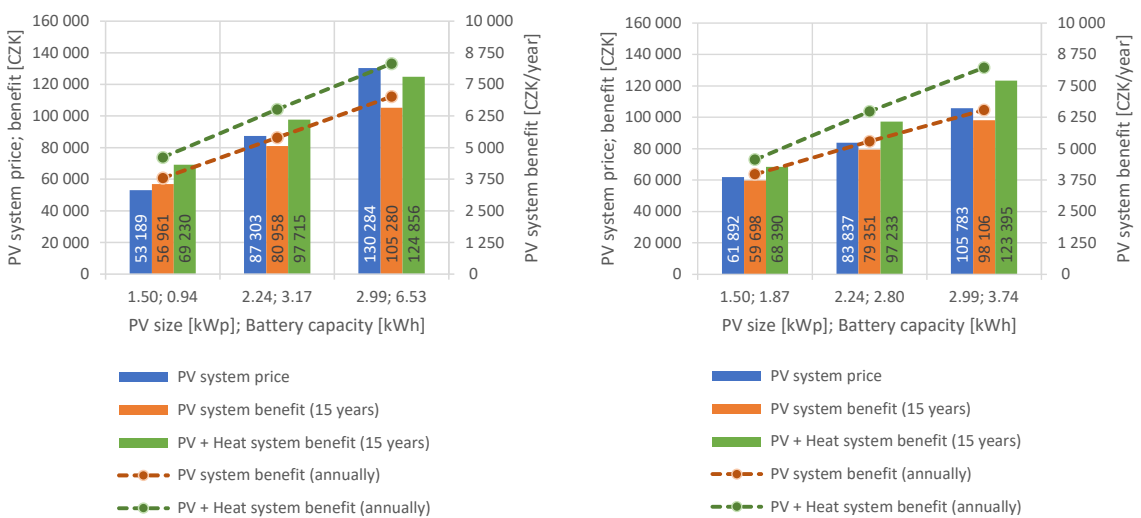
Fig. 6.17: PV system price and profit, having the system set up for
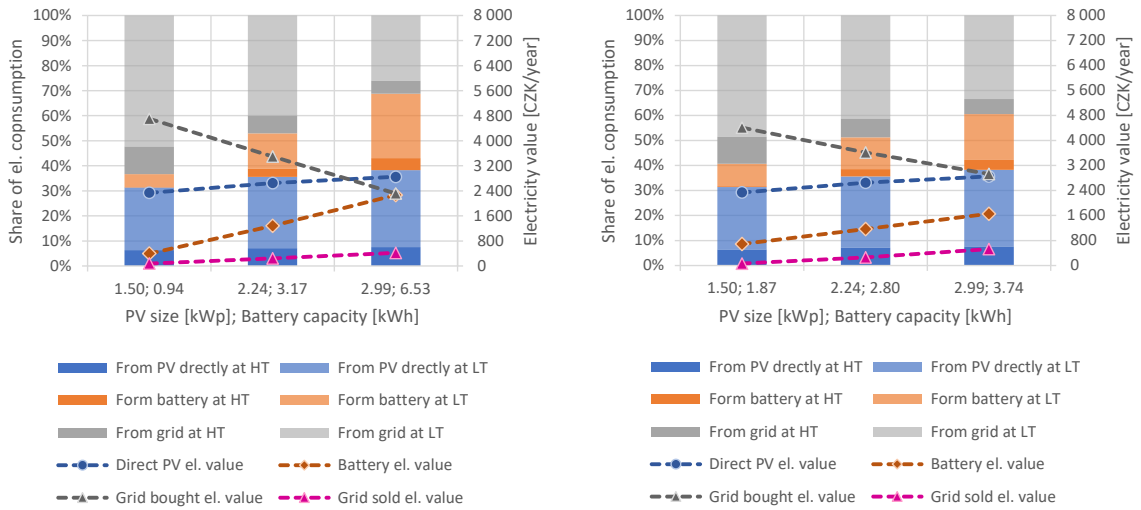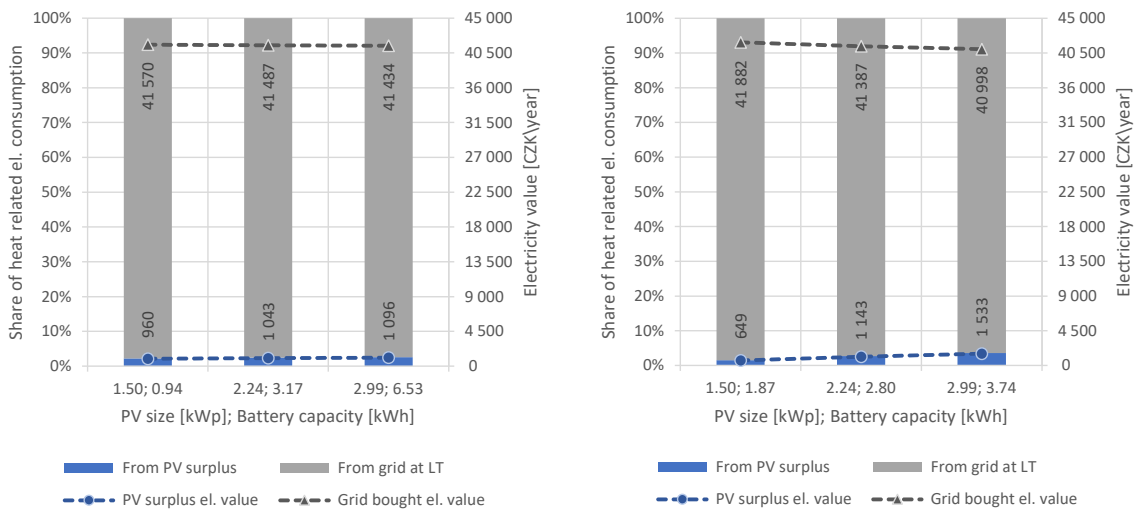a 70 % utilization (left) or with solar array size to battery capacity at 1:1.25 (right)
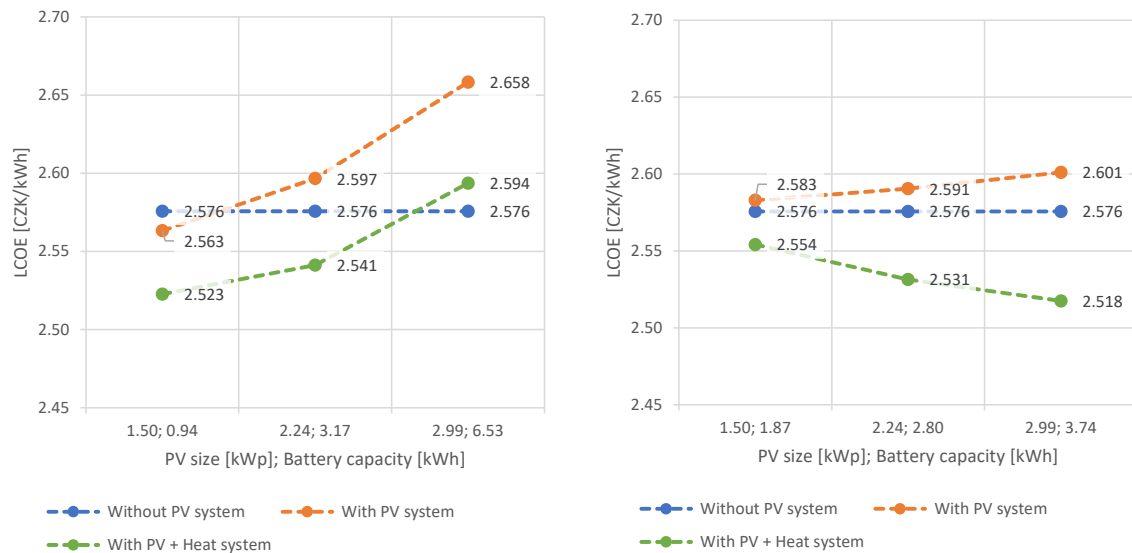
Fig. 6.18: Household LCOE, having the system set up for
a 70 % utilization (left) or with solar array size to battery capacity at 1:1.25 (right)

Looking at the Figures 6.8 and 6.15, the only disparity to be seen is the change in the "Electricity value" due to the different pricing of tariffs D25d and D26d. Aside from that, the photovoltaics systems underwent no changes, while the low tariff periods stay the same.

A more significant change can be observed when comparing Figures 6.9 and 6.16, where because of the space heating load addition in a current household type, a relative amount of the thermal demand covered from PV system decreased.

Analyzing the economic evaluation of PV setups under the conditions of **V3.1_DHW+SH**, again, the negative effect of a lower electricity value goes against the positive effect of an increased utilization rate. To properly judge the outcome, numerical values are provided in Table 6.5, seconded with Figure 6.18.

Table 6.5 PV systems price, profit and payback period under **V3.1_DHW+SH**

System setup **70%_UT**	1.50; 0.94 kWp; kWh	2.24; 3.17 kWp; kWh	2.99; 6.53 kWp; kWh
PV system price	53 189 CZK	87 303 CZK	130 284 CZK
PV annuall benefit	*3 797* CZK	5 397 CZK	7 019 CZK
PV+DHW+SH annuall benefit	*4 615* CZK	6 514 CZK	8 324 CZK
PV payback period	*14.01* years	16.17 years	18.56 years
PV+DHW+SH payback period	*11.52* years	13.40 years	15.65 CZK

System setup **1:1.25_RT**	1.50; 1.87 kWp; kWh	2.24; 2.80 kWp; kWh	2.99; 3.74 kWp; kWh
PV system price	61 892 CZK	83 837 CZK	105 783 CZK
PV annuall benefit	3 980 CZK	5 290 CZK	6 540 CZK
PV+DHW+SH annuall benefit	4 559 CZK	6 482 CZK	8 226 CZK
PV payback period	15.55 years	15.85 years	16.17 years
PV+DHW+SH payback period	13.58 years	12.93 years	12.86 CZK

6.3.1 Optimized variant

In order to determine the optimal PV system setup for **V3.1_DHW+SH**, calculation was performed two more times, optimizing for the best ratio of photovoltaic plant price and annual system benefit first, and next for the smallest household levelized cost of electricity.

Table 6.6 Optimization results

Optimization criteria	System setup kWp; kWh	Utilization efficiency	Yearly benefit	Payback period
System payback p.	2.89; 3.61	91.85 %	7 998 CZK	12.86 years
Household LCOE	3.88; 4.85	85.83 %	10 108 CZK	13.04 years
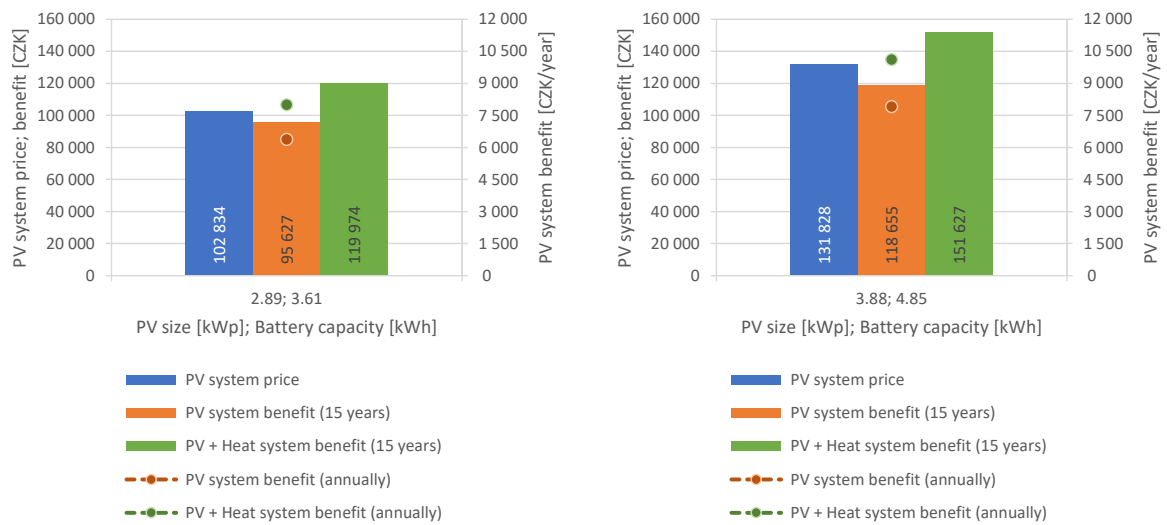
Fig. 6.19: PV system price and profit, having the system optimized for
shortest bare payback period (left) or smallest LCOE (right)

Fig. 6.20: Household LCOE, having the system optimized for
shortest bare payback period (left) or smallest LCOE (right)

6.4 V3.2_DHW+SH

Household utilizing electricity for common electrical loads, water heating and space heating. Both water heating and space heating is assumed to be single system, sharing heating element and accumulation tank. Electricity is billed at two-tariff rate, D57d, while heater operates during the low tariff only, being active 20 hours a day.
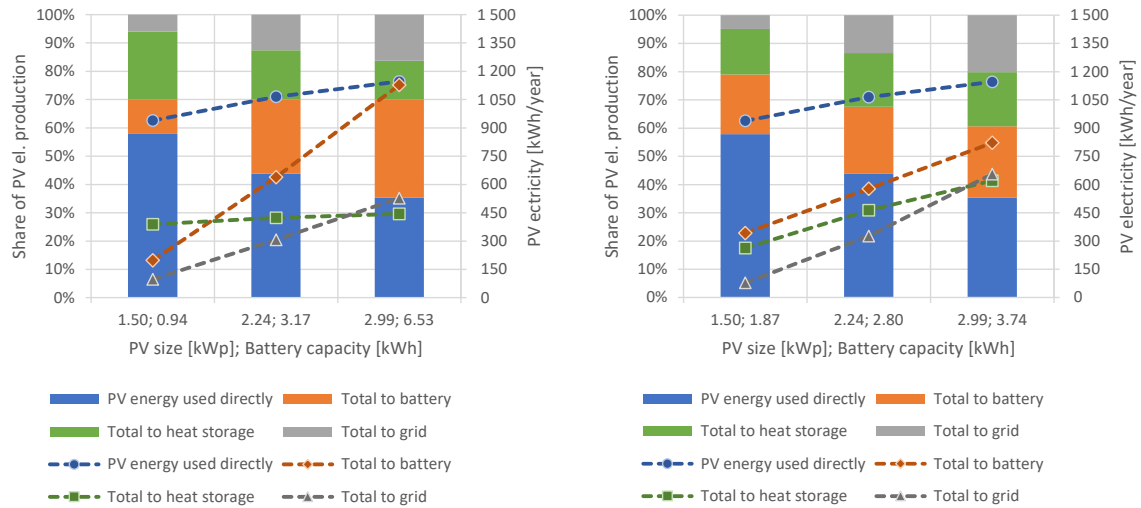
Fig. 6.21: Means of utilizing PV plant electricity, having PV system set up for
a 70 % utilization (left) or with solar array size to battery capacity at 1:1.25 (right)

Switching from 8-hour LT two tariff billing to 20-hour LT two tariff billing, an important change happens in the heater & accumulation assembly. Provided that the low tariff is running for 20 hours a day, requirements on both, heater and storage tank change. There is no longer need to accumulate the heat for lengthy periods of high tariff, and thus the necessary size of thermal storage tank is reduced. Similarly, as the heater is allowed to run for the greater part of the day, lower power output is sufficient. (See the Appendix B. for a proof.) The said setup corresponds to hybrid or heat pump systems.

Speaking of uncontrolled systems, the outcome of such modification is adverse. Given the reduced storage tank volume combined with heater running for greater part of the day, capacity for PV surplus utilization is decreased. The result can be seen by comparing Figures 6.14 and 6.21, or more precisely, from Table 6.7.

Table 6.7 Comparison of **V3.1_DHW+SH** and **V3.2_DHW+SH** PV energy utilization rate

System setup **70%_UT**	1.50; 0.94 kWp; kWh	2.24; 3.17 kWp; kWh	2.99; 6.53 kWp; kWh
V3.1; Total utilization rate	99.68 %	97.02 %	93.71 %
V3.2; Total utilization rate	94.00 %	87.38 %	83.74 %
System setup **1:1.25_RT**	1.50; 1.87 kWp; kWh	2.24; 2.80 kWp; kWh	2.99; 3.74 kWp; kWh
V3.1; Total utilization rate	100.00 %	96.35 %	91.21 %
V3.2; Total utilization rate	95.19 %	86.57 %	79.78 %

Fig. 6.22: Means of covering el. loads demand, having PV system set up for
a 70 % utilization (left) or with solar array size to battery capacity at 1:1.25 (right)

Fig. 6.23: Means of covering thermal demand, having PV system set up for
a 70 % utilization (left) or with solar array size to battery capacity at 1:1.25 (right)
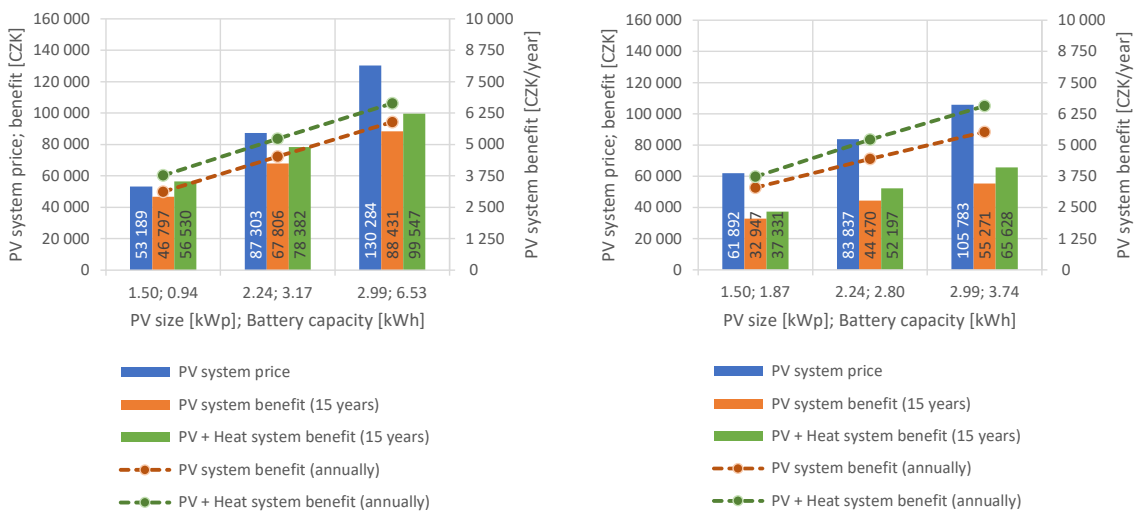
Fig. 6.24: PV system price and profit, having the system set up for
a 70 % utilization (left) or with solar array size to battery capacity at 1:1.25 (right)
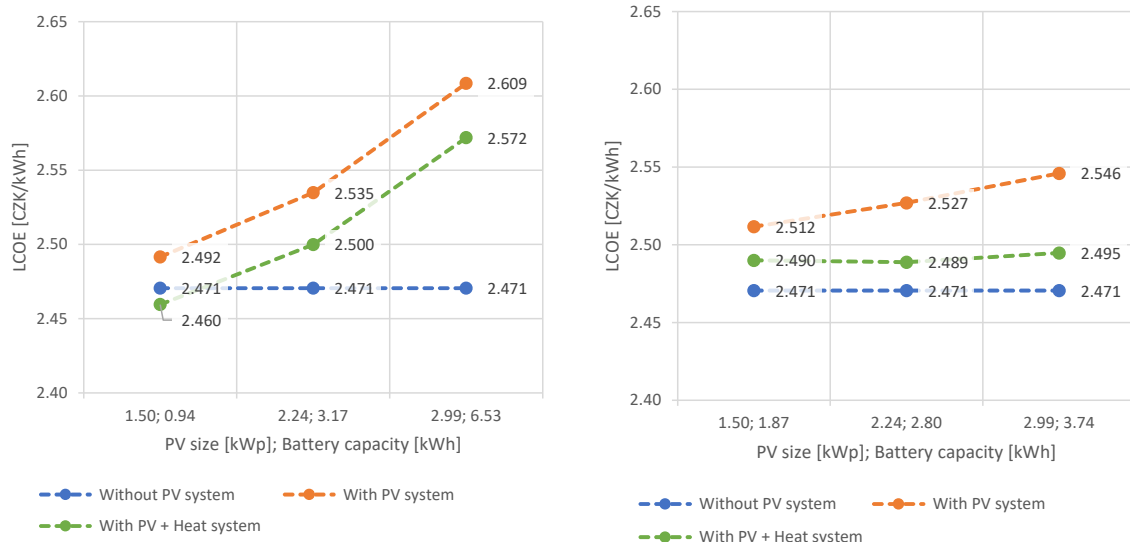
Fig. 6.25: Household LCOE, having the system set up for
a 70 % utilization (left) or with solar array size to battery capacity at 1:1.25 (right)

Examining the Figure 6.22, a crucial difference from Figure 6.15 can be recognized. Due to the extended periods of low tariff, also the majority of electricity obtained by PV plant is supplied at a low tariff rate. As mentioned previously, such issue diminish the PV system profits, yet given the price per kWh for D57d tariff, at HT: 2.567 CZK/kWh; at LT: 2.468 CZK/kWh, neither supplying the PV electricity at HT would fundamentally improve the balance.

On top of that, if a heat pump is used in the system, the assumption of 100 % efficient conversion of electricity into heat is not appropriate. Considering the usual coefficient of performance of heat pumps in the range of 3 to 4, out of single unit of electricity about 3.5 units of heat are produced. Such behavior is however not implemented within the model, where only one-to-one electricity to heat conversion is employed.

Under ideal conditions, it may be presumed, that the heat pump would utilize the same amount of PV surplus, as in one-to-one conversion, yet producing three to four times more heat. In such case the PV system profit and LCOE would stay unchanged. That might be considered the theoretical best of both values (for given case). In reality though, the heat production needs to somewhat meet the heat demand and thus it is expected, that the profit would be lessened while the LCOE would rise.

The effect of decreased electricity price and lowered utilization rate can be seen from the comparison of Figures 6.18 and 6.25, Figures 6.17 and 6.24, or more accurately, comparing Tables 6.5 and 6.8.

Table 6.8 PV systems price, profit and payback period under **V3.2_DHW+SH**

System setup **70%_UT**	1.50; 0.94 kWp; kWh	2.24; 3.17 kWp; kWh	2.99; 6.53 kWp; kWh
PV system price	53 189 CZK	87 303 CZK	130 284 CZK
PV annuall benefit	*3 120* CZK	4 520 CZK	5 895 CZK
PV+DHW+SH annuall benefit	*3 769* CZK	5 225 CZK	6 636 CZK
PV payback period	*17.05* years	19.31 years	22.10 years
PV+DHW+SH payback period	*14.11* years	16.71 years	19.63 CZK

System setup **1:1.25_RT**	1.50; 1.87 kWp; kWh	2.24; 2.80 kWp; kWh	2.99; 3.74 kWp; kWh
PV system price	61 892 CZK	83 837 CZK	105 783 CZK
PV annuall benefit	3 295 CZK	4 447 CZK	5 527 CZK
PV+DHW+SH annuall benefit	3 733 CZK	5 220 CZK	6 563 CZK
PV payback period	18.79 years	18.85 years	19.14 years
PV+DHW+SH payback period	16.58 years	16.06 years	16.12 CZK

* Values in *italic* originate from systems unqualified for subsidy, thus should serve as indicative only.

6.4.1 Optimized variant

In order to determine the optimal PV system setup for **V3.2_DHW+SH**, calculation was performed two more times, optimizing for the best ratio of a photovoltaic plant price and an annual system benefit first, and next for the smallest household levelized cost of electricity.

Table 6.9 Optimization results

Optimization criteria	System setup kWp; kWh	Utilization efficiency	Yearly benefit	Payback period
System payback p.	2.43; 3.04	84.67 %	5 570 CZK	16.05 years
Household LCOE	1.97; 2.46	89.60 %	4 698 CZK	16.13 years
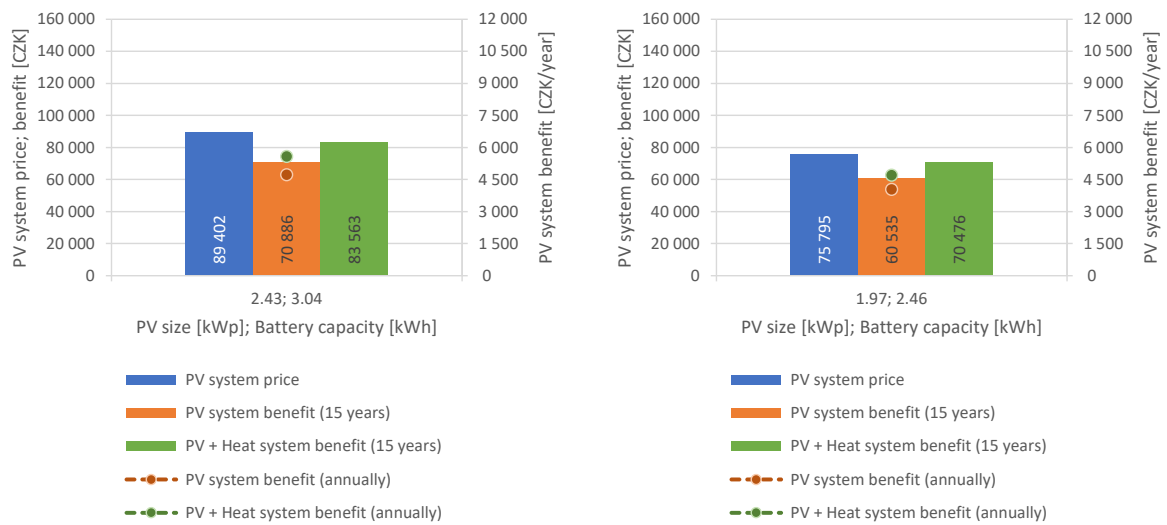
Fig. 6.26: PV system price and profit, having the system optimized for shortest bare payback period (left) or smallest LCOE (right)
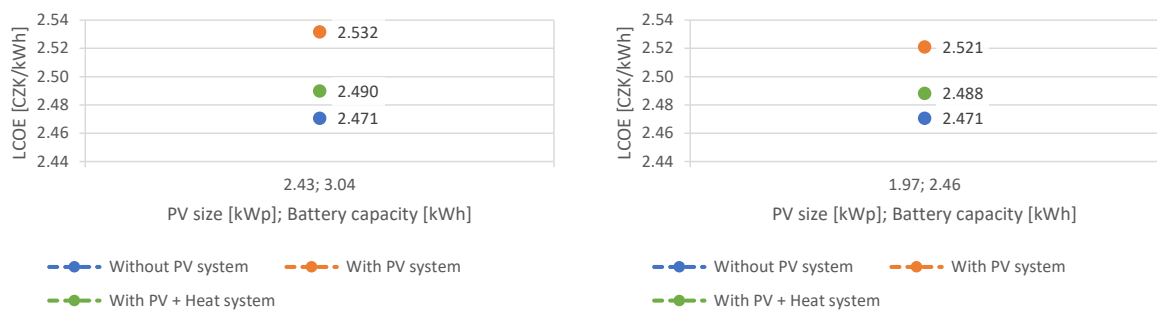
Fig. 6.27: Household LCOE, having the system optimized for shortest bare payback period (left) or smallest LCOE (right)

6.5 Results evaluation

In order to easily analyze the overall performance of various PV system setups, summary of the payback periods and LCOE change is provided in the Table 6.10. Additionally, values regarding the optimized PV systems for all four household types are presented in Table 6.11 and Table 6.12.

Table 6.10 Summary comparison of payback periods and LCOE of individual systems

System setup **70%_UT**	1.50; 0.94 kWp; kWh	2.24; 3.17 kWp; kWh	2.99; 6.53 kWp; kWh
PV system price	53 189 CZK	87 303 CZK	130 284 CZK
V1_El.App payback period	*10.03* years	11.39 years	13.04 years
V2_DHW payback period	*9.20* years	11.05 years	13.02 years
V3.1_DHW+SH payback p.	*11.52* years	13.40 years	15.65 years
V3.2_DHW+SH payback p.	*14.11* years	16.71 years	19.63 years
V1_El.App LCOE change	*-0.389* CZK/kWh	-0.612 CZK/kWh	-0.438 CZK/kWh
V2_DHW LCOE change	*-0.363* CZK/kWh	-0.338 CZK/kWh	-0.215 CZK/kWh
V3.1_DHW+SH LCOE chng.	*-0.053* CZK/kWh	-0.035 CZK/kWh	+0.018 CZK/kWh
V3.2_DHW+SH LCOE chng.	*-0.011* CZK/kWh	+0.029 CZK/kWh	+0.101 CZK/kWh
V1_El.App LCOE change	*-8.69 %*	-13.67 %	-9.79 %
V2_DHW LCOE change	*-11.36 %*	-10.58 %	-6.73 %
V3.1_DHW+SH LCOE chng.	*-2.06 %*	-1.36 %	+0.70 %
V3.2_DHW+SH LCOE chng.	*-0.45 %*	+1.17 %	+4.09 %

System setup **1:1.25_RT**	1.50; 1.87 kWp; kWh	2.24; 2.80 kWp; kWh	2.99; 3.74 kWp; kWh
PV system price	61 892 CZK	83 837 CZK	105 783 CZK
V1_El.App payback period	10.83 years	*11.18* years	*11.59* years
V2_DHW payback period	10.75 years	10.77 years	11.08 years
V3.1_DHW+SH payback p.	13.58 years	12.93 years	12.86 years
V3.2_DHW+SH payback p.	16.58 years	16.06 years	16.12 years
V1_El.App LCOE change	*-0.157* CZK/kWh	*-0.638* CZK/kWh	*-0.696* CZK/kWh
V2_DHW LCOE change	*-0.265* CZK/kWh	-0.357 CZK/kWh	-0.405 CZK/kWh
V3.1_DHW+SH LCOE chng.	*-0.022* CZK/kWh	-0.045 CZK/kWh	-0.058 CZK/kWh
V3.2_DHW+SH LCOE chng.	*+0.019* CZK/kWh	+0.018 CZK/kWh	+0.024 CZK/kWh
V1_El.App LCOE change	*-3.51 %*	*-14.25 %*	*-15.55 %*
V2_DHW LCOE change	*-8.29 %*	-11.17 %	-12.68%
V3.1_DHW+SH LCOE chng.	*-0.85 %*	-1.75 %	-2.25 %
V3.2_DHW+SH LCOE chng.	*+0.77 %*	+0.73 %	+0.97 %

* Values in *italic* originate from systems unqualified for subsidy, thus should serve as indicative only.

Quickly examining the values of systems payback period and LCOE, clear correlation can be seen. If the bare payback time outreaches the assumed lifespan of photovoltaic system, LCOE for given household type increases in comparison to LCOE of household without PV system. The same is also applicable other way round.

Table 6.11 Payback period optimized systems comparison

Household variant	System setup kWp; kWh	PV system price	Profit per year	Payback period
V1_El.App	1.27; 1.59	55 330 CZK	5 132 CZK	10.78 y
V2_DHW	1.81; 2.26	71 005 CZK	6 647 CZK	10.68 y
V3.1_DHW+SH	2.89; 3.61	102 834 CZK	7 998 CZK	12.86 y
V3.2_DHW+SH	2.43; 3.04	89 402 CZK	5 570 CZK	16.05 y

Household variant	System setup kWp; kWh	Utilization rate	LCOE change	LCOE change
V1_El.App	1.27; 1.59	83.95 %	-0.482 CZK/kWh	-10.77 %
V2_DHW	1.81; 2.26	97.64 %	-0.311 CZK/kWh	-9.73 %
V3.1_DHW+SH	2.89; 3.61	91.85 %	-0.057 CZK/kWh	-2.21 %
V3.2_DHW+SH	2.43; 3.04	84.67 %	+0.019 CZK/kWh	+0.77 %

Table 6.12 LCOE optimized systems comparison

Household variant	System setup kWp; kWh	PV system price	Profit per year	Payback period
V1_El.App	2.04; 2.55	77 960 CZK	7 039 CZK	11.08 y
V2_DHW	3.54; 4.42	121 844 CZK	10 694 CZK	11.39 y
V3.1_DHW+SH	3.88; 4.85	131 828 CZK	10 108 CZK	13.04 y
V3.2_DHW+SH	1.97; 2.46	75 795 CZK	4 698 CZK	16.13 y

Household variant	System setup kWp; kWh	Utilization rate	LCOE change	LCOE change
V1_El.App	2.04; 2.55	70.00 %	-0.616 CZK/kWh	-13.76 %
V2_DHW	3.54; 4.42	77.58 %	-0.418 CZK/kWh	-13.08 %
V3.1_DHW+SH	3.88; 3.88	85.83 %	-0.066 CZK/kWh	-2.56 %
V3.2_DHW+SH	1.97; 2.46	89.60 %	+0.017 CZK/kWh	+0.69 %

Comparing the values from Tables 6.10, 6.11 and 6.11, it is fairly noticeable that the systems designed for **V2_DHW** show the best bare payback period. Out of such observation, it may be concluded, that the benefit of using the DHW storage tank for PV surplus utilization outweighs the decline in the electricity value, compared to **V1_El.App**. That can not be said of PV systems under conditions of **V3.1_DHW+SH**, where despite the general increase in PV energy utilization (see the Table 6.4) negative effect of reduced electricity price prevails, extending the payback period. This adverse trend is even more pronounced in the PV systems for **V3.2_DHW+SH**, resulting in the worst performance out of all studied household types and PV system combinations.

On the other hand, examining the LCOE criteria, it can be seen that the household type **V1_El.App** profits the most from the combination with photovoltaic system. The reason behind is fairly simple, given by the highest absolute price of electricity out of all studied variants.

Visualizing the results for clearer comparison, Figures 6.28, 6.29 and 6.30 are provided. In addition to the established marking, **OPT_P.P.** and **OPT_LCOE** is used here, standing for systems "Optimized for the shortest Payback Period" and "Optimized for lowest LCOE". In order to better distinguish between household types, **V1_El.App** is colored yellow, **V2_DHW** blue, **V3.1_DHW+SH** red and **V3.2_DHW+SH** green.

Within the first figure, all subsidy-eligible variants are organized by their payback period. It comes as no surprise, that for each household type, the first of its kind presented is always the optimized one. Portrayed results further support the claims, that the **V2_DHW** generate the fastest bare return rate, closely seconded by **V1_El.App**. Both households types combined with PV systems stand above the other variants, if constructed properly. As a deterrent example of faulty design, variants V1_El.App; 70%_UT; 2.99; 6.53 and V2_DHW; 70%_UT; 2.99; 6.53 may serve.

Figures 6.29 and 6.30 display outputs of LCOE criteria, where for both, results are sorted in accordance with absolute LCOE change (compared to the household without photovoltaic system). Confirming the aforementioned conclusions, household type **V1_El.App** is proved to have the best potential for LCOE decrease, both in absolute and relative numbers. Speaking of the latter, **V2_DHW** does not lag behind.

Regarding the **V3.1_DHW+SH** and **V3.2_DHW+SH**, both households types provide unsatisfactory results, once connected with a photovoltaic system. For the second mentioned, such investment would even increase the LCOE overall. Such outcome is mainly caused by the low electricity price in a first place, whereas assuming only "uncontrolled" systems also plays its role.
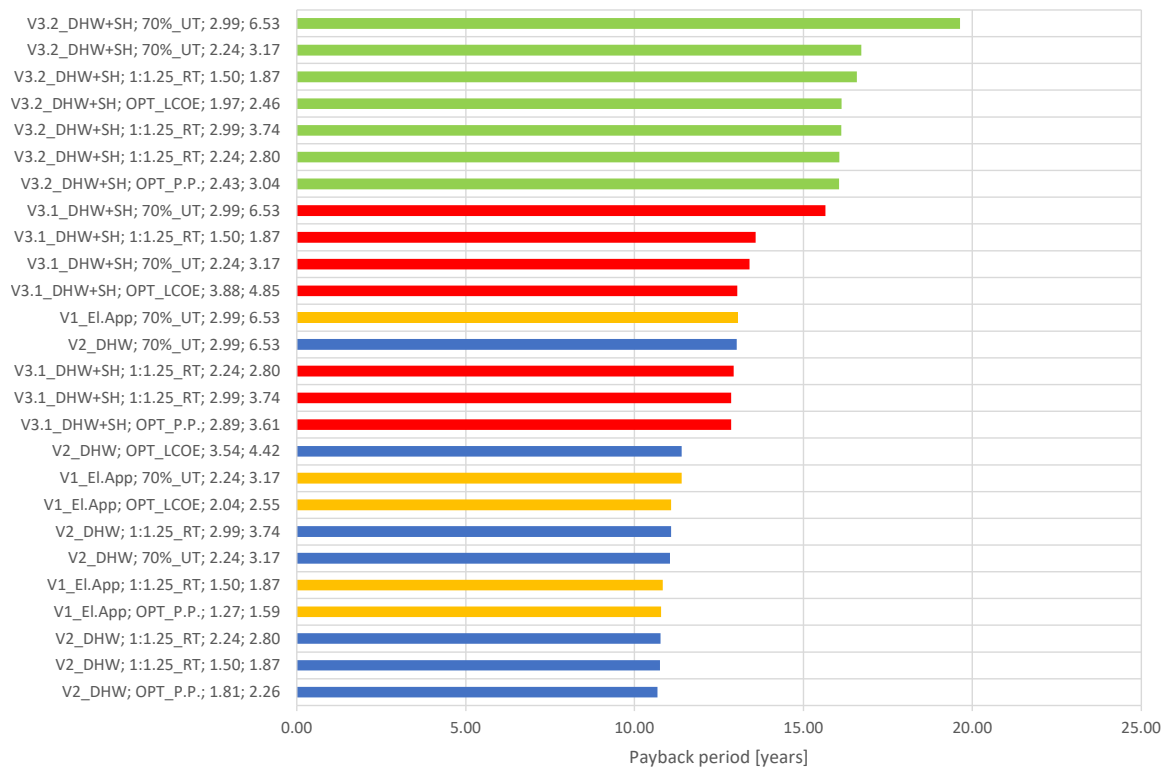
Fig. 6.28: Household setups comparison based on the bare payback period
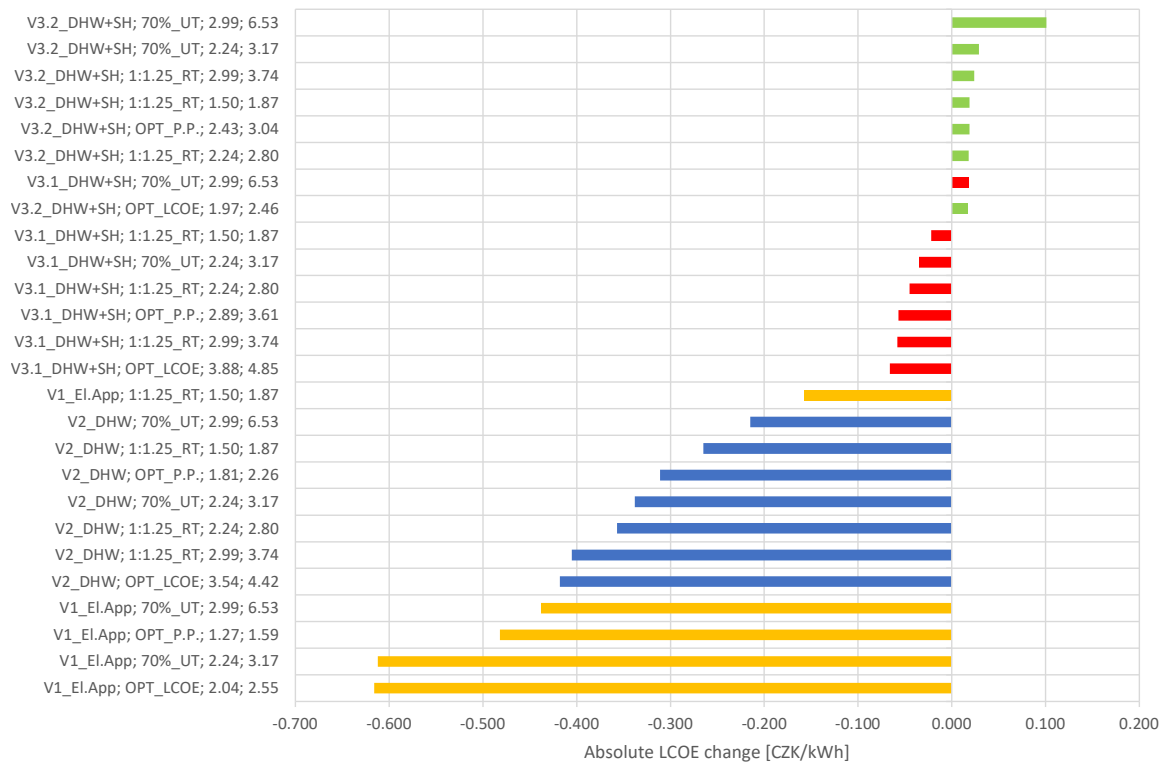
Fig. 6.29: Household setups comparison based on the absolute LCOE change
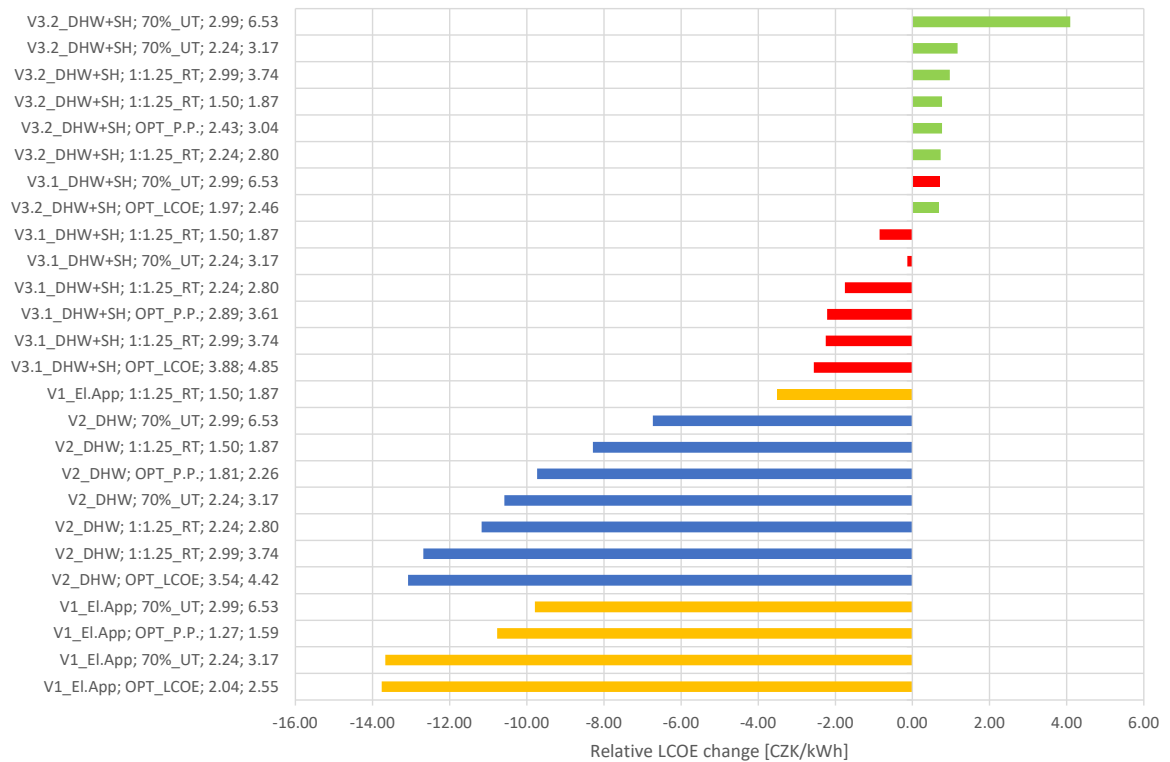
Fig. 6.30: Household setups comparison based on the relative LCOE change

Generally speaking, investment in simple hybrid photovoltaic system with battery storage can by only justified in case of either households with high electricity price, or above-average electrical demands (not focused in the study). Under such conditions, it is certain to repay the costs of the system prior to its end of life.

Regarding the two studied approaches to PV system sizing, if focused on quick payback time, rather a smaller photovoltaic setups should be preferred. On the other hand, if the investor has sufficient funds, optimizing the PV system for the lowest LCOE may prove itself worth it. Such concept provides slightly increased payback period, yet over the system service life brings higher absolute benefit. Contrarily, in relative values, PV system benefit compared the to system price is lower (bare return on investment).

Table 6.13 Absolute vs relative benefit of optimized PV systems

Household variant	System price	Service life benefit	Absolute bare benefit	Realtive bare benefit
V1_El.App; OPT_P.P.	55 330 CZK	76 974 CZK	21 644 CZK	39.12 %
V1_El.App; OPT_LCOE	77 960 CZK	105 578 CZK	27 618 CZK	35.43 %
V2_DHW; OPT_P.P.	71 005 CZK	99 699 CZK	28 694 CZK	40.41 %
V2_DHW; OPT_LCOE	121 844 CZK	160 422 CZK	38 578 CZK	31.66 %

Aside from these suggestions, it would be hard to provide more precise guidelines for PV systems size, solely based on household consumption, as the electricity billing tariff seemingly plays a crucial role. Also, more extensive study focused on each household type PV system setups would be necessary is that case.

On top of that, design of photovoltaic power plant may not always follow strictly economic indicators. For example the added value of potential back-up power source, or the effect of stabilizing users energy prices for the future may also justify "non-optimal" systems.

All in all, from the study it is possible to get a basic idea of suitable variants of photovoltaic systems for average households types, which can serve as a starting point for choosing a specific system for a particular household.

6.6 Broader perspective

As it can be seen from the achieved results, PV system revenue is highly dependent on electricity prices, whereas only a slight change crucially affects the system benefits. A parallel to that can be seen in gas heated households, where the unit value of thermal energy is even lower. For that reason it is questionable, whether it is worth investing in modifying gas heated accumulation tanks to act as PV surplus utilization capacity. In such cases, small photovoltaic hybrid system may prove itself more valuable and less technically challenging.

It is also important to note, that only simple "uncontrolled" PV + heat systems were considered, which do not utilize the full potential of such combination. Adding a basic control unit to adjust the heater operation in accordance with PV system production can lead to a considerable increase in the utilization rate and a decrease in energy bills.
Neither the combination of PV plant and plug-in hybrid or battery electric vehicle was investigated, which may serve as large PV surplus utilization capacity. Especially, once the option to discharge battery of electromobile for household needs becomes more widespread.

Speaking of cycling the battery pack, no matter whether it is part of the vehicle or standalone storage, each cycle wears out the battery, not to mention its natural aging. To perform exhaustive analysis of PV systems, both these effects needs to be considered and included within the calculation. On top of those, depth of discharge, charging and discharging rate and operational temperature considerably affects the battery life.
It is to be noted, that through the study, PV system service life was not excessively investigated due to the complexity of such task.

No matter that, results obtained during the work may serve as a guidance for a photovoltaic systems design, under the legislation and environmental conditions in the Czech Republic. Thanks to the base line - modeling of PV power plant output and household energy demands with an 1-hour time step - acquired results stand high above the "informed guess", comparing the annual household consumption with an annual photovoltaic system production. Despite its obvious inappropriateness, such approach is often used to make decisions, leading to false assumptions and an improper design.

6.7 Further work

Given the limited time, not all available model capabilities have been used to its fullest. Interesting fields of study would be comparing the performance of once optimized PV setups in different locations of Czech Republic. Also evaluating the effect of deviation of the system size from the optimized variant by 1 %; 5 %; 10 %... on the overall payback period of the system might provide valuable findings. Least but not last, the impact of simulation step size on obtained results and their precision may be examined. All of these would be achievable without any modifications to the current model.

The simulation tool however, was implemented with a high degree of versatility, allowing for further expansions. Therefore the household variant with electrical vehicle may be easily implemented and studied. Similarly, if further developed, potential of controlled PV + heat systems can be investigated.

Bibliography

Almeida, A., Fonseca, P., Schlomann, B., Feilberg, N. Characterization of the Household Electricity Consumption in the EU, Potential Energy Savings and Specific Policy Recommendations. *Energy & Buildings*, 2011, vol. 43, p. 1884–1894.

Andersen, F. M., Baldini, M., Hansen, L. G., Jensen, C. L. Households' hourly electricity consumption and peak demand in Denmark. *Applied Energy*, 2017, vol. 208, p. 607–619.

Angenendt, G., Zurmühlen, S., Rücker, F., Axelsen, H., Sauer, D. U. Optimization and operation of integrated homes with photovoltaic battery energy storage systems and power-to-heat coupling. *Energy Conversion and Management: X*, 2019, vol. 1, p. 100005.

Antonio, L., Hegedus, S. *Handbook of photovoltaic science and engineering*. Praha: John Wiley & Sons, Ltd, 2010

Atanasoae, P. Technical and Economic Assessment of Micro-Cogeneration Systems for Residential Applications. *Sustainability*, 2020, vol. 12, Č. 3, p. 1074.

Beltran, H., Ayuso, P., Perez, E. Lifetime Expectancy of Li-Ion Batteries used for Residential Solar Storage. *Energies*, 2020, vol. 13, Č. 3, p. 568.

Brownson, J. R. S. Declination, latitude and solar hour angle. https://www.e-education.psu.edu/eme810/node/484, 2020a. [Online; accessed 15-November-2020].

Brownson, J. R. S. Diagram of the multiple components of the clear sky. https://www.e-education.psu.edu/eme810/node/683, 2020b. [Online; accessed 16-November-2020].

Cooper, P. I. The Absorption of Solar Radiation in Solar Stills. *Solar Energy*, 1969, vol. 12, p. 333–346.

Demain, C., Journée, M., Bertrand, C. Evaluation of different models to estimate the global solar radiation on inclined surfaces. *Renewable Energy*, 2013, vol. 50, p. 710–721.

Erbs, D., Klein, S., Duffie, J. Estimation of the diffuse radiation fraction for hourly, daily and monthly-average global radiation. *Solar Energy*, 1982, vol. 28, p. 293–302.

Garcia, A. M., Huld, T. Performance comparison of different models for the estimation of global irradiance on inclined surfaces. 2013, .

Green Rhino Energy. Declination and latitude. http://www.greenrhinoenergy.com/solar/radiation/geometry.php, 2016. [Online; accessed 15-November-2020].

Hay, J. E., Davies, J. A. (ed.). *Calculation of the Solar Radiation Incident on an Inclined Surface*, vol. 59. Ministry of Supply and Services, 1980. Canada.

Jakhrani, A., Al-Khalid, O., Rigit, A., Samo, S., Kamboh, S. Estimation of Incident Solar Radiation on Tilted Surface by Different Empirical Methods. *International Journal of Scientific and Research Publications*, 2012, vol. 2, p. 1–6.

Klucher, T. Evaluation of models to predict insolation on tilted surfaces. *Solar Energy*, 1979, vol. 23, p. 111–114.

Knight, I., Manning, N., Swinton, M., M.R.Hajo. *European and Canadian non-HVAC electric and DHW load profiles for use in simulating the performance of residential cogeneration systems*. Tech. zpr., 2007.

Lee, S., Whaley, D., Saman, W. Electricity Demand Profile of Australian Low Energy Houses. *Energy Procedia*, 2014, vol. 62, p. 91–100.

Leeuwen, R. P., Fink, J., Wit, J. B., Smit, G. Upscaling a district heating system based on biogas cogeneration and heat pumps. *Energy, Sustainability and Society*, 2015, vol. 5, Č. 1.

Li, Z., Xing, H., Zeng, S. (ed.). *Effect of the application between anisotropic and isotropic diffuse radiation model on building diffuse radiation heat gain*, vol. 15. IBPSA Conference, 2017. USA.

Liu, B., Jordan, R. Daily insolation on surfaces tilted towards equator. *ASHRAE Transactions*, 1962, vol. 67, p. 526–541.

Loutzenhiser, P. G., Manz, H., Felsmann, C., Strachan, P. A., Frank, T., Maxwell, G. M. Empirical validation of models to compute solar irradiance on inclined surfaces for building energy simulation. *Solar Energy*, 2007, vol. 81, p. 254–267.

Lutz, J. *Hot Water Draw Patterns in Title 24*. Tech. zpr., 2017.

Medved, S., Domjan, S., Arkar, C. *Domestic Hot Water Heating in nZEB*, Cham: Springer International Publishing. ISBN 978-3-030-02822-0, 2019, p. 269–288.

Muneer, T. Solar radiation model for Europe. *Building Services Engineering Research and Technology*, 1990, vol. 11, p. 153–163.

Narayan, N., Papakosta, T., Vega-Garita, V., Qin, Z., Popovic-Gerber, J., Bauer, P., Zeman, M. Estimating battery lifetimes in Solar Home System design using a practical modelling methodology. *Applied Energy*, 2018, vol. 228, p. 1629–1639.

Olson, D., Baklen, B. E. Utility-scale solar PV: From big to biggest. 2019.

Palmer, J., Terry, N., Kane, T. *Household Electricity Survey*. Tech. zpr., UK Department of Energy & Climate Change, 2013.

Perez, R., Ineichen, P., Seals, R., Michalsky, J., Stewart, R. Modeling daylight availability and irradiance components from direct and global irradiance. *Solar Energy*, 1990, vol. 44, p. 271–289.

Perez, R., Seals, R., Ineichen, P., Stewart, R., Menicucci, D. A new simplified version of the Perez diffuse irradiance model for tilted surfaces. *Solar Energy*, 1987, vol. 39, p. 221–232.

Perez, R., Stewart, R., Seals, R., Guertin, T. The development and verification of the Perez diffuse radiation model. 1988, vol. 81.

Rehman, H., Hirvonen, J., Sirén, K. Design of a Simple Control Strategy for a Community-size Solar Heating System with a Seasonal Storage. *Energy Procedia*, 2016, vol. 91, p. 486–495.

Reindl, D. T., Beckman, W. A., Duffie, J. A. Evaluation of Hourly Tilted Surface Radiation Models. *Solar Energy*, 1990, vol. 45, p. 9–17.

REN21. *Renewables 2020 Global Status Report*. Tech. zpr., National Technical University of Athens, 2020.

SFŽP. Závazné pokyny pro žadatele RD. 2020.

Sweetnam, T., Spataru, C., Barrett, M., Carter, E. Domestic demand-side response on district heating networks. *Building Research & Information*, 2018, vol. 47, Č. 4, p. 330–343.

Temps, R. C., Coulson, K. L. Solar radiation incident upon slopes of different orientations. *Solar Energy*, 1977, vol. 19, p. 179–184.

Tian, Z., Perers, B., Furbo, S., Fan, J., Deng, J., Dragstead, J. A Comprehensive Approach for Modelling Horizontal Diffuse Radiation, Direct Normal Irradiance and Total Tilted Solar Radiation Based on Global Radiation under Danish Climate Conditions. *Energies*, 2018, vol. 11, p. 1315.

TRNSYS, T. E. S. S. (ed.). *TRNSYS 17 -Volume 7 Programmer's Guide*, vol. 7. TRNSYS: Madison, WI, 2014. USA.

Vaz, W. S. Multiobjective Optimization of a Residential Grid-Tied Solar System. *Sustainability*, 2020, vol. 12, Č. 20, p. 8648.

Watson, S., Lomas, K., Buswell, R. Decarbonising domestic heating: What is the peak GB demand? *Energy Policy*, 2019, vol. 126, p. 533–544.

Whiteman, C. D., Allwine, K. J. Extraterrestrial solar radiation on inclined surfaces. *Environmental Software*, 1986, vol. 1, p. 164–196.

Yang, D. Solar radiation on inclined surfaces: Corrections and benchmarks. *Solar Energy*, 2016, vol. 136, p. 288–302.

Zimmermann, J. P., Evans, M., Griggs, J., King, N., Harding, L., Roberts, P., Evans, C. *Household Electricity Survey - A study of domestic electrical produc usage*. Report Issue 4, Intertek Testing & Certification Ltd., 2012.

Appendices

Appendix A. - Radiation model validation figures

Fig. A.1: Total irradiance absolute (top) and relative (bottom) error - January
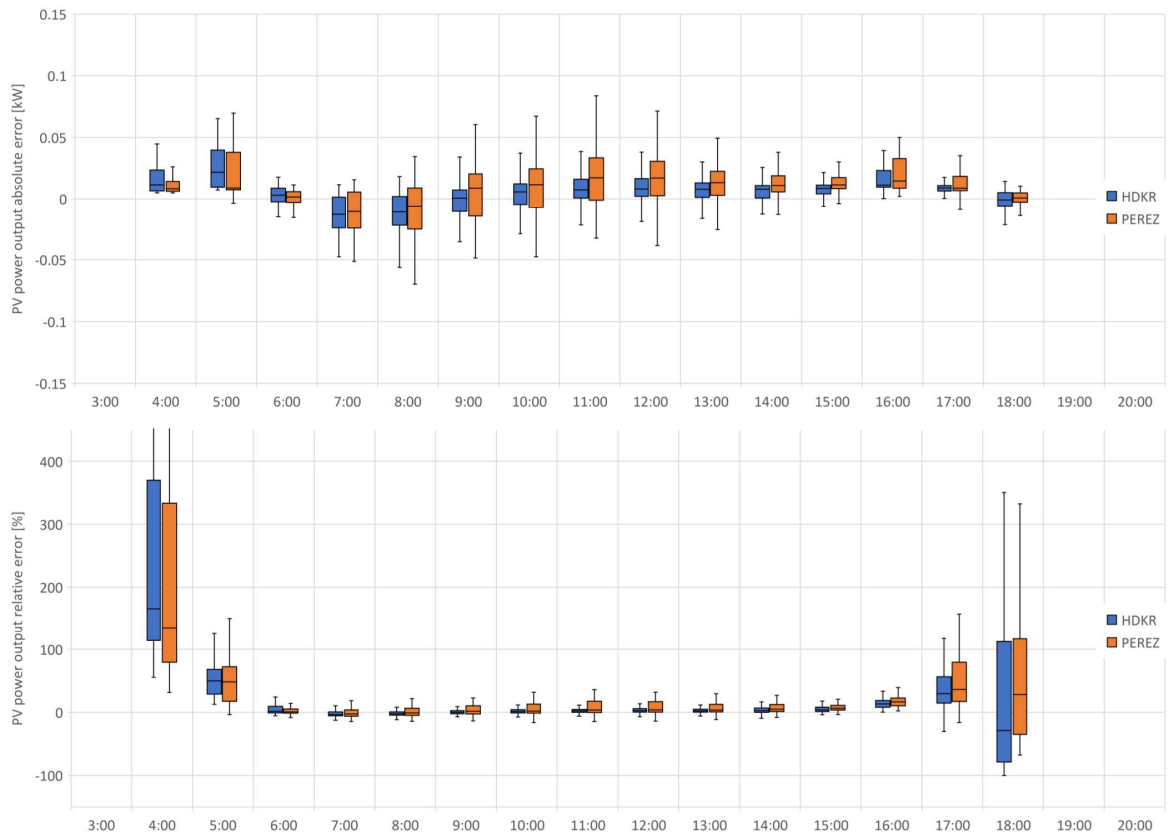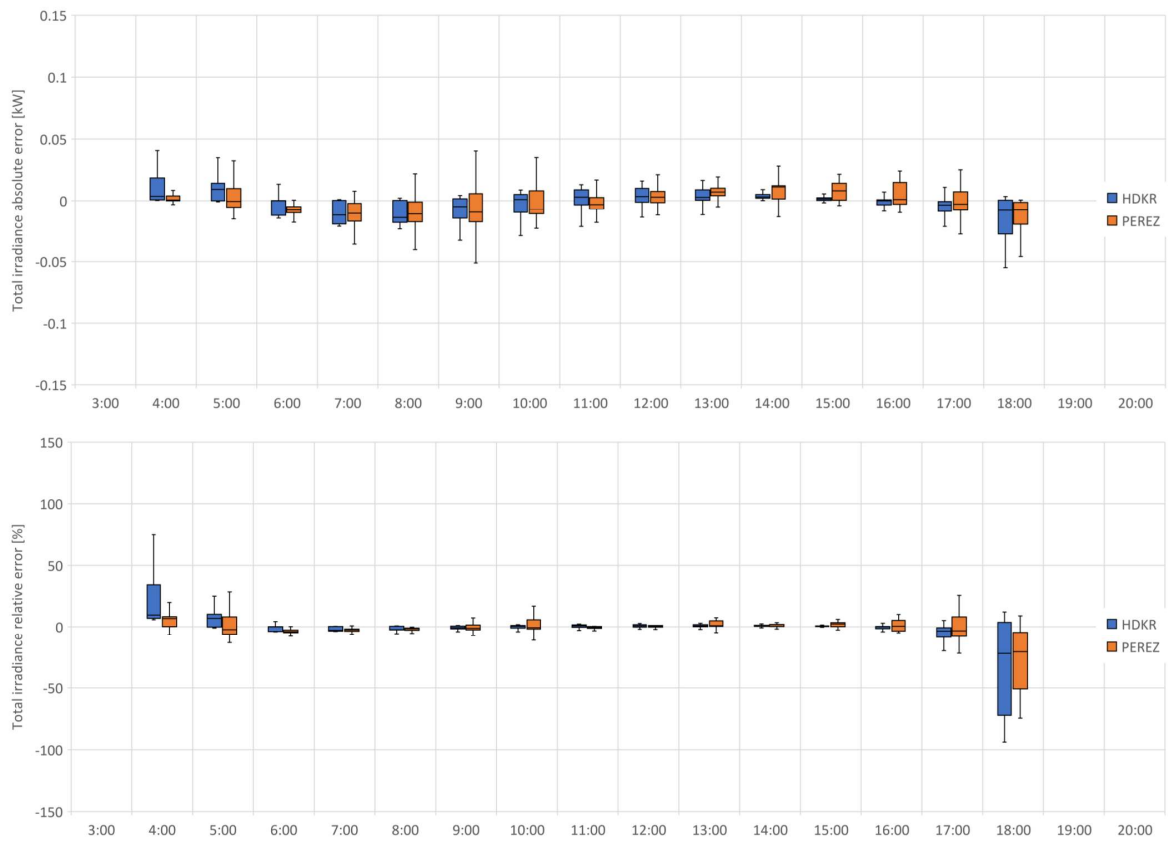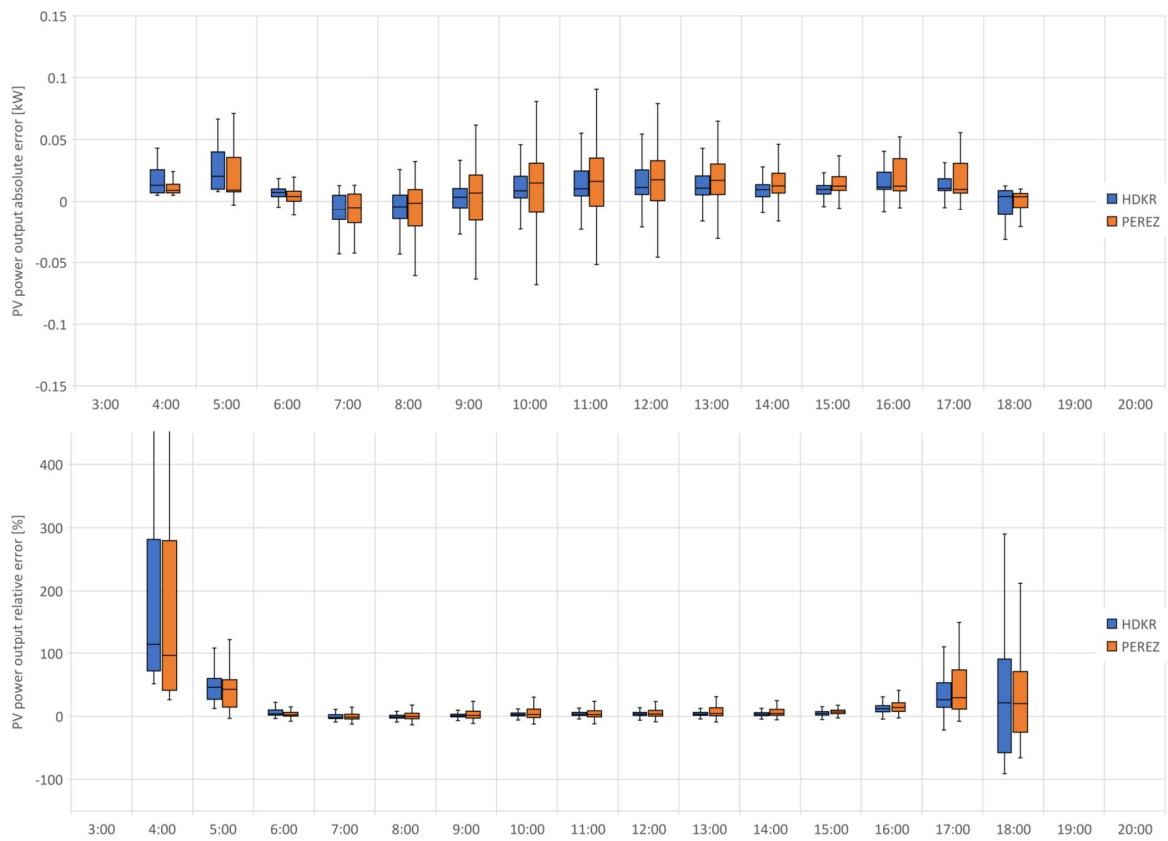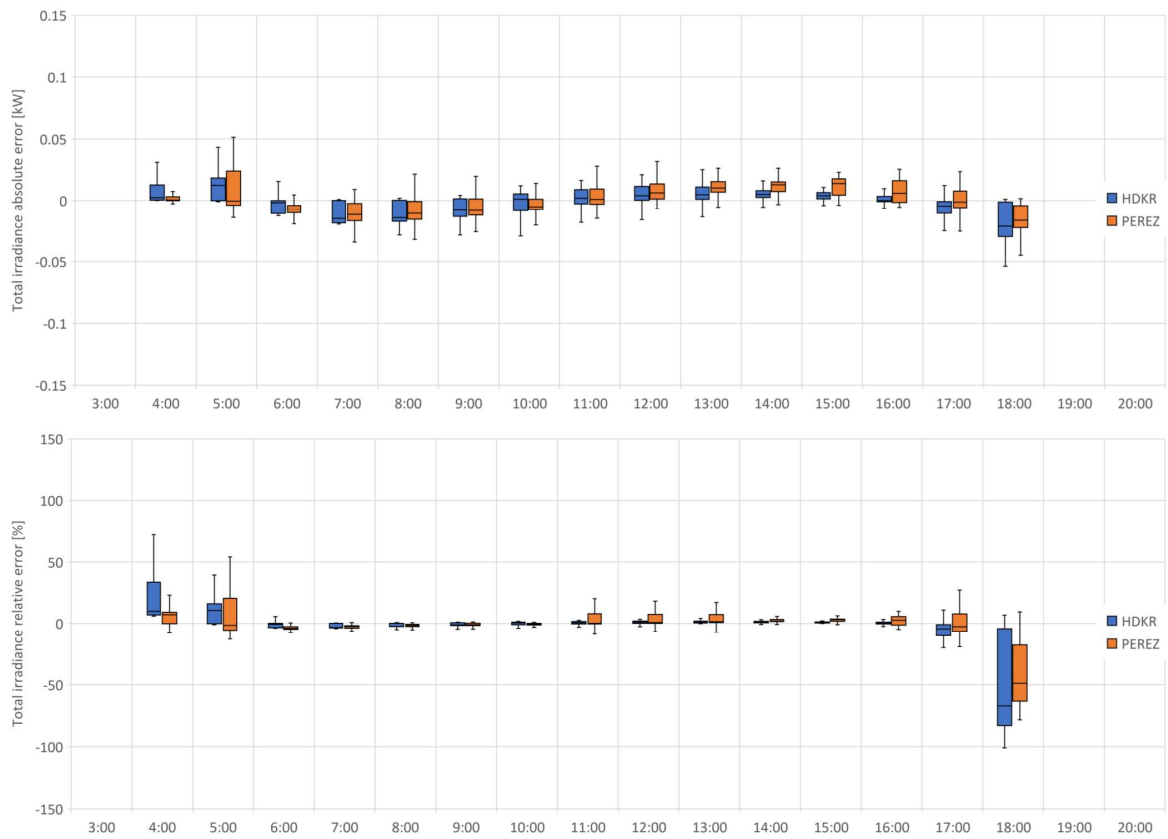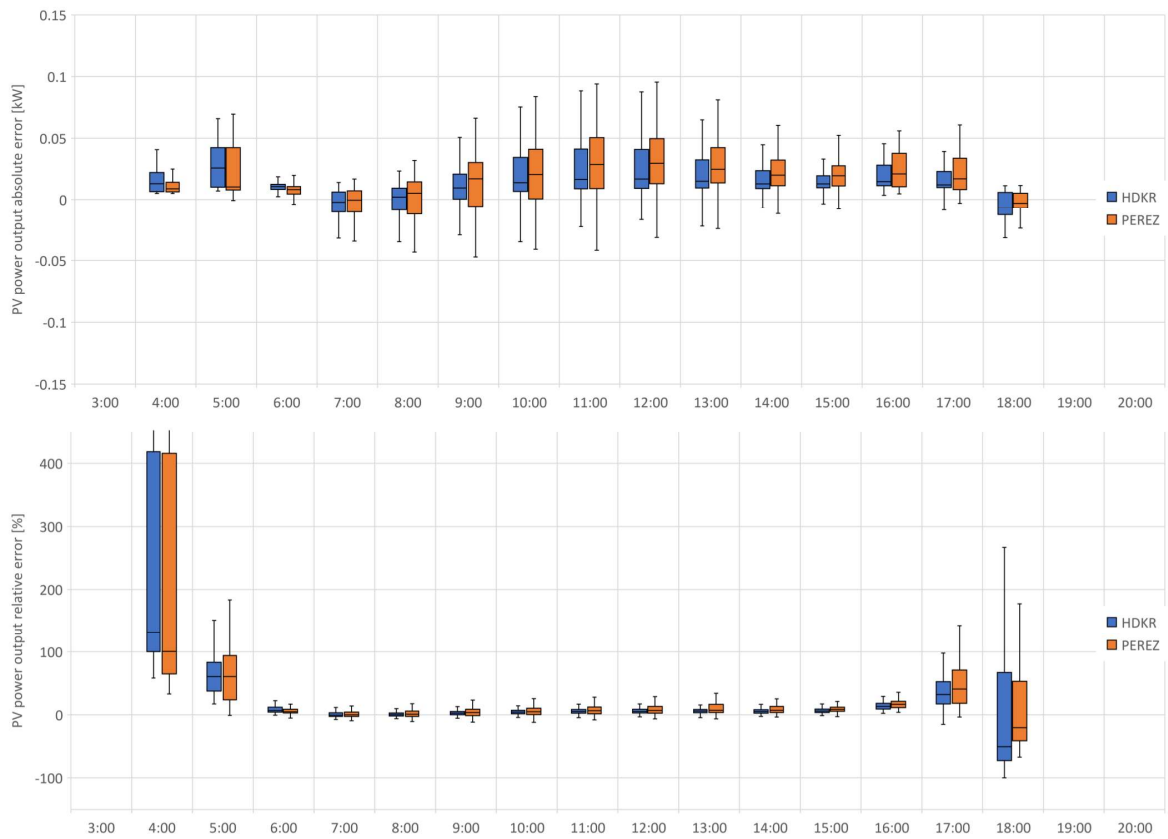

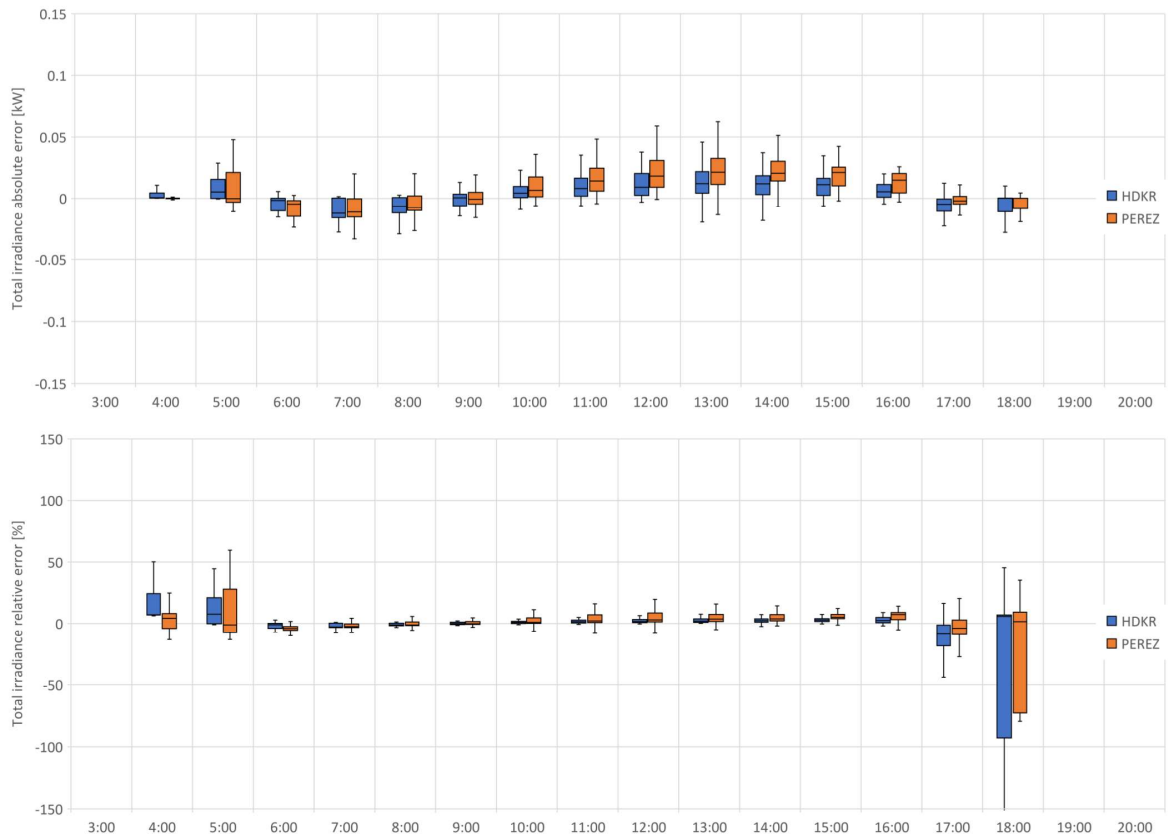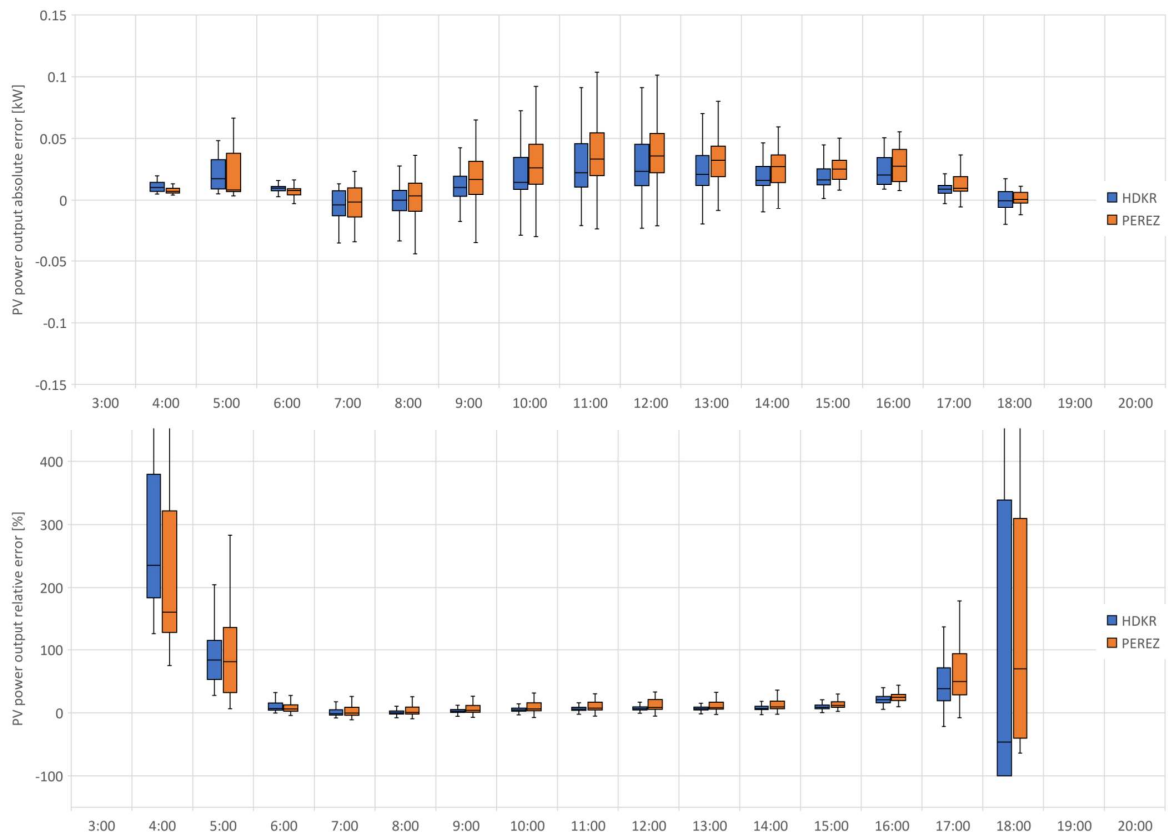Fig. A.2: Photovoltaics power output absolute (top) and relative (bottom) error - January
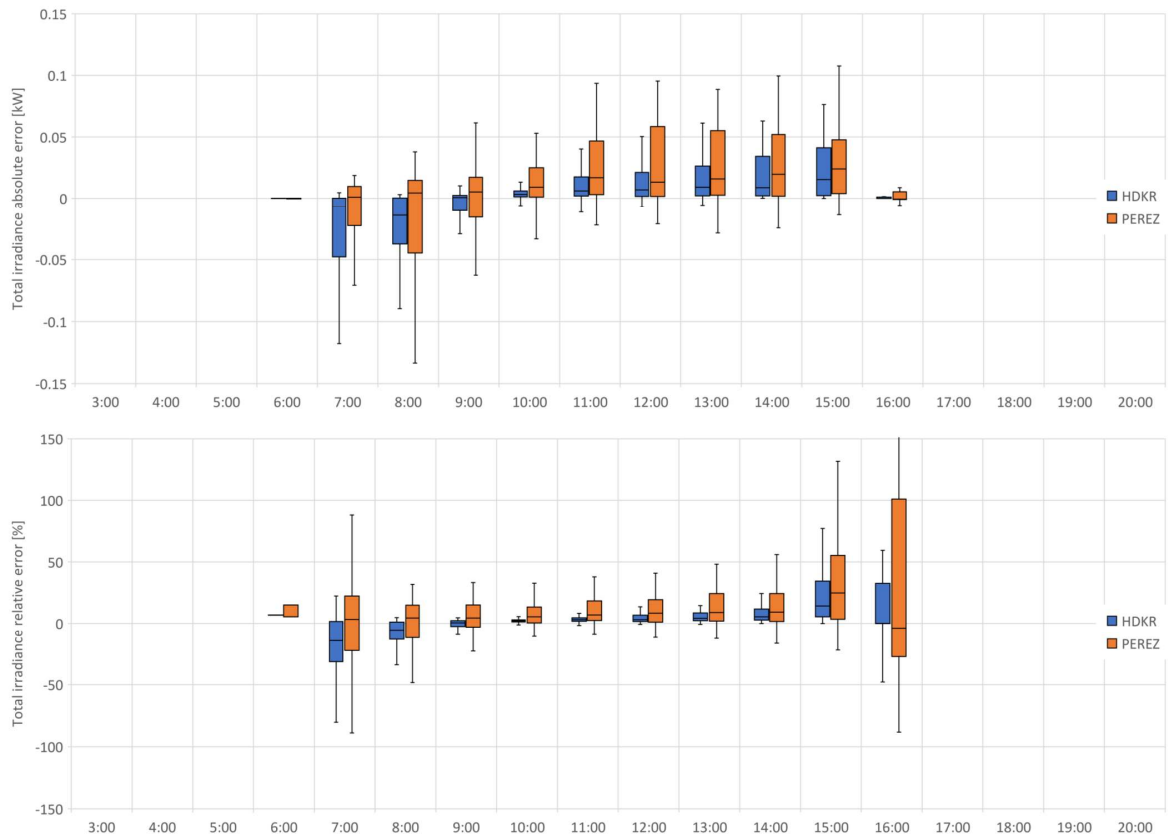
Fig. A.3: Total irradiance absolute (top) and relative (bottom) error - February
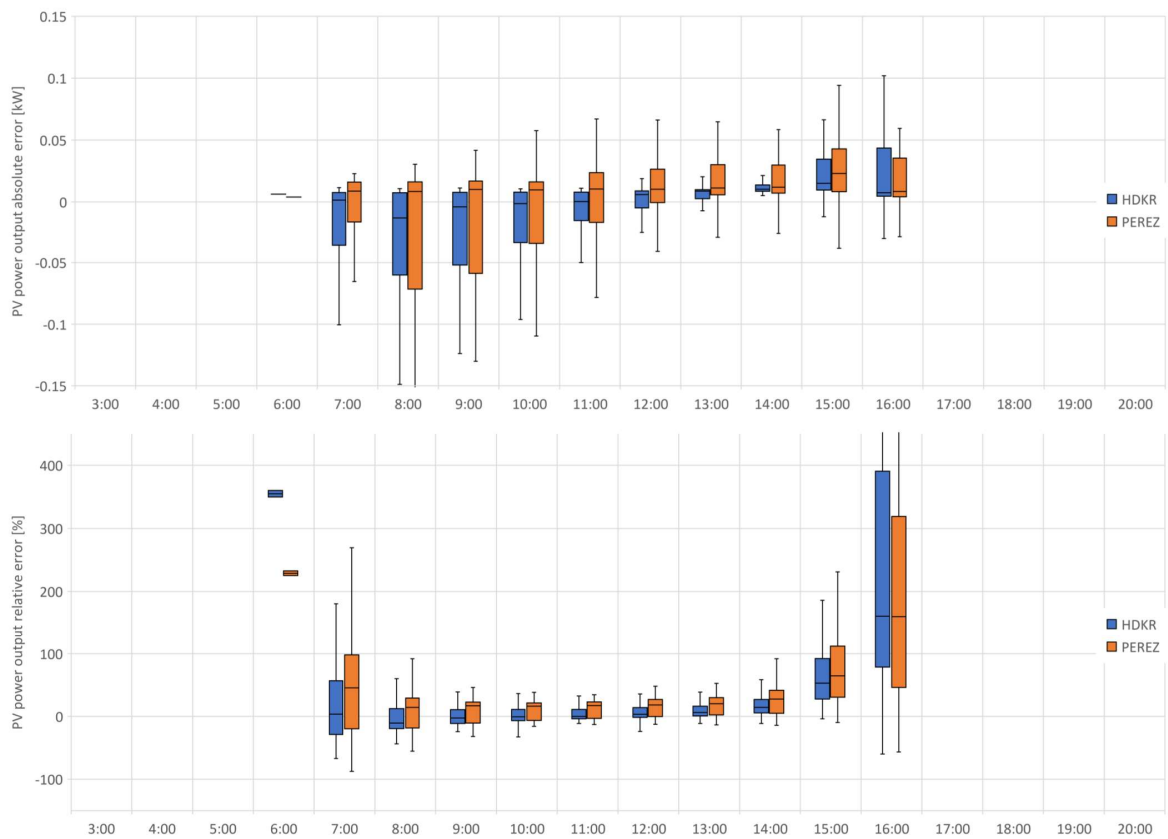
Fig. A.4: Photovoltaics power output absolute (top) and relative (bottom) error - February
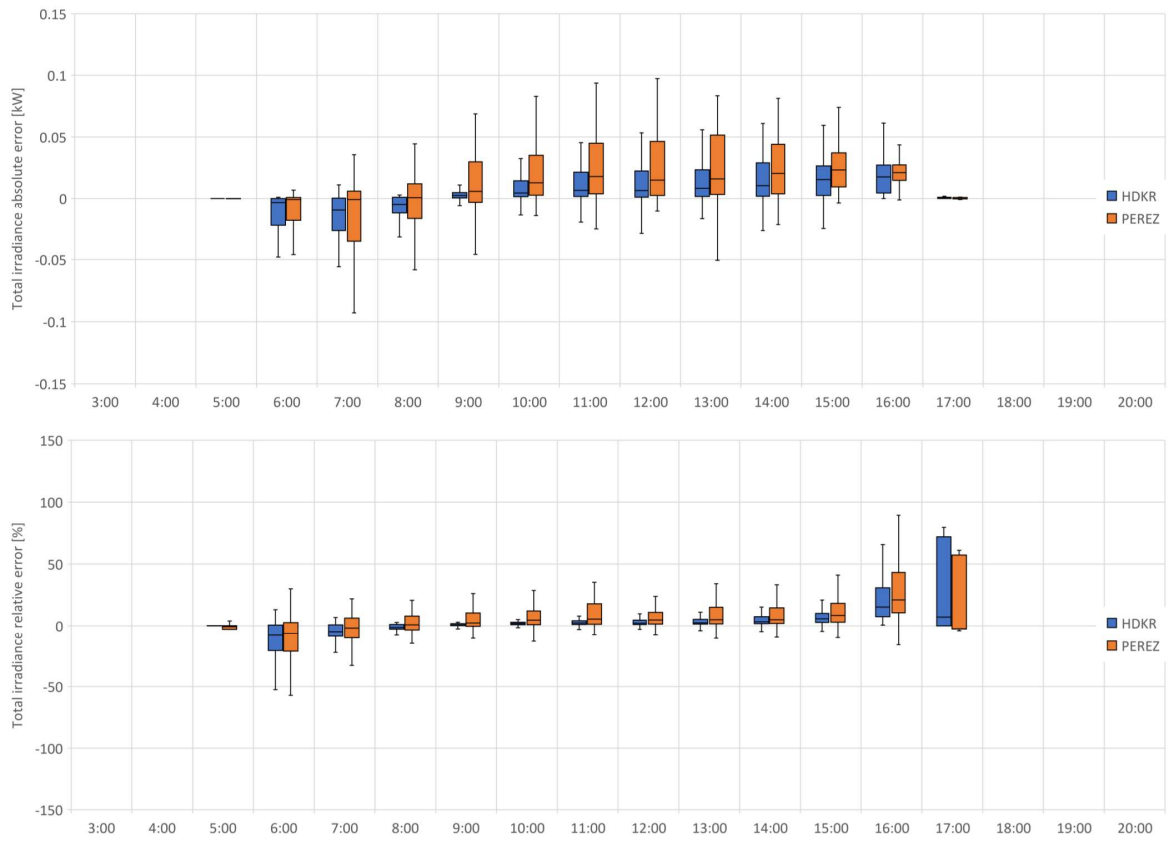
Fig. A.5: Total irradiance absolute (top) and relative (bottom) error - March
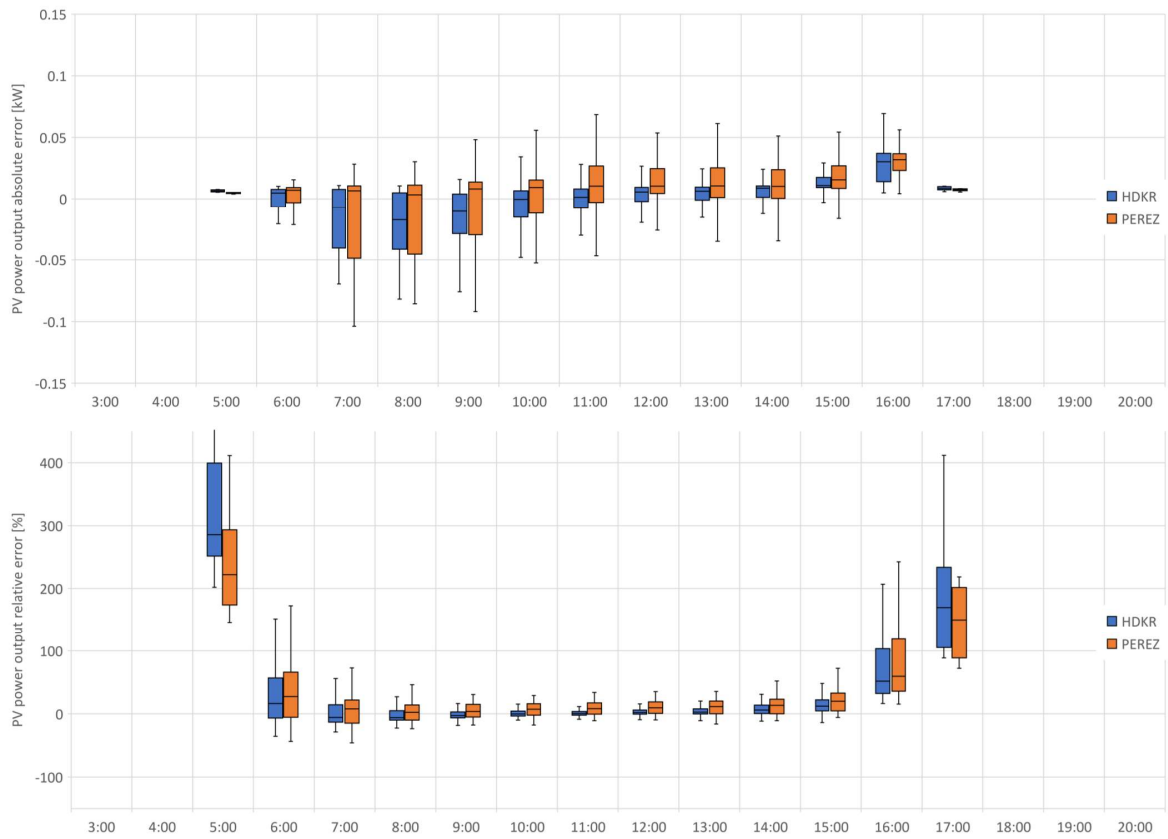
Fig. A.6: Photovoltaics power output absolute (top) and relative (bottom) error - March
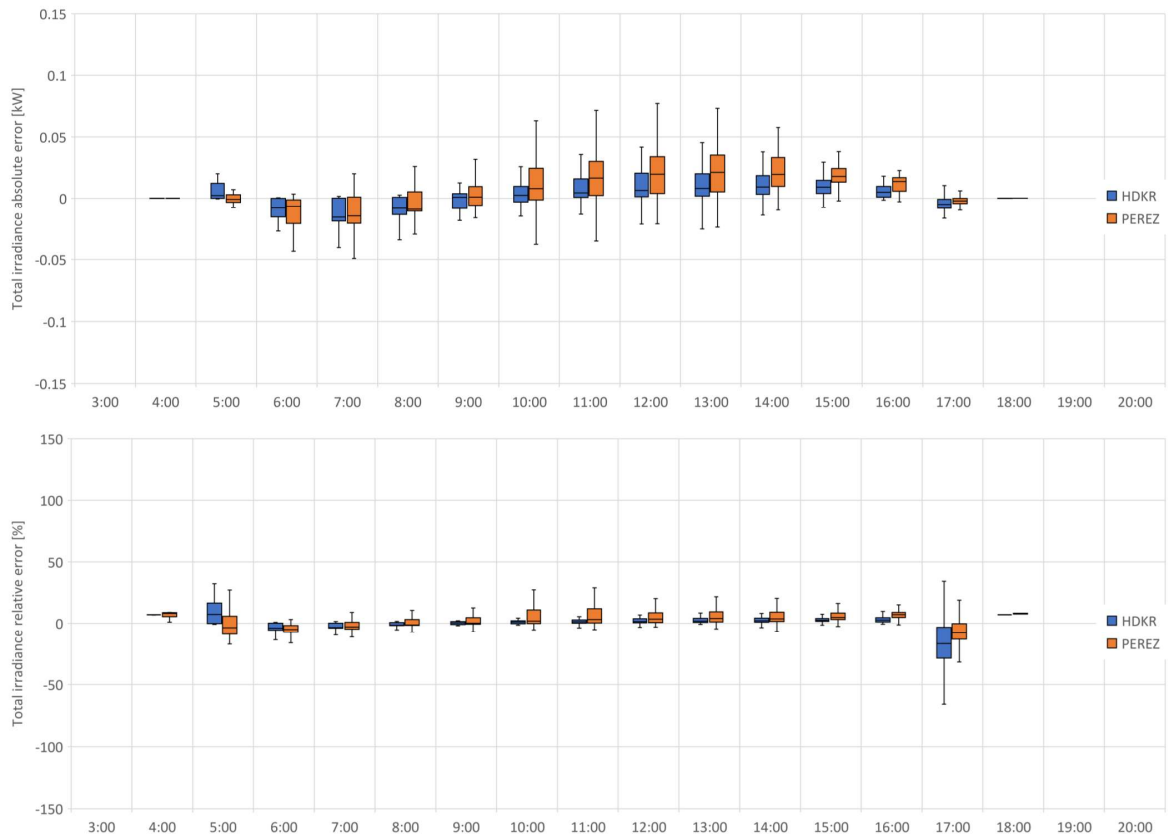
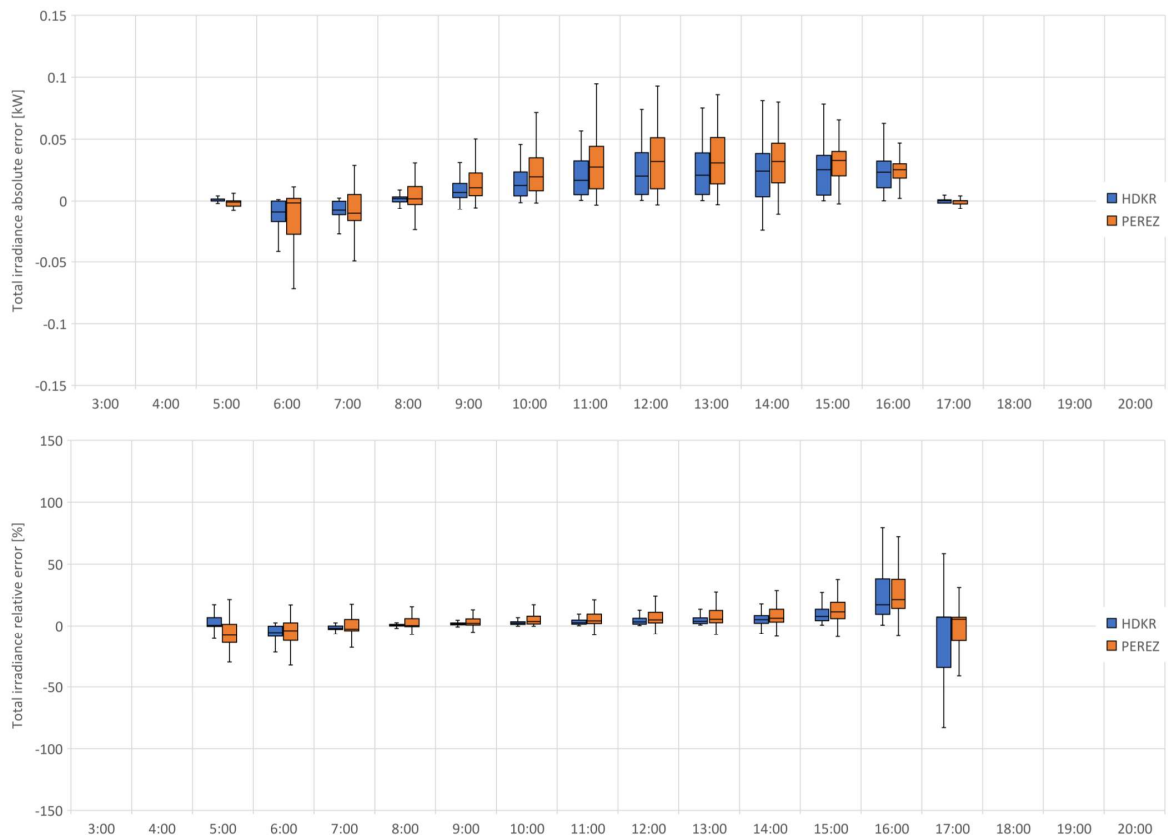Fig. A.7: Total irradiance absolute (top) and relative (bottom) error - April
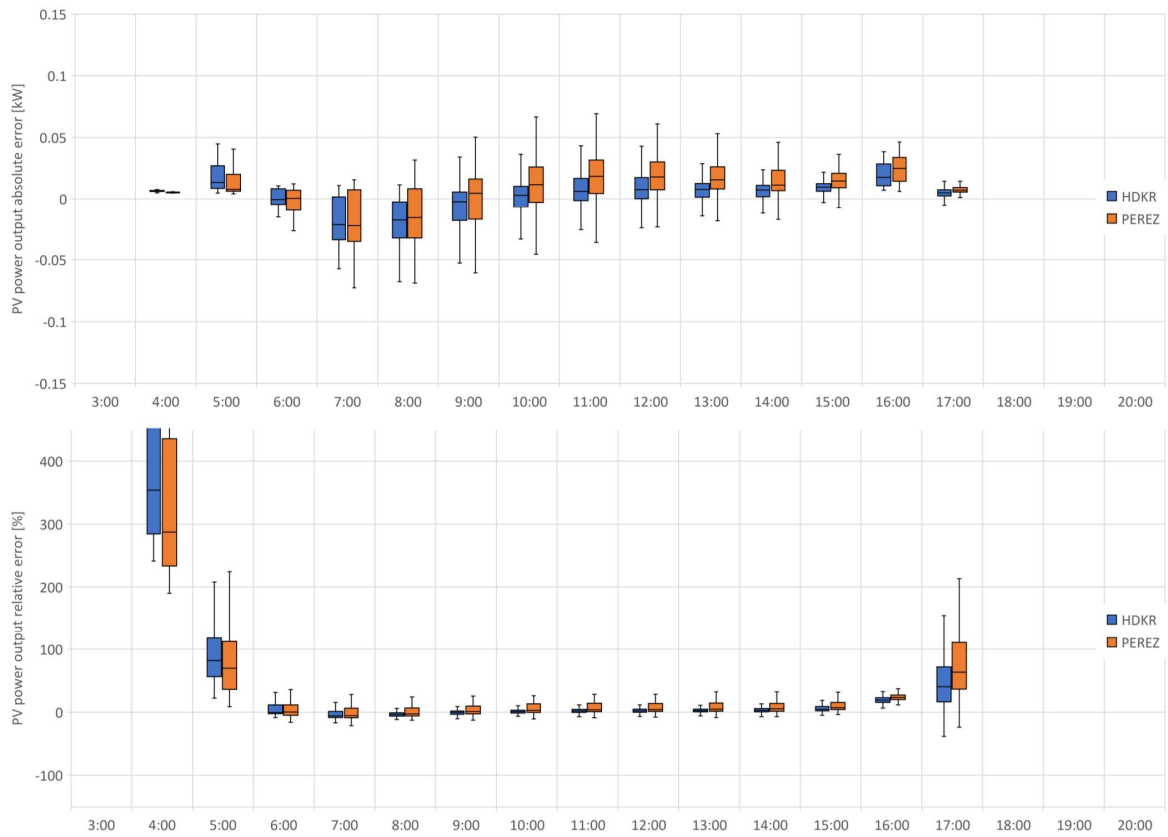
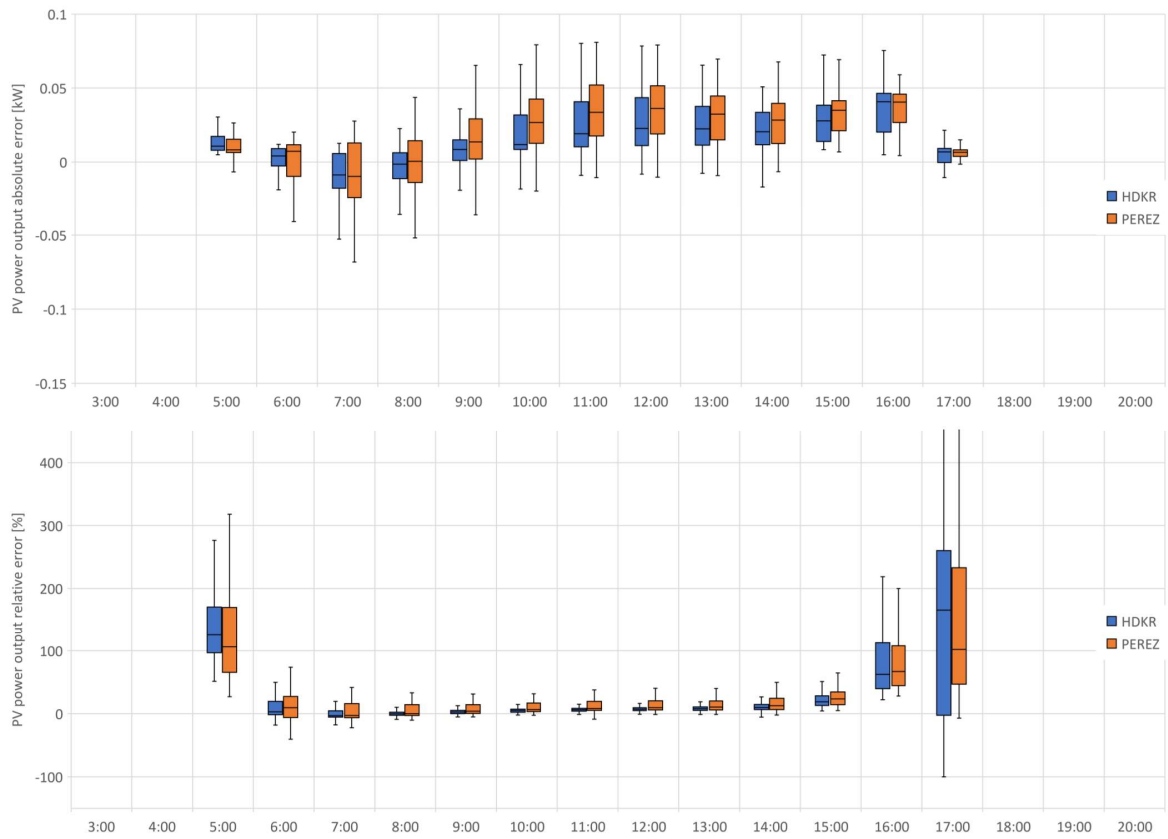Fig. A.8: Photovoltaics power output absolute (top) and relative (bottom) error - April
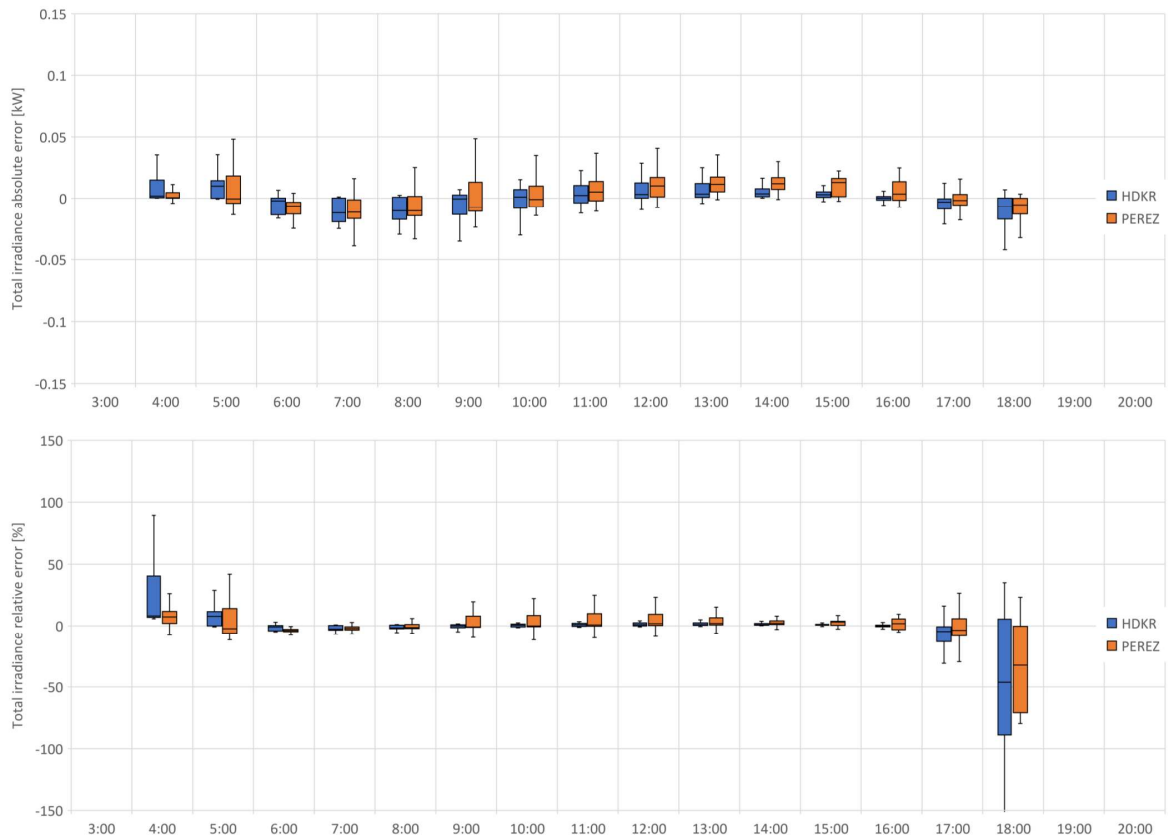
Fig. A.9: Total irradiance absolute (top) and relative (bottom) error - May

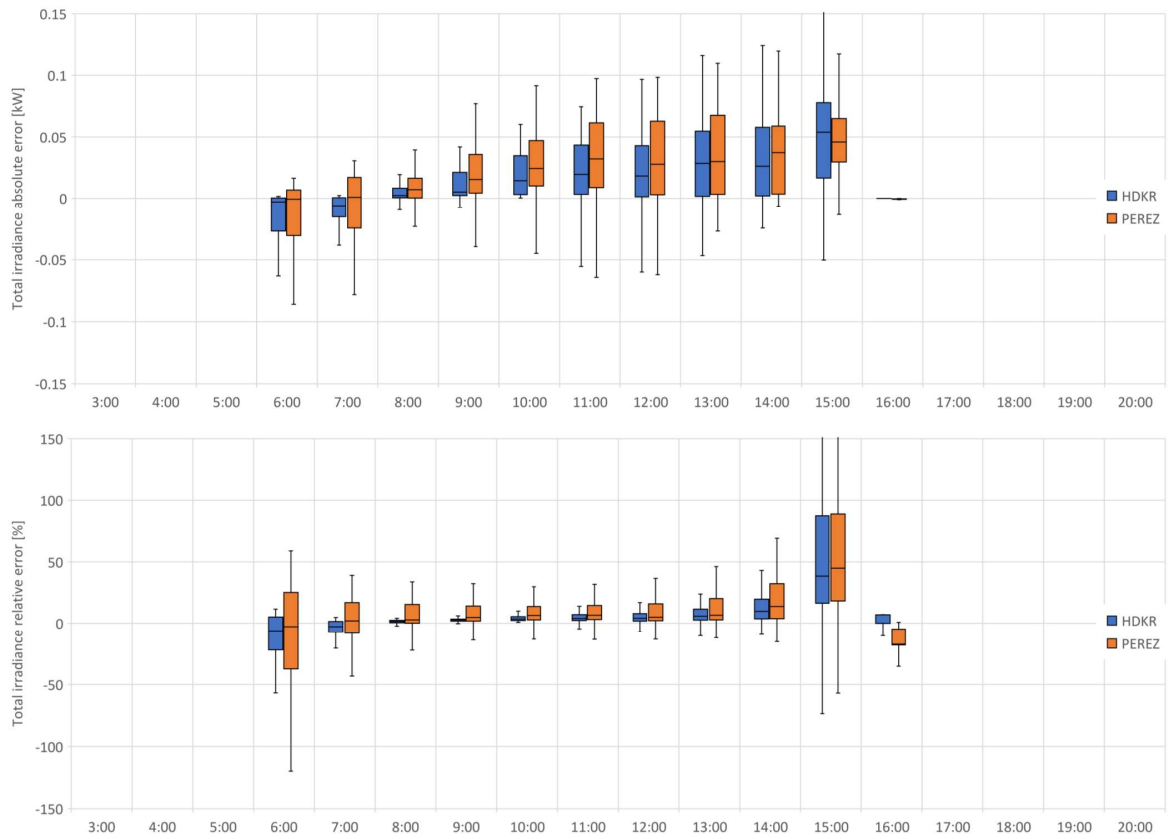Fig. A.10: Photovoltaics power output absolute (top) and relative (bottom) error - May

Fig. A.11: Total irradiance absolute (top) and relative (bottom) error - June

Fig. A.12: Photovoltaics power output absolute (top) and relative (bottom) error - June

Fig. A.13: Total irradiance absolute (top) and relative (bottom) error - July

Fig. A.14: Photovoltaics power output absolute (top) and relative (bottom) error - July

Fig. A.15: Total irradiance absolute (top) and relative (bottom) error - August

Fig. A.16: Photovoltaics power output absolute (top) and relative (bottom) error - August

Fig. A.17: Total irradiance absolute (top) and relative (bottom) error - September

Fig. A.18: Photovoltaics power output absolute (top) and relative (bottom) error - September

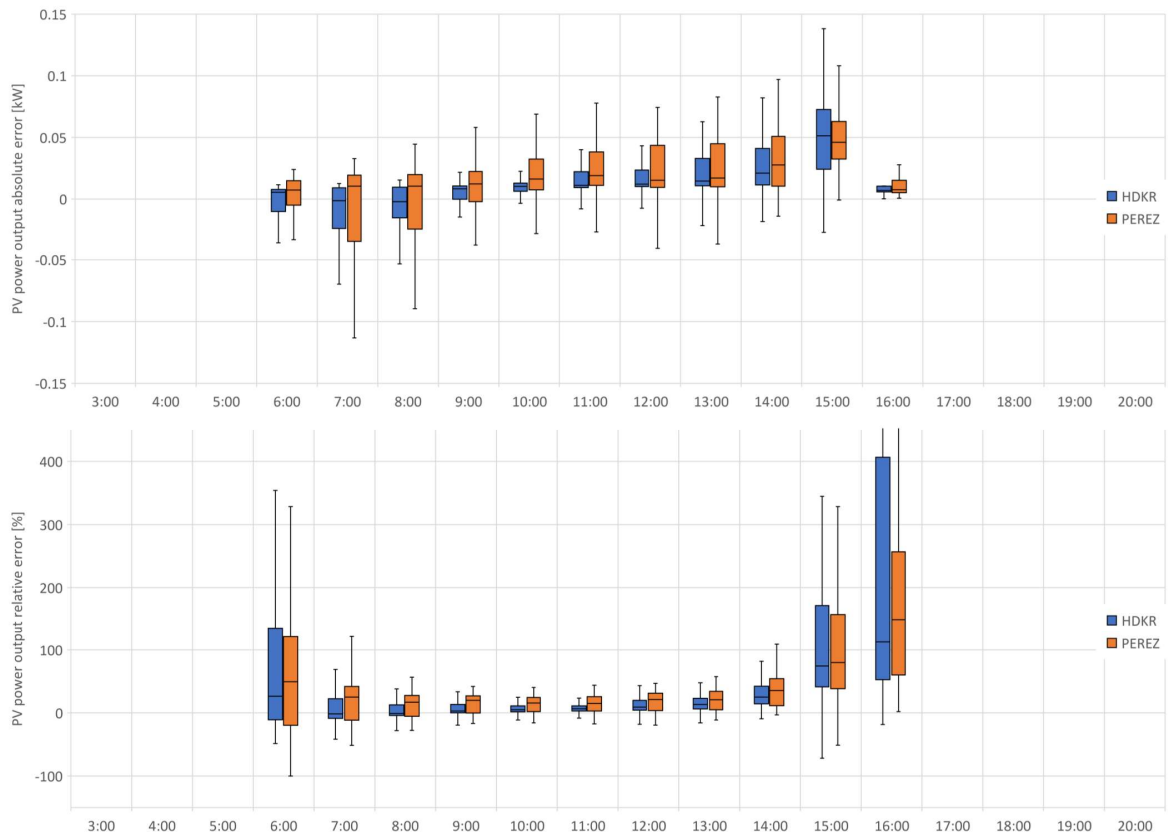Fig. A.19: Total irradiance absolute (top) and relative (bottom) error - October

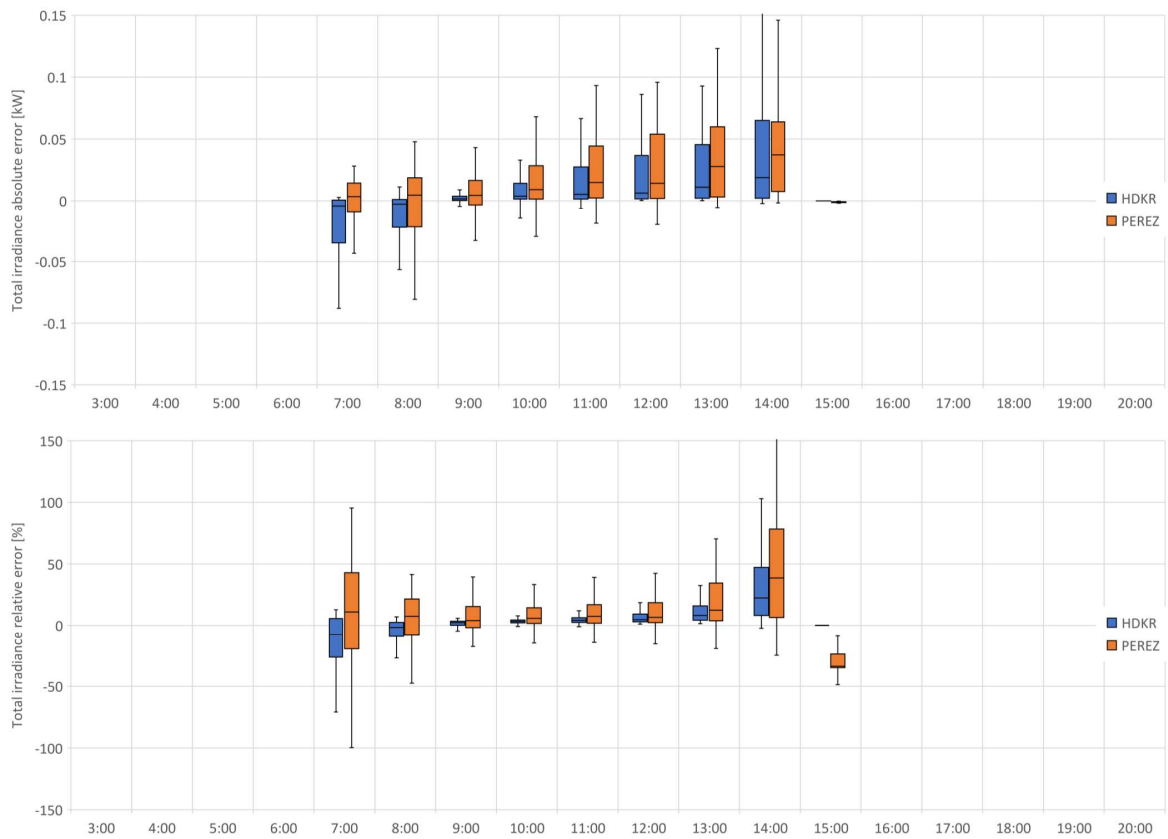Fig. A.20: Photovoltaics power output absolute (top) and relative (bottom) error - October

Fig. A.21: Total irradiance absolute (top) and relative (bottom) error - November
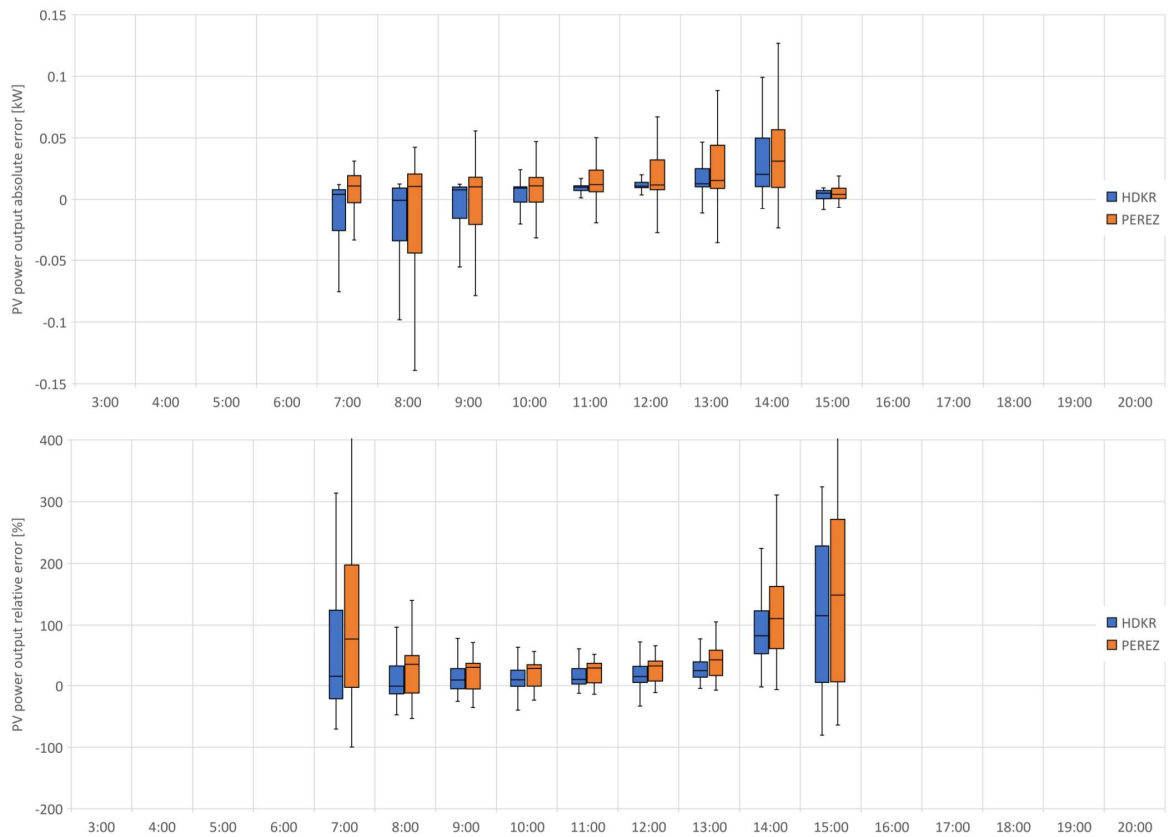

Fig. A.22: Photovoltaics power output absolute (top) and relative (bottom) error - November
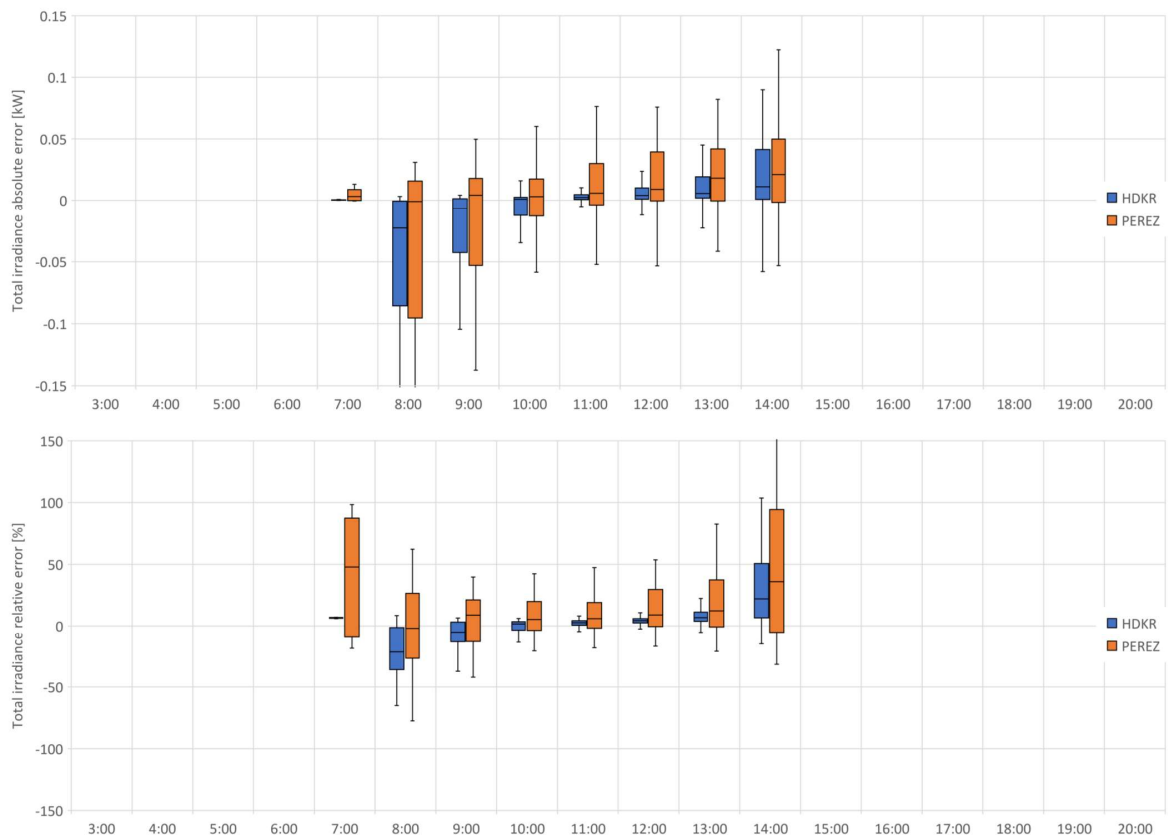
Fig. A.23: Total irradiance absolute (top) and relative (bottom) error - December
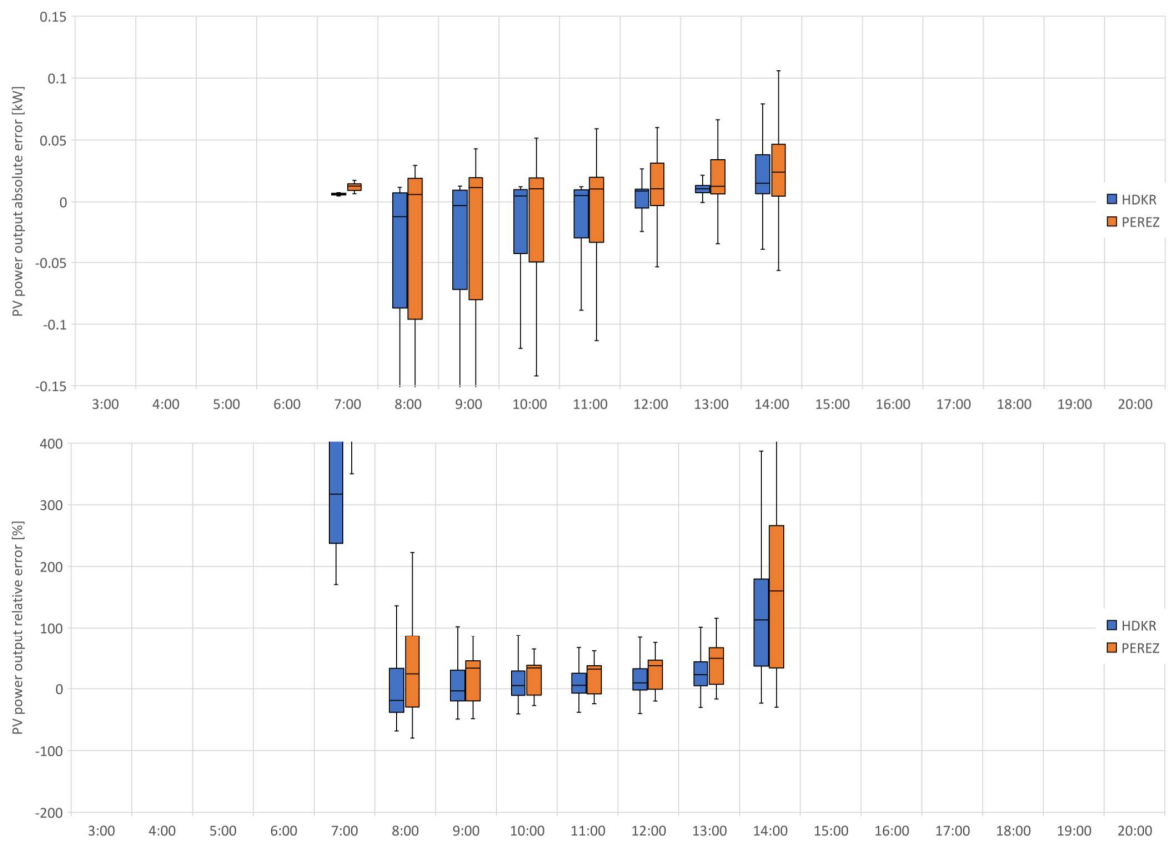

Fig. A.24: Photovoltaics power output absolute (top) and relative (bottom) error - December

91

Appendix B. - Heater & accumulation tank assemblies

Table B.1 Heater & accumulation tank setups

Household variant	Setup n.1 kW; kWh	Setup n.2 kW; kWh	Setup n.3 kW; kWh	Setup n.4 kW; kWh	Setup n.5 kW; kWh
V1_El.App	-	-	-	-	-
V2_DHW	2.220; 7.5	1.276; 10	1.271; 12.50	1.267; 15	1.262; 17.5
V3.1_DHW+SH	12.421; 45	12.285; 50	12.251; 55	12.225; 60	12.203; 65
V3.2_DHW+SH	9.218; 7.5	8.468; 10	7.718; 12.50	6.968; 15	6.218; 17.5

For each household variant, Setup n.1 was determined as the smallest possible to fulfill the condition of 10 % thermal reserve through the year, out of total storage tank capacity. Rest of the setups originate from the initial one, whereas the accumulation capacity was increased by a single step.

(In order to save computational time, in case of **V2_DHW** and **V3.2_DHW+SH**, heater power output step was designed 0.5 kW, whereas in case of **V3.2_DHW+SH**, 5 kW.)